

https://dspace.org/

The effects of inhibiting the notch signalling pathway in triple negative breast cancer cell lines

Msibi, Thandiwe

2016-02-26
http://hdl.handle.net/10539/19748

Downloaded from a DSpace repository. https://dspace.org/



The effects of inhibiting the Notch signalling pathway in triple negative breast cancer cell lines

A dissertation submitted to the Faculty of Health Sciences, School of Clinical Medicine

Department of Internal Medicine, University of The Witwatersrand, Johannesburg in fulfilment of the

Degree of Masters of Science in Medicine

Johannesburg 2015

Student: Thandiwe Msibi

Supervisor : Dr Clement Penny

DECLARATION

I declare that this dissertation is my own, unaided work. It is being submitted for the degree of Master of Science in Medicine, to the University of the Witwatersrand, Johannesburg. It has not been submitted before for any degree or examination at any other university.

Student signature: _____

On the day of 2015

DEDICATION

"FOR MY MOTHER GALLINAH CAROLINE MSIBI"

Publications and presentations arising from dissertation

- T.Msibi., P.Ruff., C.Penny., Investigating the Notch signalling pathway in Triple Negative Breast Cancer. Poster presentation at MBRT conference held at the University of the Witwatersrand Johannesburg 4th December 2013.
- T.Msibi., P.Ruff., C.Penny., Notch signal pathway in Triple Negative Breast Cancer. Poster presentation at the Faculty of science research day symposium held at the University of the Witwatersrand Johannesburg 17th September 2014
- T.Msibi., P.Ruff., C.Penny., Notch signalling pathway in Triple Negative Breast Cancer. Poster presentation at MBRT conference held at the University of the Witwatersrand Johannesburg 4th December 2014.

ABSTRACT

The molecular pathology of triple negative breast cancer (TNBC) is poorly understood, consequently, no successful forms of therapy have been developed. Thus an improvement of knowledge and subsequently the discovery of novel treatments for the disease are imperative. It has been found that deregulation of the Notch signalling pathway promotes tumourigenesis in breast tissue. Therefore, it was of interest here to investigate whether the Notch signalling pathway is deregulated in TNBC and whether its abrogation affects the proliferation and migration of TNBC cell lines. The normal growth characteristics of MCF-7 cells (hormone sensitive) were compared to those of MDA-MB-231 and MDA-MB-436 (both hormone insensitive) cell lines and were determined by real-time cell impedance assays, using the "xCELLigence" instrument. Thereafter, cells were treated with gamma secretase inhibitors (GSI) of the Notch signalling pathway. The MCF-7 cell line proliferated faster than the MDA-MB-231 and MDA-MB-436 cell lines. The proliferation of the MDA-MB-231 and MDA-MB-436 cell lines decreased significantly following treatment with inhibitors. Confocal microscopy was used to assess levels of the Notch intracellular component (a gamma secretase cleavage product) and E-cadherin (a breast tumour suppressor marker), pre- and post- treatment. Prior to drug treatments, confocal microscopy showed that the Notch intracellular component was highly expressed in the MDA-MB-231 cell line, and it was low in the MDA-MB-436 cell line, compared to the MCF-7 cell line. Following drug treatments, confocal microscopy showed a decreased expression of the Notch intracellular component in all three cell lines. Prior to drug treatment only the MCF-7 cell line expressed E-cadherin which was reduced post treatment. Subsequently the cell migration assays revealed that migration is reduced post-

drug treatment in all three cell lines, despite no statistical significance. Overall the MDA-MB-231 and MDA-MB-436 cell lines were more significantly sensitive to the gamma secretase inhibitors compared to the MCF-7 cell lines. Therefore these observations suggest that the Notch signalling pathway is a plausible novel therapeutic target in the treatment of TNBC.

ACKNOWLEDGEMENTS

I would like to thank the following groups and persons who made this work possible.

To my supervisor Dr Clement Penny, for your encouragement and advising me throughout the duration of this project, I will always be grateful for the opportunity you gave me. Being in your lab was an experience of a lifetime. God bless you.

To the head of the Research lab Dr Raquel Duarte, for being there for me when I needed someone the most, you were like a lab mother and I will pray that God blesses you thrice more than you have blessed me.

To my labmates/friends (in alphabetical order):

Aadilah Omar, Alex Kasembeli, Andrea Papadoupalous, Brenda Milner, Ezio Fok, Kiashanee Moodley, Lerato Mpye, Natasia Kruger, Nicole Crawford, and Therese Dix Peek. You guys were the best lab group I have ever been in; I appreciated and still appreciate the love and support I received from you guys. Thank you for all the help you each gave me in the lab and with other things. I will miss you all.

To the Department of Anatomy:

Ms Pamela Sharp, Ms Hasiena Ali, Ms Tanya Augustine and their students. Thank you for allowing me to use your facilities and giving me advice on my work.

To the following funding agencies:

- Mintek Dr Raymond Hewer who provided NRF sourced funding
- Faculty Research Committee, Faculty of Health Sciences, University of the Witwatersrand
- Postgraduate Merit Scholarship, University of the Witwatersrand

To my siblings Fakazi and Mlungisi you two are the best brothers a sister could ever wish for. I pray that you go as far as you can with your dreams. To the rest of my family, thank you for always believing me in me and keeping me in your prayers.

"Follow your Bliss and the Universe will open doors for you where there were only walls"- Joseph Campbell (1904-1987)

TABLE OF CONTENTS

DECLARATION ..... **II**

DEDICATION ..... **III**

PUBLICATIONS AND PRESENTATIONS ARISING FROM DISSERTATION ..... **IV**

ABSTRACT ..... **V**

ACKNOWLEDGEMENTS ..... **VII**

LIST OF FIGURES XVI

LIST OF TABLES XX

LIST OF ABBREVIATIONS XXIII

CHAPTER 1: INTRODUCTION **1**

1.1 REVIEW OF LITERATURE 1

1.1.1 Breast cancer statistics and classification *1*

1.1.2 What is Triple negative breast cancer? *3*

1.1.2.1 The difference between the Basal-like breast cancer and Triple negative breast cancer 3

1.1.2.2 Molecular classification of Triple negative breast cancer 4

1.1.2.3 Epidemiology and risk factors for Triple negative breast cancer 8

1.1.2.3.1 Racial disparities 8

1.1.2.3.2 Genetic risk factors 9

1.1.2.3.3 Reproductive risk factors 10

1.1.2.3.4 Anthropometric risk factors 11

1.1.2.3.5 Socioeconomic status risk factors 13

1.1.3 Current and novel treatment options 14

1.1.4 The Notch signalling pathway 17

1.1.4.1 The structure of the Notch receptors and their ligands 18

1.1.4.1.1 Notch receptors 18

1.1.4.1.2 Notch ligands 19

1.1.4.1.3 Notch signal transduction 22

1.1.5 Notch signalling in breast cancer 25

1.1.6 Strategies to target Notch signal pathway in Triple negative breast cancer 28

1.1.6.1 Notch1 and Delta-like 4 monoclonal antibodies 29

1.1.6.2 Notch-1 siRNA 30

1.1.6.3 γ-Secretase inhibitors 31

1.2 EXPERIMENTAL APPROACH AND RATIONALE 34

1.2.1 Experimental approach 34

1.2.1.1 Notch pathway inhibition 34

1.2.1.2 Cellular proliferation and viability 35

1.2.1.3 Evaluating cell morphology and migration 40

1.2.2 Rationale 41

1.2.2.1 Aims and objectives 42

1.2.2.1.1 Aim 42

1.2.2.1.2 Objectives 42

CHAPTER 2: MATERIALS AND METHODS 43

2.1 MAMMALIAN CELL LINES AND CELL CULTURE MAINTENANCE 44

2.1.1 Cell lines 44

2.1.2 Cell culture maintenance 45

2.2 ANALYSIS OF CELLULAR PROLIFERATION 46

2.2.1 Normal growth curve profiling 46

2.2.2 Cell viability and proliferation assays 47

2.2.2.1 xCelligence-proliferation and viability assay 47

2.2.2.2 Trypan blue exclusion cell viability assay 48

2.3 CONFOCAL IMMUNOFLUORESCENCE MICROSCOPY 49

2.3.1 Immunofluorescence staining 51

2.3.1.1 Cell preparation 51

2.3.1.2 Primary and Secondary antibody staining 52

2.3.1.3 Nuclear staining 52

2.3.1.4 Z-sectioning and 3 dimensional reconstruction analysis 53

2.4 CELL MIGRATION STUDY 53

2.4.1 Cell migration assay 54

2.5 DATA ANALYSIS 55

CHAPTER 3: RESULTS 56

3.1 DETERMINATION OF THE ACTIVITY OF NOTCH AND THE EFFECT OF GAMMA SECRETASE INHIBITION 56

3.1.1 Notch signalling is active in breast cancer cells and NIC expression decreases post- inhibitor treatment 56

3.2 EFFECT OF NOTCH ON BREAST CANCER CELLS 59

3.2.1 Oestrogen receptor positive cells grow more rapidly compared to TNBC cell lines 59

3.2.2 Notch signal pathway inhibition decreases cell proliferation and viability in breast cancer cells . 61

3.2.2.1 Trypan blue assay cell viability 61

3.2.2.2 xCelligence-RTCA cell proliferation and viability 64

3.3 EFFECT ON CELL MORPHOLOGY AND CELL MIGRATION 68

3.3.1 Notch inhibition decreases expression of E-cadherin in MCF-7 cells and alters cell morphology in MDA-MB-231 and MDA-MB-436 cell lines. 68

3.3.1.1 The expression of E-cadherin in human breast cancer cells 68

3.3.1.2 The morphology of human breast cancer cells 69

3.3.2 Notch inhibition does not affect cell migration in BC cell lines. 75

CHAPTER 4: DISCUSSION 82

4.1 NOTCH EXPRESSION AND ACTIVITY 82

4.2 THE CELLULAR GROWTH, PROLIFERATION AND VIABILITY OF HUMAN BREAST CANCER CELLS 84

4.2.1 Classical end-point assay versus real-time cell analysis assay 86

4.3 NOTCH AND CELL MIGRATION AND MORPHOLOGY 86

4.4 CONCLUSION 88

CHAPTER 5: PERSPECTIVES AND FUTURE WORK 90

5.1 PROPOSED APPROACH FOR FUTURE WORK 90

CHAPTER 6: REFERENCES 92

6.1. JOURNAL ARTICLES 92

6.2 E-REFERENCES 112

APPENDIX A: PROTOCOLS 113

A.1 PREPARATION OF SOLUTIONS AND REAGENTS 113

A.1.1 1X Phosphate Buffered Solution (PBS) 113

A.1.2 Blocking buffer *113*

A.1.3 Fixing Solution/Buffer *113*

A.1.4 Permeabilisation solution/Buffer *113*

A.1.5 F-actin cytoskeleton staining solution *113*

A.1.6 Nuclear stain *114*

A.1.7 Cell culture media *114*

A.1.8 Freezing media and thawing media *115*

A.2 PHARMACOLOGICAL INHIBITOR CONCENTRATION CALCULATIONS 115

A.2.1 DAPT stock solution *115*

A.2.2 DBZ stock solution *116*

APPENDIX B: CELL CULTURE MAINTENANCE AND ETHICS 117

B.1 CELL SUB-CULTURE 117

B.2 CELL FREEZING 117

B.3 CELL THAWING 118

B.4 CELL COUNTING 118

B.5 ETHIC WAIVER 119

APPENDIX C: CELL GROWTH, PROLIFERATION AND VIABILITY RAW DATA 121

C.1 NORMAL GROWTH PROFILE CELL NUMBER OPTIMISATION 121

C.2 TRYPAN BLUE ASSAY AND CELL VIABILITY DRUG CONCENTRATION OPTIMISATION 123

C.2.2 Trypan Blue viability assay 123

C.2.3 Cell proliferation raw data 125

APPENDIX D: INDIRECT IMMUNOFLUORESCENCE 127

D.1 NEGATIVE CONTROLS FOR THE NOTCH-1 INTRACELLULAR COMPONENT SIGNALLING EXPRESSION AND LOCALISATION ... 127

D.2 Negative controls for the expression and localisation of E-cadherin 134

D.3 MCF-7 cell line E-cadherin expression 140

APPENDIX E: SCRATCH/MIGRATION ASSAY ANALYSIS 141

E.1 CALCULATIONS OF CELL MIGRATION 141

E.2 RAW DATA FOR GAP CLOSURE PLOTS 143

APPENDIX F: STATISTICAL ANALYSES AND TURN-IT-IN REPORT 147

LIST OF FIGURES

1.1	Summary of the two different methodological approaches applied to sub-classify TNBC.	7
1.2	Schematic representation of a TNBC tumour; the current challenge in its treatment and management.	16
1.3	Diagrammatic representations of the Notch receptor and Notch-ligand.	21
1.4	A Schematic representation of the Notch pathway.	24
1.5	Potential Therapeutic targets for Notch in Triple negative Breast cancer.	33
1.6	A diagrammatic representation of the cell-electrode interaction in an E-plate.	37
1.7	Schematic diagrams showing the difference between classical endpoint assay and the xCELLigence RTCA technology.	39
2.1	Flow diagram representation of methodology applied in this study.	43
2.2	Principal of the confocal laser microscope	50
3.1	Notch signalling is active in breast cancer cells and its expression decreases post inhibitor treatment	58
3.2	Normal cell growth profile of hormone receptor positive cell line (MCF-7) compared to hormone receptor negative positive cell line (MDA-MB-231 and MDA-MB-436).	60
3.3	TB assay cell viability of breast cancer cells.	63
3.4	GSI treatment inhibits cell proliferation of MCF-7 breast cancer cell lines.	65
3.5	GSI treatment inhibits cell proliferation of MDA-MB-231 breast cancer cell lines.	66

3.6	GSI treatment inhibits cell proliferation of MDA-MB-436 breast cancer cell line.	67
3.7.**a**	Effects of Notch inhibition on the expression of E-cadherin and cell morphology in permeabilised cells.	71
3.7.**b**	3D projection, generated from Z-sectioning; Zeiss LSM 780 permeabilised cells.	72
3.8.**a**	Effects of Notch inhibition on the expression of E-cadherin and cell morphology in non-permeabilised cells.	73
3.8.**b**	3D projection, generated from Z-sectioning; Zeiss LSM 780 non-permeabilised	74
3.9.**a**	Notch inhibition does not affect cell migration in MCF-7 cell line	76
3.9.**b**	A plot representing the gap closure in Notch inhibited MCF7 cells.	77
3.10.**a**	Notch inhibition does not affect cell migration in MDA-MB-231 cell line.	78
3.10.**b**	A plot representing the gap closure in Notch inhibited MDA-MB-231 cells.	79
3.11.**a**	Notch inhibition does not affect cell migration in MDA-MB-436 cell line.	80
3.11.**b**	A plot representing the gap closure in Notch inhibited MDA-MB-436 cells	81
5.1	Diagram representing the methodology for future work.	91
C.1	Optimising cell seeding density of MCF-7 cell line	121
C.2	Optimising cell seeding density of MDA-MB-231cell line.	122
C.3	Optimising cell seeding density of MDA-MB-436 cell line	122
C.4	Real-time cell proliferation and viability of the MCF-7 cell line over 88 hours.	125
C.5	Real-time cell proliferation and viability of the MD-MB-231 cell line over	125

200 hours.

C.6 Real-time cell proliferation and viability of the MDA-MB-231 cell line over 119 hours. 126

D.1.**a** Negative controls of MCF-7 cell line in confocal microscopy. 128

D.1.**b** Negative controls of MCF-7 cell line in confocal microscopy. 129

D.2.**a** Negative controls of MDA-MB-231cell line in confocal microscopy. 130

D.2.**b** Negative controls of MDA-MB-231cell line in confocal microscopy. 131

D.3.**a** Negative controls of MDA-MB-436 cell line in confocal microscopy. 132

D.3.**b** Negative controls of MDA-MB-436 cell line in confocal microscopy. 133

D.4.**a** E-cadherin negative controls of MCF-7cell line in confocal microscopy. 134

D.4**.b** E-cadherin negative controls of MCF-7cell line in confocal microscopy. 135

D.5.**a** E-cadherin negative controls of MDA-MB-231cell line in confocal microscopy. 136

D.5.**b** E-cadherin negative controls of MDA-MB-231cell line in confocal microscopy. 137

D.6.**a** E-cadherin negative controls of MDA-MB-436 cell line in confocal microscopy. 138

D.6.**b** E-cadherin negative controls of MDA-MB-436 cell line in confocal microscopy. 139

D.7 The E-cadherin expression and localisation in MCF-7 cell line. 140

E.1 Scratch image analyses. 141

E.2 Scratch image analyses 142

E.3 Scratch image analyses. 142

E.4 Scratch image analyses. 143

LIST OF TABLES

1.1	Molecular classification of the five major breast cancer subtypes.	3
1.2	Clinical characteristics of the Triple Negative Breast Cancer phenotype (as described by Dent et.al, 2007.	15
2.1	A summary of the characteristics of the breast cell lines.	45
2.2	Optimised cell seeding density for xCelligence studies.	46
A.1	Media preparation for MCF-7, MDA-MB-231 and MDA-MB-436 cell lines.	114
C.1	Dilution series for cell seeding densities for growth signature optimisation.	121
C.2	Average percentage values of MCF-7 cell viability.	123
C.3	Standard deviation values of MCF-7 cell viability.	123
C.4	Average percentage values of MDA-MB-231 cell viability.	123
C.5	Standard deviation values of MDA-MB-231 cell viability.	124
C.6	Average percentage values of MDA-MB-436 cell viability.	124
C.7	Standard deviation values of MDA-MB-436 cell viability.	124
E.1	The average distances of MCF-7 cell line pixel/µm calculated on ImageJ.	143
E.2	The standard deviations of MCF-7 cell line pixel/µm calculated on ImageJ.	144
E.3	The average distances of MDA-MB-231 cell line pixel/µm calculated on ImageJ.	144
E.4	The standard deviation MDA-MB-231cell line pixel/µm calculated on ImageJ.	145
E.5	The averages distances of MDA-MB-436 cell line pixel/µm calculated on ImageJ.	145
E.6	The standard deviations of MDA-MB-436 cell line pixel/µm calculated on ImageJ.	146

F.1 Results from the Kruskal-Wallis test of the effect of DBZ on MCF-7, MDA-MB-231 and MDA-MB-436 cell lines. 147

F.2 Results from the Kruskal-Wallis test of the effect of DAPT on MCF-7, MDA-MB-231, and MDA-MB436 cell lines. 148

F.3 Results from the Kruskal-Wallis test of the normal growth curves of MCF-7, MDA-MB-231, and MDA-MB-436 cell lines. 148

F.4 Results from the unpaired student's t-test between the growth curves of MCF-7 and MDA-MB-231 cell lines. 149

F.5 Results from the unpaired student's t-test between the growth curves of MCF-7 and MDA-MB-436. 150

F.6 Results from the unpaired student's t-test between the effects of DAPT on the cell proliferation and viability of the MCF-7 and MDA-MB-231 cell lines. 151

F.7 Results from the unpaired student's t-test between the effects of DAPT on the cell proliferation and viability of the MCF-7 and MDA-MB-436 cell lines. 152

F.8 Results from the unpaired student's t-test between the effects of DBZ on the cell proliferation and viability of the MCF-7 and MDA-MB-231 cell lines. 153

F.9 Results from the unpaired student's t-test between the effects of DBZ on the cell proliferation and viability of the MCF-7 and MDA-MB-436 cell lines. 154

F.10 Results from the paired student's t-test between the effects of DAPT vs DBZ on the cell proliferation and viability of the MCF-7 cell line. 155

F.11 Results from the paired student's t-test between the effects of DAPT vs DBZ on the cell proliferation and viability of the MDA-MB-231 cell line. 156

F.12 Results from the paired student's t-test between the effects of DAPT vs DBZ 157

on the cell proliferation and viability of the MDA-MB-436 cell line.

F.13 Results from the Kruskal-Wallis test on the cell migration of MCF-7 cell lines. 158

F.14 Results from the Kruskal-Wallis t-test on the cell proliferation and viability of the MDA-MB-231 cell line. 158

F.15 Results from the Kruskal-Wallis t-test on the cell migration of the MDA-MB-436 cell line. 159

F.16 Results from the paired student's t-test between the effects of DAPT vs DBZ on the cell migration of the MCF-7 cell line. 160

F.17 Results from the paired student's t-test between the effects of DAPT vs DBZ on the cell proliferation and viability of the MDA-MB-436 cell line. 161

F.18 Results from the paired student's t-test between the effects of DAPT vs DBZ on the cell proliferation and viability of the MDA-MB-231 cell line. 162

LIST OF ABBREVIATIONS

3D	3 dimension
AAW	African American Women
APH1	Anterior pharnx-defective 1
ADAM	A Disintergrin Metalloprotease
ANK	Ankyrin
ATCC	American Type Cell Culture
BC	Breast cancer
BL1	Basal Like 1
BL2	Basal Like 2
BLBC	Basal Like Breast Cancer
BMI	Body Mass Index
BSA	Bovine Serum Albumin
BSA	Bovine serum albumin
BWHS	Black Women's Health Study
CBCP	Clinical Breast Care Project
CBF-1	C-promoter binding factor-1
CHBH	Chris-Hani Baragwanath Hospital
CI	Cell Index
CK	Cytokeratin
CRD	Cysteine Rich Domain
CSC	Cancer Stem Cell
CW	Caucasian women

DAPT	N-(N-3,5-Diflurophenacetyl-L-alanyl)-S-phenyl glycine t-Butyl Ester
DBZ	N-[(1S)-2-[[(7S)-6,7-Dihydro-5-5methyl-6-oxo-5H-dibenz[b,d] azepin-7-yl]amino-1-methyl-2-oxoethyl]-3,difluorobenzeneacetamide
DMSO	Dimethyl Sulphoxide
DOS	Delta and OSM-11-like repeats
DSL	Delta/serrate/lag-2
DsRNA	Double stranded
E-cadherin	Epithelial Cadherin
EDTA	Ethylenediaminetetraacetic acid
EGF	Epithelial Growth Factor
EGFR	Epithelial Growth Factor Receptor
EMT	Epithelial-to-mesenchymal transition
E-plates	Electronic plates
ER	Oestrogen Receptor
RER	Rough endoplasmic Reticulum
FBS	Foetal Bovine Serum
FDA	Food and Drug Administration
GSI	γ-Secretase Inhibitor
GTPase	Guanosine triphosphate hydrolase
HD	Heterodimerization
HER-2	Human Epidermal Growth Factor-2
IHC	Immunohistochemistry

L-15	Leibovitz
LAR	Luminal Androgen Receptor
LNR	Lin12-Notch Repeats
mAb	monoclonal antibody
MAML	Mastermind-like
MCF-7	Michigan Cancer Foundation–7
MDA-MB-231	M.D Anderson-Metastatic Breast-231
MDA-MB-436	M.D Anderson-Metastatic Breast-436
miRNA	Micro-ribonucleic acids
ML	Mesenchymal Like
MNNL	Module at the N-terminus of Notch Ligand
mRNA	messenger ribonucleic Acid
MSL	Mesenchymal Stem Like
N1IC	Notch-1 Intracellular Component
N-cadherin	Neural Cadherin
NEC	Notch Extracellular Component
NIC	Notch Intracellular Component
N1IC	Notch-1 Intracellular Component
NLS	Notch Localising Sequence
NRR	Negative Regulatory Region
NTM	Notch transmembrane
OC	Oral contraceptives
PBS	Phosphate Buffered Saline

PDZL	post synaptic density protein (PSD95), Drosophila disc large tumor suppressor (Dlg1), and zonula occludens-1 protein (zo-1) Ligand
PEN2	Presenilin enhancer 2
PR	Progesterone Receptor
RAM	RBPjk Association Module
RBPJκ	Recombination signal-binding protein for immunoglobulin kappa j
RER	Rough endoplasmic reticulum
RIP	Regulated Intramembrane Proteolysis
RISC	RNA Induced Silencing Complex
RNA	Ribonucleic acid
RNAi	RNA interference
RT	Room Temperature
RTCA	Real Time Cell Analysis
SA	South Africa
SDV	Standard Deviation
SES	Socioeconomic status
siRNA	short interfering RNA
TAD	Transactivation Domain
T-ALL	T-cell Acute Lymphoblastic Leukemia/Lymphoma
TB	Trypan Blue
TNBC	Triple Negative Breast Cancer
USA	United States of America
Ɣ-secretase	Gamma secretase

CHAPTER 1: INTRODUCTION

1.1 Review of literature

1.1.1 Breast cancer statistics and classification

Breast cancer (BC) is the most common cause of cancer related deaths among women worldwide and it is now estimated that it represents one in four cancers afflicting women Ferlay *et al*. (2015). The most recent GLOBOCAN study reveals that BC incidences have risen by approximately 20% between 2008 and 2012 (Ferlay *et al*., 2015). In South Africa (SA), it is estimated that one in thirty five women will be diagnosed with the disease making it the leading cause of cancer related deaths in South African women (CANSA, 2014).

BC is a heterogeneous complex of diseases that have been classified into five subtypes namely: Luminal A; Luminal B; Human epidermal growth factor-2 receptor (HER-2) positive (HER-2^{+}); Normal breast-like and Basal-like BC (BLBC) (see Table 1.1) (Sotiriou and Pusztai, 2009, Perou *et al*., 2000, Sorlie *et al*., 2003). The classification was based on gene expression patterns, wherein each subtype displayed distinct biological features (Yersal and Barutca, 2014, Rakha and Ellis, 2011), which give rise to the differences in the

response patterns to various treatment modalities and to clinical outcomes (Yersal and Barutca, 2014, Liu *et al*., 2014).

The Luminal subtype arises from the luminal epithelium of the breast ducts and is sub-classified into Luminal A and Luminal B breast tumours (Vuong *et al*., 2014). While both express oestrogen receptors (ER) and progesterone receptors (PR), the Luminal A tumours have higher levels of ER, compared to the Luminal B tumours (Sorlie *et al*., 2001, Zhang *et al*., 2014). Furthermore, the Luminal A tumours have a lower proliferation index and are highly sensitive to current endocrine therapeutics and to aromatase inhibitors (Ignatiadis and Sotiriou, 2013). The Luminal B tumours express HER-2, thus these tumours have a higher proliferative index than Luminal A tumours (Zhang *et al*., 2014). This feature enhances their sensitivity to current anti-HER-2 therapies (Network, 2012, Ignatiadis and Sotiriou, 2013).

Those tumours classified as normal breast-like, express genes characteristic of adipose tissues, and are negative for the basal myoepithelial markers, cytokeratin (CK) 5 and epithelial growth factor receptor (EGFR) (Yersal and Barutca, 2014, Vuong *et al*., 2014). This subtype however, remains controversial, as some researchers believe that it very likely represents normal breast cell samples that have been contaminated during technical work (Weigelt *et al*., 2010).

The last subtype is the BLBC subtype. These tumours which originate from the basal myoepithelium are the most aggressive of all the tumour subtypes. They express high levels of basal myoepithelial markers, such as, CK5, CK14, CK17 and laminin; and they

lack the expression of ER, PR and HER-2 receptor, a feature described as "triple negativity". Currently, there is no specific therapy for BLBC tumours.

Table 1.1: Molecular classification of the five major breast cancers subtypes (Sorlie *et al*., 2003).

Subtypes	Molecular classification	Prevalence
Luminal A	$ER^+/PR^+/HER\text{-}2^-$	50-60%
Luminal B	$ER^+/PR^+/HER\text{-}2^+$	15-20%
HER-2 Positive	$ER^-/PR^-/HER\text{-}2^+$	15-20%
Basal-like	$ER^-/PR^-/HER\text{-}2^-$	8-37%
Normal like	ER-/PR-HER-2- / CK5-	5- 10%

1.1.2 What is Triple negative breast cancer?

1.1.2.1 The difference between the Basal-like breast cancer and Triple negative breast cancer

BLBCs are the most aggressive BC subtype of the five discussed. They are diagnosed more frequently in young women of African ancestry (Badve *et al*., 2011). As mentioned above, a characteristic feature of BLBC is the lack of ER, PR, and HER-2 expression. In the research setting, this disease is defined via gene expression array analysis (Perou *et al*., 2000). Since this approach is economically unfeasible in the clinical setting, immunohistochemical (IHC) analyses of hormone and growth receptors are used as markers for BLBC. As a consequence of this approach, BLBC became more commonly

known as triple negative breast cancer (TNBC) (Prat *et al*., 2013). However, research has demonstrated that as there is approximately 25% discordance between BLBC and TNBC, as not all BLBC are TNBC and *vice versa (*Yersal and Barutca, 2014, Prat *et al.*, 2013).

Microarray based studies on 12 publicly available TNBC data sets, which were composed of TNBC human tumours and TNBC cell lines revealed that only 70-80% of the tumours possessed the basal like phenotype and 20-30% were either luminal or had basoluminal phenotypes (Prat *et al*., 2013).Other microarray studies demonstrated that between 50-75% of TNBC tumours were of the basal like phenotype (Rakha *et al*., 2009, Perou, 2011, Nielsen *et al*., 2004). Moreover, up to 45% of BLBCs expressed the ER, PR and HER-2 and 40-80% of TNBC expressed basal markers (Carey *et al*., 2010). It is also noted that a characteristic feature of the controversial normal breast-like tumours, lack ER, PR and HER-2 expression, which implies that they may also be considered "triple negative". Evidently, research has shown that TNBC is not a reliable surrogate for BLBC and therefore, the terms should not to be used synonymously (Prat *et al*., 2013, Rakha *et al*., 2009).

Therefore, TNBCs are defined as breast tumours that lack ER, PR and HER-2 expression, and may fall into any of the other BC subtypes (Perou, 2011, Eiermann *et al*., 2012, Prat and Perou, 2011) .

1.1.2.2 Molecular classification of Triple negative breast cancer

The heterogeneity of this group has lead researchers to the inclination that TNBC may be comprised of a variety of molecularly distinct subgroups (Prat and Perou, 2011). In this regard the most prominent publication is by Lehmann and colleagues who analysed

ribonucleic acid (RNA) expression from 14 BC gene expression datasets that used breast tumours from women in the United States of America (USA), Europe and China as a training set, to develop gene signatures for TNBC subgroups (Lehmann *et al*., 2011). Through their analyses 2,188 genes from 386 TNBC tumours were identified (Lehmann *et al*., 2011). Consensus and k-means clustering of the tumour profiles revealed that there were six TNBC sub-groups which consisted of Basal-like 1 (BL1), Basal-like 2 (BL2), Mesenchymal like (ML), Mesenchymal stem like (MSL), and Luminal Androgen Receptor (LAR) (summarised Figure 1.1) (Lehmann *et al*., 2011) .

Other researchers have employed different approaches to investigate or validate the "TNBC sub-group" hypothesis (Prat *et al*., 2013). Elsawaf and colleagues demonstrated that there are four distinct TNBC subgroups (Elsawaf *et al*., 2013). By using IHC combined with hierarchical clustering, they analysed 147 patient derived TNBC tumours, to assess the expression of basal and luminal cytokeratins. The subgroups were classified as Basal A, Basal B, Basoluminal and Luminal, with respect to the predominant pattern of cytokeratin expression (Figure 1.1) (Elsawaf *et al*., 2013).

Each of these studies employed a different approach to test the hypothesis, each having advantages and disadvantages. The Lehmann study was larger and distinguished their subgroups based on the identification and clustering of 2,188 genes. In contrast, the Elsawaf study was smaller and evaluated the biomarker expression patterns on the tumours. The former study is more statistically and biologically powerful *versus* the latter. However, the Elsawaf approach is more economically and practically feasible for routine clinical diagnostics, more especially in an African setting.

Furthermore, Prat and colleagues (Prat *et al*., 2010) identified another sub-group characterised by lower claudin expression levels through micro-ribonucleic acid (miRNA) expression analyses. Claudins represent a group of cell adhesion molecules that are associated with the formation and stabilisation of tight junctions (Escudero-Esparza *et al*., 2011). These tumours were observed to be most aggressive compared to other subgroups (Prat *et al*., 2010). The clinical relevance of this subgroup as well as the aforementioned groupings is still under investigation, since subject of TNBC sub-classification is controversial.

Therefore, further research is warranted in order to reach a general consensus as to which approach is best suited to determine the molecular subgroup of a tumour. It is imperative that both the researcher and clinician agree to avoid tumour misclassifications, when diagnosing patients or when beginning a clinical trial or laboratory research.

Despite the controversy, the research discussed provides valuable information concerning the complicated nature of TNBC and it is this complexity in addition to the lack of hormone and growth receptor expression as to why TNBC remains a challenge to treat and manage.

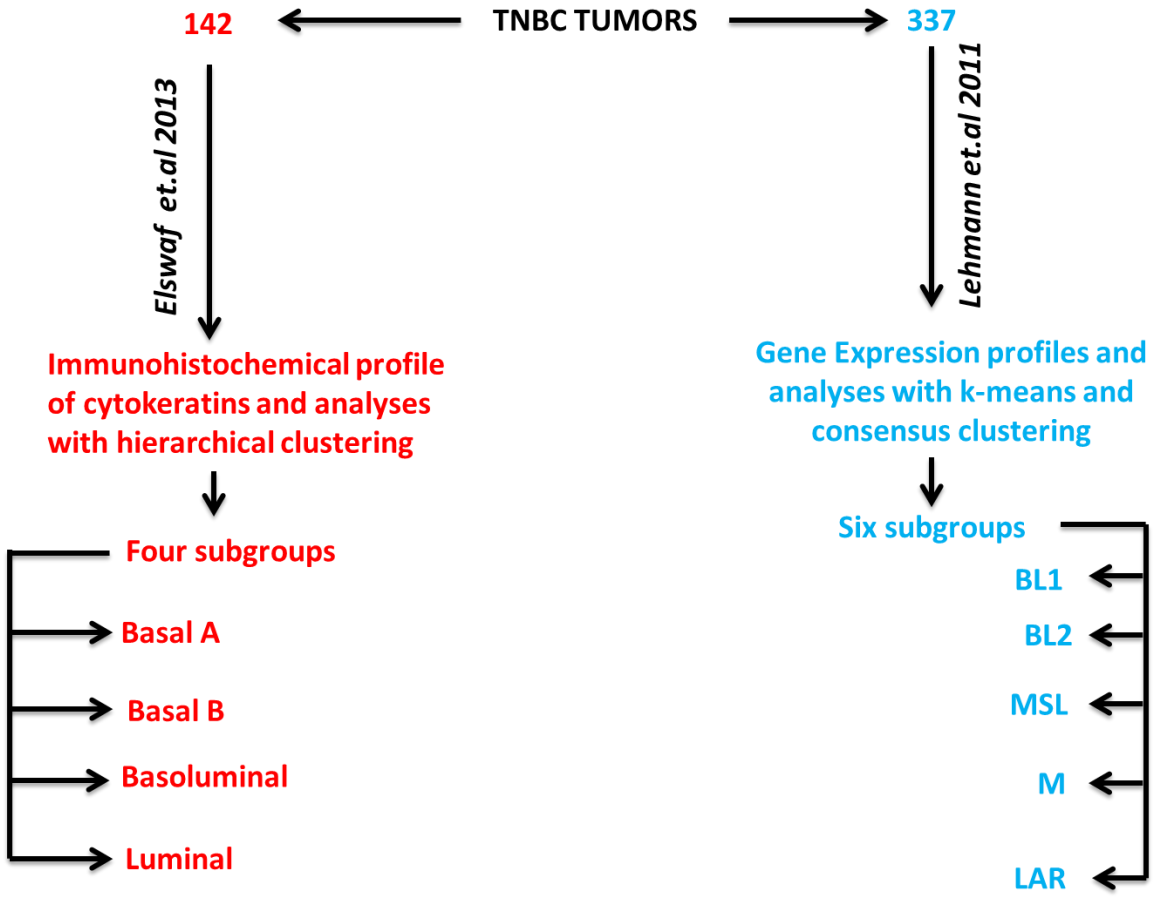


Figure 1.1 Summary of the two different methodological approaches applied to sub-classify TNBC. Immunohistochemical analyses of 147 TNBC tumours (red) based on hierarchical clustering of predominant patterns of basal and luminal cytokeratins revealed four distinct subgroups Basal A; Basal B; Basoluminal and Luminal TNBCs. Gene expression analyses of 337 TNBC tumours (blue) were analysed by k-means and consensus clustering of 2,188 genes. The six distinct sub-groups identified in this study were Basal-like 1 (BL1); Basal-like 2 (BL2), Mesenchymal-stem-like (MSL); Mesenchymal (M) and Luminal Androgen Receptor (LAR) (Elsawaf *et al*., 2013, Lehmann *et al*., 2011) .To-date the sub-classification of TNBC tumours is a topic of debate.[Diagram was created on Microsoft PowerPoint, 2010; Msibi, 2015]

1.1.2.3 Epidemiology and risk factors for Triple negative breast cancer

1.1.2.3.1 Racial disparities

It has been reported that TNBC is more prevalent in young black women compared to women of other races (Swede *et al*., 2011, Galukande *et al*., 2014). Stead and colleagues published data, collected from 415 female patients with invasive BC between 1998 and 2006(Stead *et al*., 2009). This study consisted of an ethnically diverse population. It was observed that TNBC constitutes 20% of all tumours and 64% of these were tumours obtained from pre-menopausal black patients (age less than 50 years). The Clinical Breast Care Project (CBCP) studied the racial disparities between African American women (AAW) and Caucasian women (CW) with BC (Sturtz *et al*., 2014). It was found that TNBC diagnosis was significantly higher in AAW (28%) compared to CW (12%) (Sturtz *et al*., 2014). Most epidemiological studies on the disease have been conducted in the Western and European countries.

Hitherto only two BC subtype studies have been published in SA. McCormack and colleagues examined the BC characteristics of 1,092 patients who attended Chris-Hani Baragwanath Hospital (CHBH), between 2006 and 2012(McCormack *et al*., 2013). From a racially diverse population they observed that TNBC was most prevalent in black women. The data is comparable to that obtained from USA based studies. Although informative, this study was limited to patients attending CHBH. A larger study with 10,047 BC patients from SA and Namibia was conducted between 2011 and 2013(Dickens *et al*., 2014a). The data concurred with others, that is, TNBC is more prevalent in black women and statistically it represents 17.4% - 21.9% of all BCs (Dickens *et al*., 2014a).

In other sub-Saharan countries epidemiological studies are few and small (Sayed *et al*., 2014, Eng *et al*., 2014). This emphasises the need for extensive epidemiological data collection in SA, as well as the rest of the sub-continent.

1.1.2.3.2 Genetic risk factors

Genomic instability and mutation is an enabling hallmark of tumorigenesis (Hanahan and Weinberg, 2011). Mutations in the genes enhance the susceptibility of cancer. Certain gene mutations are associated with particular cancers. The breast cancer susceptibility (BRCA) gene is a well-known BC gene. It's been reported that women with a BRCA1 mutation have a more than 50% chance of development of TNBC (Zhang *et al*., 2012, Haiman *et al*., 2011). In the Hellenic Cooperative Oncology Group study (HCOG), it was found that, that there were 65 deleterious BRCA1 mutations among the 403 TNBC patients that participated (Fostira *et al*., 2012). Additionally when the age at onset of the disease was considered, BRCA1 carriers increased dramatically with some 27% of women with TNBC diagnosed at or before the age of 50, whilst 36% diagnosed at or before the age of 40 had a BRCA1 mutation (Fostira *et al*., 2012). A report on similar observations was provided in a cohort of 469 TNBC patients (70% Caucasian and 19% AAW), 31% of the group had a BRCA1 and BRCA2 mutation (Greenup *et al*., 2013). When age at diagnosis was taken into account, the likeli-hood of carrying a BRCA1 or BRCA2 mutation increased (Greenup *et al*., 2013).

Couch *et al*. assessed the frequency of mutation in 17 BC predisposition genes among 1.824 TNBC patients when unselected for family history (Couch *et al*., 2015). Across the cohort, 14.6% of women had at least 1 deleterious gene mutation, predominantly BRCA1,

identified in 8.5% and BRCA2 identified in 2.7 % (Couch *et al*., 2015). Sporadic TNBC cases with BRCA1/2 mutations were strongly associated with younger age (Couch *et al*., 2015). Furthermore the study discovered that the 15 other mutations were present at varying degrees in 3.7% of the women (Couch *et al*., 2015). The most frequent after BRCA1/2, were mutations in the Partner and Localizer of BRCA2 (PALB2) gene found in 21 patients (1.2%) (Couch *et al*., 2015). The Couch study concurs with the HCOG study as 38 % of mutations were found in women younger than 40 and the presence of mutation was associated with diagnosis at a significantly young age.

In view of the high prevalence of TNBC in women of African ancestry than of European ancestry, genetics researchers have undertaken the task to discover gene susceptibility loci for this subtype of BC. A Meta-analysis of genome-wide association studies (GWAS) of ER negative BC in a mixed population of African and European ancestry identified a novel TERT-rs10069690 SNP in chromosome 5P15 for TNBC risk; however, allele frequency of rs10069690 was greater in women of African than of European ancestry (Haiman *et al*., 2011). The data was confirmed in the Black Women's Health Study (BWHS) in which only AAWs were examined (1199 cases and 1948 controls) (Palmer *et al*., 2013). While the functional significance of the findings are unknown, the results do however support a genetic cause of TNBC that might partly contribute to racial or ethnic origin differences in the incidence of the disease (Palmer *et al*., 2013).

1.1.2.3.3 Reproductive risk factors

Reproductive factors are among the earliest and most well established BC risk factors. However, there are a few studies that evaluate the effects of these factors on the risk of

developing any one of the BC subtypes. It has been shown that early parity correlates with a reduced risk of TNBC and an increase in the overall survival of the patients (Ma *et al*., 2010, Li *et al*., 2013). It has also been reported that longer duration of breastfeeding has protective effects on TNBC (Li *et al*., 2013, Sturtz *et al*., 2014, Ma *et al*., 2010).

The use of oral contraceptives (OC) has been associated with an increased risk of TNBC. Rosenberg and colleagues conducted a prospective follow-up study of the BWHS and found that the use of OCs caused a 2.5 fold increase in the risk of TNBC (Rosenberg *et al*., 2010). Others report that longer duration of contraceptive use caused an increase risk, compared to women who had never used OCs (Dolle *et al*., 2009, Beaber *et al*., 2014, Li *et al*., 2013). However, Turkoz and colleagues conducted a cross-sectional retrospective study with 2005 women and discovered that OC, hormone replacement therapy and *in vitro* fertilisation had no significant impact on TNBC outcome and survival, regardless of menopausal status (Turkoz *et al*., 2013).

A great deal of research on the effects of reproductive factors and their association with TNBC development and patient prognosis must be undertaken, in order to prevent, treat and manage the disease effectively (discussed further below).

1.1.2.3.4 Anthropometric risk factors

Research has shown that women with a higher body mass index (BMI) are at a greater risk of developing BC. It is thought that the association appears to be driven by distinct molecular mechanisms which are based on a woman's menopausal status (Pierobon and Frankenfeld, 2013). In post-menopausal women, upper body obesity is associated with the

risk of developing BC. The same cannot be conclusively stated about pre-menopausal women (Pierobon and Frankenfeld, 2013). Clinically post-menopausal women often present with a less aggressive phenotype and with oestrogen dependent tumours, which are most likely driven by steroidal hormones produced by the adipocytes (Rose and Vona-Davis, 2010).On the other hand, pre-menopausal women who develop BC often present with more aggressive tumours that are hormone-independent (Rose and Vona-Davis, 2010).

Evidence to suggest that obesity is associated with TNBC is contradictory. A retrospective study which included 448 TNBC patients found that a higher BMI was more prevalent among AAWs, however there was no significant difference associated with the disease within the three (normal weight, overweight and obese) BMI groups with regards to age at diagnosis, menopausal status or pathological tumour stage or grade (Tait *et al*., 2014). Similar findings were observed by Dawood and colleagues, where overweight and obese women were predominantly AAW and their height, weight and waist-to-hip ratio were not associated with TNBC (Dawood *et al*., 2012). Moreover a prospective study showed that higher BMI is mostly associated with AAWs (Mowad *et al*., 2013). Although obese patients had presented with significantly larger tumours and higher T-stage, recurrence and death were not significantly different among the three BM1 groups that were assessed (Mowad *et al*., 2013).

Contradictory to the above mentioned studies, the retrospective study by Turkoz and colleagues showed that overweight and obese pre-menopausal women had a significantly higher risk of developing TNBC (Turkoz *et al*., 2013). Another population based case

control study which analysed the BMI change of women from the age of 18-44 years demonstrated that obesity was associated with increased risk of TNBC among parous women only (Kawai *et al*., 2014).

In a meta-analysis, in which 11 studies were examined, it was discovered that the association between TNBC and obesity is dependent on menopausal status (Pierobon and Frankenfeld, 2013). In pre-menopausal women a BMI of 30 or more resulted in a significant increase risk of developing TNBC; however, in post-menopausal women the same BMI did not increase the risk (Pierobon and Frankenfeld, 2013). Looking at the studies overall, it is clearly necessary to undertake further research on the role of anthropometry and its role in TNBC development together with overall patient survival. Moreover further investigations are needed to evaluate the molecular mechanisms that link obesity and its relationship with TNBC.

1.1.2.3.5 Socioeconomic status risk factors

Socioeconomic status (SES) is intrinsically linked with lifestyle behaviours, including physical activity, diet, reproductive experiences, such as having more children and screening behaviours, which vary in prevalence across different populations of women(Brewster *et al*., Dunn *et al*., 2010) . It has been shown that women with lower income brackets are often black and they generally tend to have more children than women from more affluent backgrounds (Davies *et al*., 2013, Sineshaw *et al*., 2014, Shariff-Marco *et al*., 2014). Also their survival outcome after cancer treatment is lower than that of women from a higher income bracket (Shariff-Marco *et al*., 2014).

In a cohort of 1,000 women, it was discovered that of BC patients diagnosed at CHBH, those who lived farther away and whom were from low income brackets presented with late stage BC diagnosis, compared to their wealthier counterparts (Dickens *et al*., 2014b). Further it was seen that other contributing factors that resulted in delayed diagnosis included a lack of education concerning where to go to seek help, poor knowledge of symptoms, lack of breast awareness, fear and beliefs held on the causes of cancer and whether it is curable (Dickens *et al*., 2014b). Internationally it has been shown that in general women from poor backgrounds or rural areas are most likely to present with more aggressive forms of BC, due to lack of access to healthcare (Davies *et al*., 2013, Seneviratne *et al*., 2015, Newman *et al*., 2006). In terms of studies concerning the effect of low SES on the disease, data from the California Cancer Registry showed that irrespective of race or ethnic origin, women living in areas of low SES were more likely than women living in areas of high SES to be diagnosed with TNBC than any other type of BC (Parise and Caggiano, 2013).

These observations may be one of the contributing factors as to why TNBC is mostly prevalent in women AAWs and other African women in other countries.

1.1.3 Current and novel treatment options

At present there are no Food and Drug Administration (FDA) approved drugs for the treatment of BC (Andre and Zielinski, 2012). Currently, surgery, radiation and chemotherapy are the only treatment options available (Yagata *et al*., 2011), however, some challenges remain (see Figure 1.2). Although chemotherapy is associated with a complete pathological response in some patients, other patients do not respond and may

relapse often resulting in worse overall survival (Gluz *et al*., 2009, Cortazar *et al*., 2014). Population based studies on TNBC have shown that the disease is more aggressive than other forms of BC(Lee *et al*., 2014, Yagata *et al*., 2011). These studies have also shown that there is a higher risk of recurrence within the first three years after initial treatment and that the majority of deaths occur within the first five years (Dent *et al*., 2007, Bayoumi *et al*., 2014, Solin *et al*., 2009, Pogoda *et al*., 2013) (Table 1.2).

Table 1.2: Clinical characteristics of the Triple Negative Breast Cancer phenotype (as described by (Dent *et al*., 2007).

Often present as interval cancers
Rapid rise in risk of recurrence following diagnosis
Distal recurrence rarely preceded by local recurrence
Increased mortality rate in the first 5years
Rapid progression from distant recurrence
Weak relationship between tumour size and node status
Peak risk of recurrence at 1-3 years
Local recurrence not predictive of distal recurrence
Majority of deaths occur in first 5 years

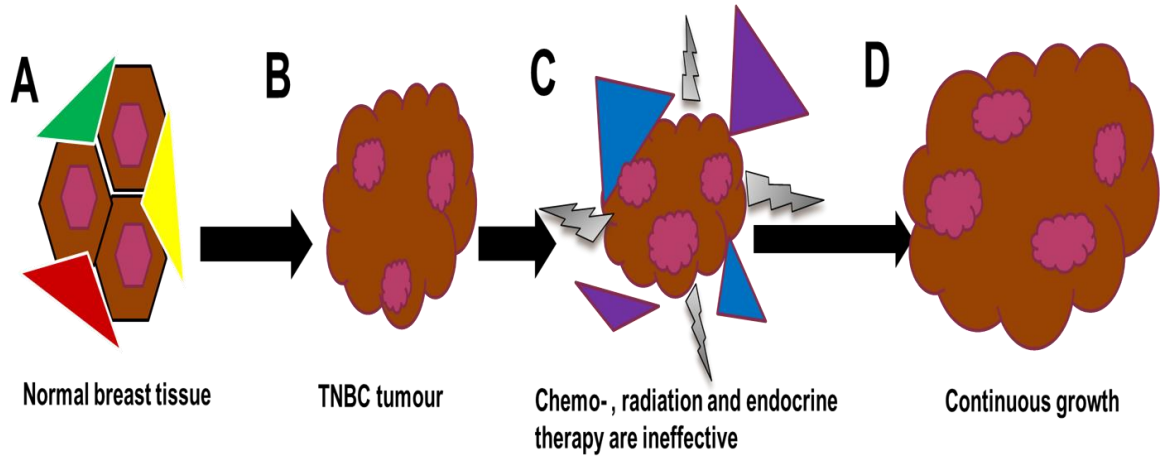


Figure 1.2.Schematic representation of a TNBC tumour; the current challenge in its treatment and management. **A)** The normal breast tissue expresses oestrogen receptors (ER, green), progesterone receptors (PR, yellow) and human epidermal growth factor-2 receptors (HER-2, red). **B)** A TNBC tumour lacks the expression of the hormone receptor and the growth factor receptor. **C)** Endocrine (mauve), radiation (silver) and chemo (blue) therapy are ineffective in tumour treatment. **D)** Ineffective treatment leads to continuous growth. [Diagram was created in Microsoft PowerPoint, 2010; Msibi, 2014].

There are many obstacles encountered in the treatment and management of TNBC. These include: a lack of targeted therapies, an absence of reliable prognostic and diagnostic markers coupled with a poor knowledge of the mechanism of pathology of the disease (Podo *et al*., 2010). These challenges surrounding TNBC have drawn a lot of attention from cancer researchers. The mission is to discover and develop novel therapeutics to treat and manage the disease effectively.

Novel approaches proposed in the literature include among others, the use of monoclonal antibodies (mAb), targeting of angiogenesis, targeting DNA repair and damage mechanisms , cell signalling pathways and cancer stem cells (CSCs) (Yagata *et al*., 2011, Koziol *et al*., 2012, Aulmann *et al*., 2010, Miki *et al*., 2014) . However, thus far none of these have been particularly successful. This emphasises the crucial need to better understand the mechanisms of TNBC pathogenesis as this will subsequently lead to the development of more effective novel therapeutics. In this regard, it is suggested here that the Notch signalling pathway is worthy of investigation as a potential therapeutic target. The importance of this pathway, and its role in BC development, is described below.

1.1.4 The Notch signalling pathway

The elucidation of the Notch signalling pathway began in 1913 when John Smith Dexter observed that a mutation of a particular gene in *Drosophila ampelophila* resulted in the development of a notch at the end of the fly's wings. Consequently, he called them "perfect Notched". Subsequently, in 1917, Thomas Hunt Morgan identified the alleles of the fly gene now known as *NOTCH*. The gene was eventually cloned and definitively identified during 1985-1986 (Olsauskas-Kuprys *et al*., 2013, Wharton *et al.*,

1985, Kidd *et al.*, 1986). Since then, research has shown that the pathway is transduced via receptor-ligand activation, when neighbouring cells come into contact with one another(Kopan and Ilagan, 2009). The pathway is involved in multiple cellular processes, including cell fate decisions, tissue homeostasis and stem cell maintenance (Takebe *et al*., 2014, Ntziachristos *et al*., 2014, Bolos *et al*., 2007) .

1.1.4.1 The structure of the Notch receptors and their ligands

1.1.4.1.1 Notch receptors

There are four trans-membrane Notch receptors in mammals; these being termed NOTCH1 to 4, (Figure 1.3). The receptors are comprised of 29-36 tandem epidermal growth factor like-repeats (EGF) (Kopan and Ilagan, 2009). Many of the repeats are bound to calcium that determines the structure and affinity of the receptors to its ligand (Chillakuri *et al*., 2012). A negative regulatory region (NRR) that inhibits the activation of the receptor in the absence of a ligand follows the EGF repeats (Olsauskas-Kuprys *et al*., 2013, Chillakuri *et al*., 2012). The NRR region consists of three cysteine-rich Lin12-Notch repeats (LNR) and a heterodimerization domain (HD) (Stanley and Okajima, 2010, Chillakuri *et al*., 2012). Together, the repeats and the NRR form the Notch extracellular component (NEC) (Kopan and Ilagan, 2009, Chillakuri *et al*., 2012).

The Notch intracellular component (NIC) is comprised of the recombination signal binding protein for immunoglobulin kappa j (RBPjk) association module (RAM) domain that contains 12-20 amino-acids (Kopan and Ilagan, 2009). The RAM together with the LNR

and HD form the Notch transmembrane (NTM) domain. RAM is also linked to seven ankyrin (ANK) repeats by a long and unstructured linker containing one Notch localising sequence (NLS) followed by bipartite NLS(Kopan and Ilagan, 2009) . In the NOTCH-1 and NOTCH-2 receptor, these are then followed by an evolutionarily divergent transactivation domain (TAD); this region is however, absent in NOTCH-3 and NOTCH-4 (Kopan and Ilagan, 2009, Chillakuri *et al*., 2012). The TAD is followed by a conserved proline/glutamic acid/serine/threonine-rich motif (PEST) which contains degrons that regulate the stability of NIC (Chillakuri *et al*., 2012) .

1.1.4.1.2 Notch ligands

There are five ligands, including JAGGED 1 to 2 and DELTA-LIKE 1, 3, and 4, all of which are classified as type 1 transmembrane proteins that belong to the Delta-like and Serrate/Jagged families(Stanley and Okajima, 2010). They are characterised by three related structural motifs (Chillakuri *et al*., 2012). The N-terminus consists of a module of an unknown structure that is stabilised by a disulphide bond called Module at the N-terminus of Notch Ligands (MNNL). This module precedes the delta/serrate/lag-2 (DSL) motif, which is followed by specialised tandem EGF repeats known as Delta and OSM-11-like repeats or DOS(Kopan and Ilagan, 2009) . The DOS is followed by calcium binding and non-calcium binding EGF-like repeats; the repeats range in number from 16 (Jagged family) to 5-9 (delta-family). A cysteine rich domain (CRD) which is only present in the Jagged family precedes the EGF repeats. The intracellular component of the ligand is a post synaptic density protein (PSD95), Drosophila disc large tumour suppressor (Dlg1), and zonula occludens-1 protein (zo-1) Ligand (PDZL) domain that is present only

on JAGGED-1 and DELTA-LIKE-1 and 4. This domain facilitates the integration of proteins at the adherens junction to promote cell-cell adhesion and inhibit cell motility.

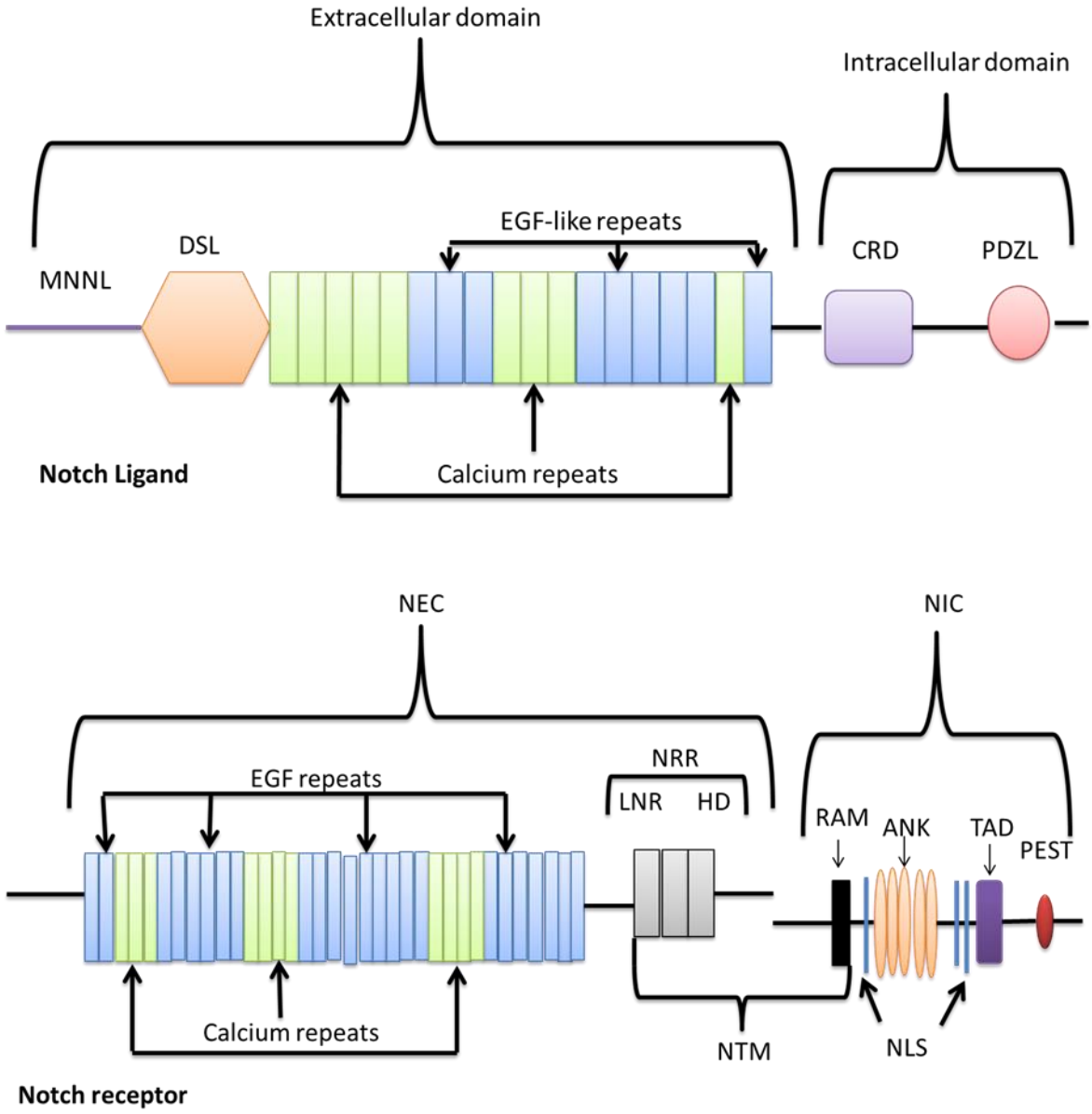


Figure 1.3 Diagrammatic representations of the Notch receptor and Notch-ligand. The extracellular domain of the receptor is comprised of epithelial growth factor like (EGF) repeats and calcium repeats and the negative regulatory region (NRR). The transmembrane domain is composed of the lin12-notch repeats (LNR) and heterodimerization (HD) of the NRR and the RBPjk Association Module (RAM) component of the notch intracellular component (NIC). The intracellular component is comprised of the RAM, ankyrin repeats (ANK), transactivation domain (TAD) and proline/glutamic acid/serine/threonine-rich (PEST) domains. The Notch ligand is comprised of the module at the n-terminus of notch ligand (MNNL) which precedes the delta/serrate/lag-2 (DSL) domain. The domain is preceded by the EGF repeats. These regions all form the extracellular domain of the ligand. The Intracellular domain consists of the cysteine rich domain and the post synaptic density protein (PSD95), Drosophila disc large tumor suppressor (Dlg1), and zonula occludens-1 protein (zo-1) Ligand (PDZL) domain. [Diagram was created on Microsoft PowerPoint, 2010; Msibi, 2015]

1.1.4.1.3 Notch signal transduction

The NOTCH receptors (see Figure 1.3) are derived from large (>300 kD) precursor polypeptides in the rough endoplasmic reticulum (RER) (Figure 1.4). The precursor molecule is subjected to post-translational modifications before reaching maturation. The molecule is glycosylated by *O*-fucose on its EGF repeats. The addition of *O*-linked Fucose is mediated by *O*-fucosyl transferase 1. The NOTCH precursor is then transported to the *trans*-Golgi apparatus by the guanosine triphosphate hydrolase (GTPase) Rab-protein 6. There, the *O*-fucose is extended by the addition of carbohydrate chains on the serine and threonine residues, the elongation is mediated by the fringe family, specifically the β1, 3-N acetylglucosaminyl-transferases Lunatic, Manic or Radical.

The modification by the fringe proteins controls the ligand-mediated activation. The fully modified Notch pre-protein then experiences its first of three proteolytic cleavages in the Golgi. A Furin-like convertase (at site 1) (Figure 1.4) creates the first cleavage at the N and C terminus of the protein which forms the mature NOTCH receptor. The receptor is then transported to the plasma membrane where it interacts with its membrane-associated ligand (Figure 1.4). Upon ligand-receptor engagement, a second cleavage is initiated by a disintegrin metalloproteases 10 and 17 (ADAM 10 and ADAM 17, respectively) (at site 2) (Figure 1.4). which releases the NEC to be trans-endocytosed into the ligand-expressing cell. This then leaves NTM vulnerable to the third and final cleavage by Gamma-secretase (γ-secretase) (at site 3) (Figure 1.4) complex, liberating the NIC. The component is then trans-located into the nucleus where it forms a transcriptional activated complex with the following: DNA-binding factor, C-promoter binding factor-1(CBF-1), a constitutive

transcriptional repressor, a displacing co-repressor and recruiting co-activators such as Mastermind-like (MAML) (Figure 1.4). Formation of these complexes results in the expression of various NOTCH target genes, such as *HES*/*HEY* family genes and *C-MYC*, which are involved in cell growth, differentiation, and survival (Figure 1.4).

Notch activates many genes associated with cell differentiation and/or survival. Following receptor-ligand binding, NIC bound to CBF-1 in the nucleus at the time of receptor activation is marked for proteosomal degradation by the E3 ubiquitin ligases Numb and Itch. The deregulation of this pathway is associated with cancer and developmental disorders.

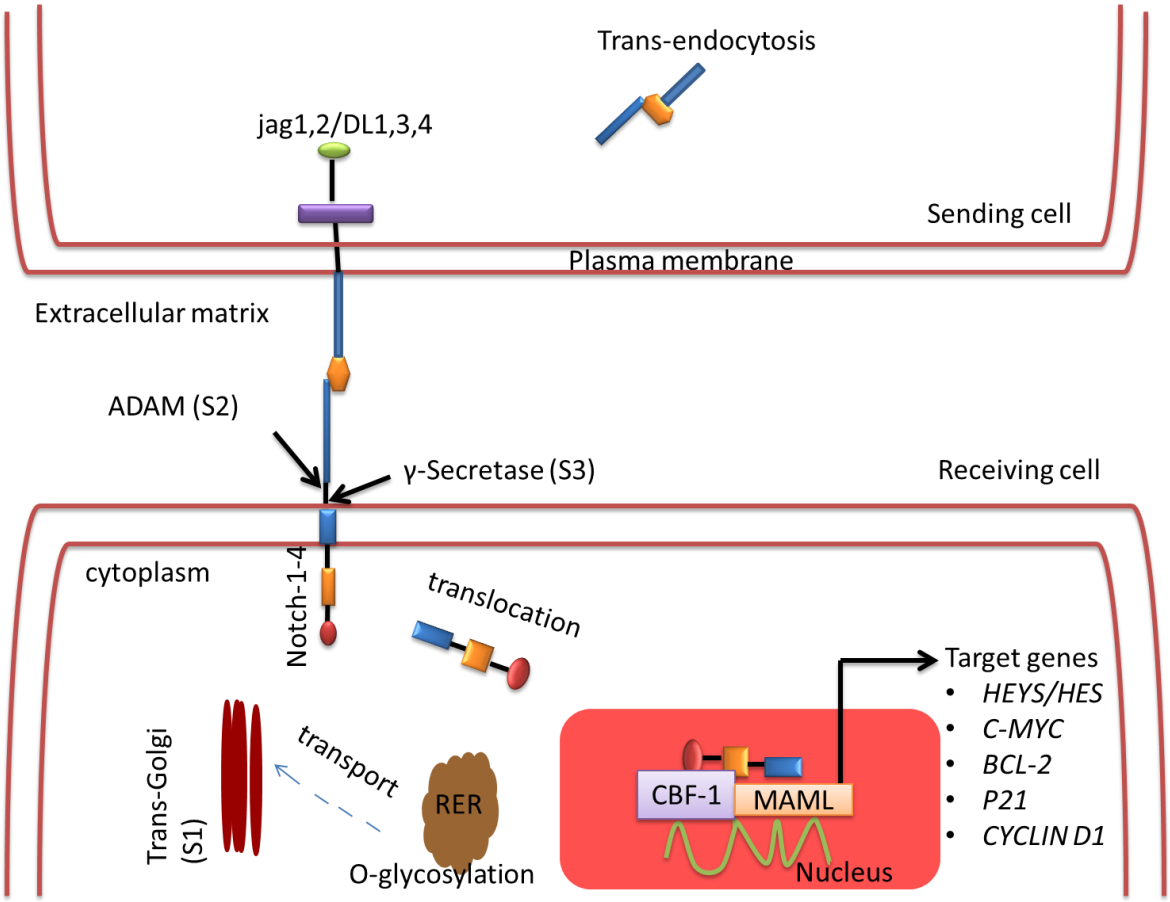


Figure 1.4 A Schematic representation of the Notch pathway. Notch precursor protein is glycosylated in the rough endoplasmic reticulum (RER) and transported to the Golgi-apparatus where it is cleaved by Furin-like convertase (S1). This cleavage results in a mature NOTCH receptor being placed on the plasma membrane where it awaits ligand activation. A Disintegrin Metalloprotease (ADAM) makes the second cleavage causing receptor vulnerability to cleavage by gamma secretase (γ-secretase) (S3). The third cleavage results in the generation of the notch intracellular component (NIC), which is translocated into the nucleus where it binds with C-promoter binding factor-1 (CBF-1), thus repressing or activating target gene expression such as *HEYS/HES;C-MYC;P21;BCL-2;CYCLIN D1* [Diagram was created in Microsoft PowerPoint, 2010; Msibi; 2015].

1.1.5 Notch signalling in breast cancer

The earliest indication that Notch signalling plays a role in human carcinogenesis was observed in 1991 in T-cell acute Lymphoblastic Leukaemia/Lymphoma (T-ALL) (Ellisen *et al*., 1991). It was found that the *NOTCH-1* chromosomal translocation t(7;9)(q34;q34.3), which is responsible for producing NRR, was altered thus causing defects in the signal(Ellisen *et al*., 1991).Subsequently, *NOTCH-1* gain-of-function mutations were discovered in approximately 50% of T-ALL and in other haematologic cancers (Aster *et al*., 2011).Furthermore, aberrant NOTCH signalling has been detected in many solid tumours for example, cervical, colon, liver, lung, pancreatic, prostate, ovarian and renal cancers(Rose *et al*., 2010, Wang *et al*., 2010, Du *et al*., 2012, Yong *et al*., 2011, Gao *et al*., 2014, Theys *et al*., 2013, Shao *et al*., 2012) . Of particular interest here is the function of the Notch signal in BC development.

Evidence that Notch receptors are possible breast oncogenes was first seen in experiments conducted on mice, where activation of NOTCH-1 and NOTCH-4 via mouse mammary tumour virus induced neoplasms. Moreover, the up-regulation of NOTCH-4 resulted in the transformation of mammary epithelium *in vitro* and *in vivo* (Farnie and Clarke, 2007). In humans, the first direct correlation of dysregulated Notch signal and breast malignancy was published by Reedijk *et al*. in 2005 (Reedijk *et al*., 2005).Using immunohistochemistry, the group's findings suggested that high expression of the NOTCH-1 receptor, together with the ligand JAGGED-1, correlated with poor BC prognosis and overall survival. They also noted that the overexpression was more prominent in ER negative tumours than ER positive ones (Reedijk *et al*., 2005). In an independent study by Dickson and colleagues, the expression of miRNAs was evaluated

using *in-situ* hybridisation (Dickson *et al*., 2007). Their findings verified those obtained by Reedijk and colleagues, as they were able to show that high levels of JAGGED-1 correlated with a lower five year survival rate in BC patients (Reedijk *et al*., 2005) . These data were reinforced by Speiser *et al*. (2012) who demonstrated that TNBC tumours express high levels of NOTCH-1 and NOTCH-4. However; their study did not prove that high expression levels of these receptors are correlated with poor clinical outcome (Speiser *et al*., 2012). The limitation of their study was a small sample size of 50 tumours.

Research on NOTCH-2 and NOTCH-3 is scarce, with approximately two studies that directly investigated the role of NOTCH-2 in human BC and only one study that investigated NOTCH-3. In 2004, Parr *et al.* suggested that NOTCH-2 activation increased tumour survival and that tumours expressing higher levels of this receptor were well differentiated compared those that expressed NOTCH-1(Parr *et al*., 2004). The tumour xenografts from ER negative cells displayed slowed growth when NOTCH-2 was up-regulated (O'Neill *et al*., 2007). These data imply that NOTCH-2 is a tumour suppressor gene in the breast.

Yamaguchi and colleagues reported that in HER-2 negative BC cell lines, down-regulation of NOTCH-3 resulted in suppressed proliferation and increased apoptosis (Yamaguchi *et al.*, 2008). Evidently, Notch signal activation appeared to be a "double edged sword" where it can either exert oncogenic or tumour suppressive effects depending on the receptor that is activated (Capaccione and Pine, 2013, Roy *et al.*, 2007, Lobry *et al*., 2014). However, the role that the Notch signal plays within each BC subtype remains unclear since most of the available data relates to ER positive BC. Moreover, the relationships

between ER, PR, HER-2 and Notch are uncertain as data is limited. It has however been suggested that oestrogen plays a role in the regulation of Notch signalling.

This notion was extrapolated from a study by Rizzo *et al.* (2009) (Rizzo *et al*., 2009). They reported that oestrogen deprivation of the ER positive cell line Michigan Cancer Foundation – 7 (MCF7) resulted in increased NOTCH-1 activity (Rizzo *et al*., 2009). Osipo *et al.* (2008) demonstrated that HER-2 overexpressing cells had low Notch transcriptional activity compared to HER-2 negative cells (Osipo *et al*., 2008). Subsequently, in 2009, Korkaya and Wicha suggested the following concerning the relationship between HER-2 overexpression and Notch pathway activity (Korkaya and Wicha, 2009):

1. The HER-2 promoter contains Notch binding sequences
2. HER-2 overexpressing cells display activated Notch signal
3. Inhibition of the Notch signal using an siRNA or γ-secretase inhibitors results in the down-regulation of HER-2 expression, resulting in decreased mammo- sphere formation

In the same year, Graham *et al.* (2009) demonstrated that in normal breast cells, progesterone increased the expression of DELTA-LIKE 1 and 3 ligands which showed that a lack of progesterone may decrease the activity of the Notch pathway(Graham *et al*., 2009). Other factors that may influence Notch pathway activity include hypoxia and cross talk with other pathways such as WNT, Sonic hedgehog and Ras(Kikuchi *et al.*, 2011, Han *et al*., 2011). Taken together, the literature shows that aberrant Notch signalling has tumourigenic effects on the breast, and that additional data is required in order to

understand its function in TNBC. Supplementary data may add to the rationale to target Notch signal as a therapeutic strategy in treating TNBC, as this cancer currently lacks FDA approved agents.

1.1.6 Strategies to target Notch signal pathway in Triple negative breast cancer

As there is a lack of targeted therapeutic agents for treating TNBC, and that there is strong evidence suggesting that the aberrant Notch signalling pathway is a key event in the aetiology of BC, targeted therapies aimed at modulating the pathway in TNBC are emerging. In 2008, Rizzo, *et al.* rationalised targeting the pathway based on the reasons mentioned below:

- Firstly, as the cascade is triggered by a receptor-ligand interaction that does not require an enzymatic amplification step, the "signal intensity" can be modulated very precisely by cellular regulatory mechanisms. Therefore, the downstream effects of Notch activation are exquisitely dose dependent (Rizzo *et al.*,2008b) . Furthermore, complete shutdown of the pathway may not be necessary to achieve a therapeutic effect.
- Secondly, the intracellular half-life of the active form Notch is generally very short and-
- Thirdly, the effects of Notch are remarkably context dependent as each receptor exerts a different effect on the breast cells.

There are three main strategies to modulate the signal proposed as treatment options in TNBC, including the administration of mAbs, short interfering RNAs (siRNA) and γ-

secretase inhibitors (GSI) (see Figure 1.5); and each of these approaches are explained below.

1.1.6.1 Notch1 and Delta-like 4 monoclonal antibodies

The overexpression of NOTCH receptors and ligands makes mAb therapy an attractive treatment option, as they are effective in eliminating tumour cells and have a low toxicity profile (Shuptrine *et al*., 2012). Furthermore, mAbs are designed to target tumours through specific or associated antigens, without the need for hepatic metabolism. An ideal example of a successful mAb in BC therapy is Trastuzumab which is administered to patients with ER positive BC, in combination with chemotherapy. Attempts to address the potential use of Notch mAbs have been made by a few research groups.

Qui and collegues, developed neutralising antibodies against human NOTCH-1(Qiu *et al*., 2013). They found that inhibiting the pathway with mAbs resulted in decreased expression of NOTCH-1 signal target genes in ER negative BC cells (Qiu *et al*., 2013). They also reported that blocking the signal enhanced the anti-tumour efficacy of Docetaxel. Sharma and colleagues characterised and determined the effects of several mAbs on ligand binding and consequent receptor activation (Sharma *et al*., 2012). They observed that a mAb specific to the EGF repeats 11 to 12, appeared to be the most effective in inhibiting JAGGED-1 and DELTA-LIKE-4 binding to the NOTCH-1 receptor (Sharma *et al*., 2012). Subsequently, these antibodies reduced the CSC population present in BC cell lines, as well as the expression of NOTCH-1 target genes. Since breast tumours co-express NOTCH receptors, mAb therapy is highly attractive, as a specific receptor and/or receptors may be

targeted effectively, eliminating the need to "shut down" the entire pathway. Currently, the use of Notch mAbs for the treatment of TNBC has not been used in clinical trials.

1.1.6.2 Notch-1 siRNA

RNA interference (RNAi) is an evolutionary conserved post-transcriptional gene-silencing pathway that was first discovered in the nematode (Fire *et al*., 1998). It may be modulated by double stranded RNA (dsRNA) molecules which are 21-23 nucleotides in length, and are referred to as short interfering RNAs (siRNAs) (Karagiannis and El-Osta, 2005) . Briefly, double stranded (dsRNA) is cleaved into siRNAs by the enzyme dicer and its associated proteins. One strand, the guide strand, is integrated into the RNA induced silencing complex (RISC), whereas the other strand is subjected to degradation. The guide strand binds to a complementary mRNA which triggers its degradation by RISC.

The siRNAs are designed to interfere with the expression of specific genes, to ultimately knock-down gene expression. The knock-down of *NOTCH-1* or *NOTCH-4* has strong anti-proliferative effects in BC cell lines (Rizzo *et al*., 2008a). Zang and colleague reported that down-regulating the expression of the NOTCH-1 receptor results in an increase in chemo-sensitivity (Zang *et al*., 2010). These results show that siRNA may be a promising target for BC treatment. However, the tissue and organ specific delivery; of siRNAs remains a challenge. The central considerations include chemical modification and delivery strategy; and here as appropriate chemical modifications help siRNA duplexes avoid immune-stimulation and allow them to withstand degradation from nucleases. However, efficient and tissue specific delivery may be the biggest challenge in the application of siRNA to

humans. To date, there are no clinical trials that have utilised *NOTCH* siRNAs in BC patients.

1.1.6.3 γ-Secretase inhibitors

γ-secretase is an intramembrane aspartyl protease with a molecular weight of approximately 230 kiloDaltons (Wolfe, 2009, Lu *et al*., 2014). This is composed of four subunits those are: Nicastrin, presenilin enhancer 2 (PEN2); presenilin; and anterior pharnx-defective 1(APH1) (Golde *et al*., 2013). It cleaves more than 30 type 1 transmembrane proteins within their membrane spanning regions (Lu *et al*., 2014, Tolia and De Strooper, 2009) and these cleaved products serve as signalling molecules. This process is known as regulated intramembrane proteolysis (RIP) (Lu *et al*., 2014). Two of its most extensively studied substrates are the amyloid precursor protein and the NOTCH receptors (Lewis *et al*., 2003, 2014, Kim *et al*., 2004). Other substrates include HER-2, epithelial cadherin (E-cadherin), Neural cadherin (N-cadherin), CD44, Nectin-1 and the low density lipoproteins receptor (Wolfe, 2009). In the Notch pathway, it participates in the final cleavage of the NOTCH receptor resulting in a NIC which is translocated to the nucleus where it activates target gene expression (see Figure 1.4). Inhibiting this cleavage step with small molecules could prove beneficial as it has previously been demonstrated that targeting Notch with GSI suppressed survivin levels, induced apoptosis, abolished colony formation of BC cells on soft agar and inhibited metastatic tumour growth in mice (Lee *et al*., 2008b). Furthermore, other studies have shown that cell proliferation decreases with GSI treatment in ER negative cell lines (Han *et al*., 2009, McClements *et al*., 2013, Wang *et al*., 2010).

GSIs are divided into the following three classes: peptide isosteres, azepines and sulphonamides. They may further be classified as Type 1 and 2 depending on their structure and binding site (Olsauskas-Kuprys *et al*., 2013). Type 1 GSIs are transition-state analogues, peptide isosteres that mimic the transition state of a substrate's cleavage by γ-secretase and competitively bind to the catalytic active site of presenilins (Olsauskas-Kuprys *et al*., 2013). Type 2 GSIs are small non-transitional-state inhibitory molecules that bind non-competitively to a site other than the active site, possibly at the interface of the γ-secretase complex dimer (Olsauskas-Kuprys *et al*., 2013). These inhibitors target all four NOTCH receptors, as well as other substrates; these side interactions may result in gastrointestinal toxicities (Takebe *et al*., 2014, Espinoza and Miele, 2013). However, it has been shown that glucocorticoid administration protects against GSI-induced gut toxicity, as they antagonise the effects of NOTCH receptor inhibition in the intestinal epithelium. Thus combining GSIs and glucocorticoids may improve the safety of GSIs when treating human cancers (Wei *et al*., 2010) .

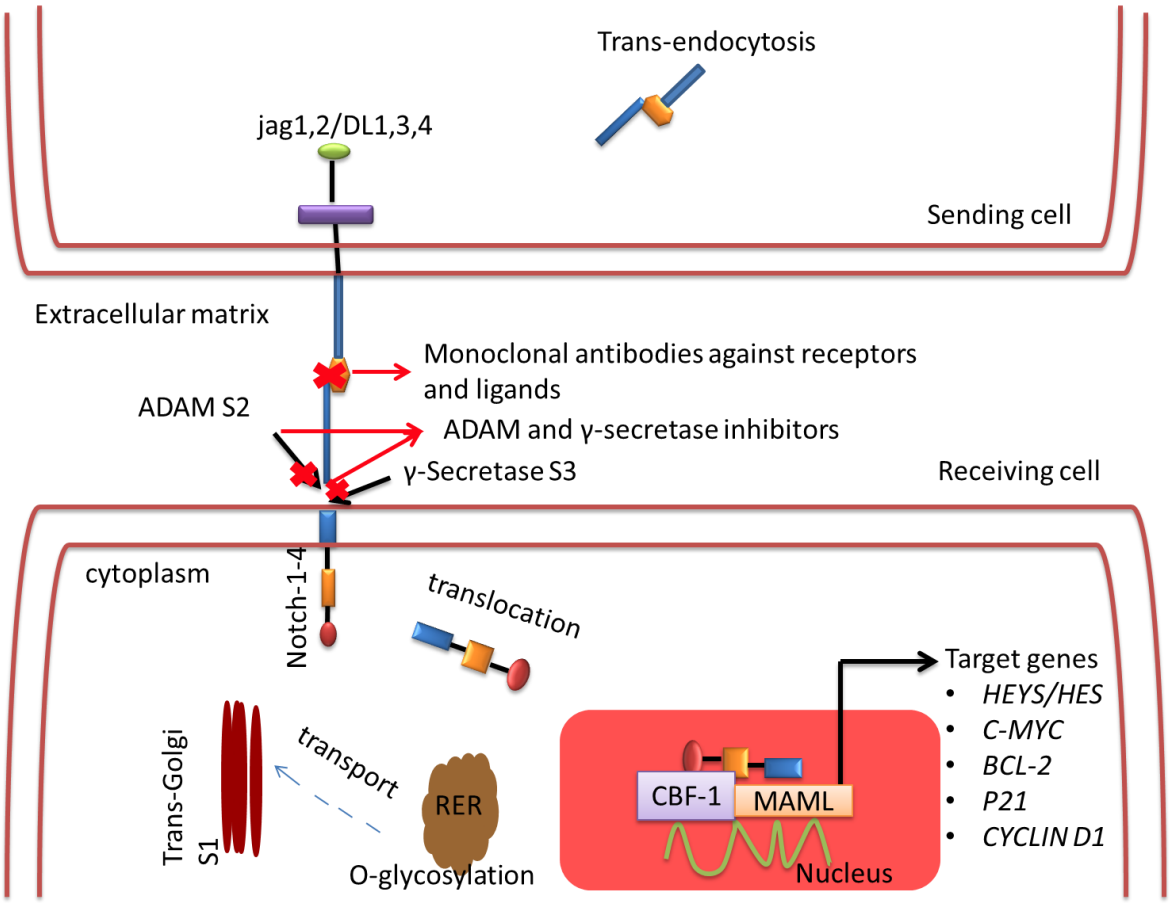


Figure 1.5 Potential Therapeutic targets for Notch in Triple negative Breast cancer. . The pathway may be targeted by either: inhibiting receptor-ligand binding with monoclonal antibodies, which would prevent activation of specific genes depending on which of the four receptors or five ligands are targeted. Site2 (S2) may be blocked with mAb; siRNA. Site (S3) may be inhibited with gamma secretase inhibitors. [Diagram was created on Microsoft Powerpoint 2010 (Msibi, 2015)].

1.2 Experimental approach and rationale

In view of the current literature on the Notch signal pathway and its association with TNBC, it is valid to further investigate its effects on the manifestation and progression of the disease.

Differences between Notch signalling in TNBC and Notch signalling in receptor positive BC since as mentioned earlier majority of the research has been aimed at receptor positive BC and there is also the thought that absence of oestrogen intensifies the signal. The methodological approach applied in this study is briefly discussed below.

1.2.1 Experimental approach

To interrogate the effects of the pathway on TNBC, an *in vitro* approach will be employed. Receptor negative cells that represent TNBC will be evaluated in comparison with receptor positive cells which represent hormone sensitive BC. The receptor positive cells are treated as the control group while the receptor negative group is treated as the experimental group.

1.2.1.1 Notch pathway inhibition

The pathway will be evaluated by inhibiting the pathway with pharmacological inhibitors N-(N-3,5-Diflurophenacetyl-L-alanyl)-S-phenyl glycine t-Butyl Ester (DAPT) and N-[(1S)-2-[[(7S)-6,7-Dihydro-5-5methyl-6-oxo-5H-dibenz[b,d] azepin-7-yl]amino-1-methyl-2-oxoethyl]-3,difluorobenzeneacetamide (DBZ). Although both are classified as an azapines, they represent a non-transitional state analogue and a transitional state analogue (a competitive and non-competitive inhibitor) respectively.

1.2.1.2 Cellular proliferation and viability

The effects of Notch pathway inhibition on cell proliferation and viability of the cell lines, in response to pharmacological inhibition will be evaluated by cell impedance assays, using the xCELLigence (Roche Diagnostics, ACEA Biosciences Inc., USA) real time cell analyses (RTCA), hereafter referred to as xCELLigence assays.

The xCELLigence (Roche) instrument is a microelectronic biosensor system that monitors cell behaviour in real time, by measuring the resistance which is conferred by cells as they attach and spread on electronic plates (E-plates). The E-plate consisting of 16 individual wells has gold electrodes at the base of each well, that sense resistance. This resistance is referred to as impedance, which is defined as the measure of the total opposition to the electric current flow in an alternating current circuit, made up of two components: the *ohmic* resistance and reactance (Figure 1.6). To quantify the status of cells based on impedance, a parameter termed the Cell Index (CI) is derived according to the equation: CI = max (R_{cell} (f_i) / $R_b(f_i)$ – 1) i= 1,….N; where $R_b(f)$ and R_{cell} represents the frequency-dependant electrode resistances with cells and without cells respectively; and N represents the number of the frequency points at which the impedance is measured. Thus the CI is a quantitative measure of the overall status of the cells in a particular well, wherein an increase in the number of cells that attach and spread on the electrode surface confers an increase in the CI. There are several advantages of this technology compared to so-called end-point assays (see Figure 1.6 below):

That it is a label-free detection system, resulting in minimal interference with normal cell function.

Since measurement is read in real time, the physiological effects of any compound can be assessed immediately as compared to an end-point assay, where cells are usually harvested and results are read after a certain amount of hours (Figure 1.7).

It can be used to gather information on different cellular processes, such as, cell proliferation, migration, compound-mediated cytotoxicity, apoptosis, and real-time detection of viral cytopathic effects, cell adhesion, cell viability and proliferation.

The main disadvantage of this system is that it expensive and thus other simple assays are applied to first optimise compound concentrations. In the present study the alternative assay used to test drug concentrations was the Trypan Blue (TB) exclusion dye assay - a classical end-point assay (see Figure 1.7 below).

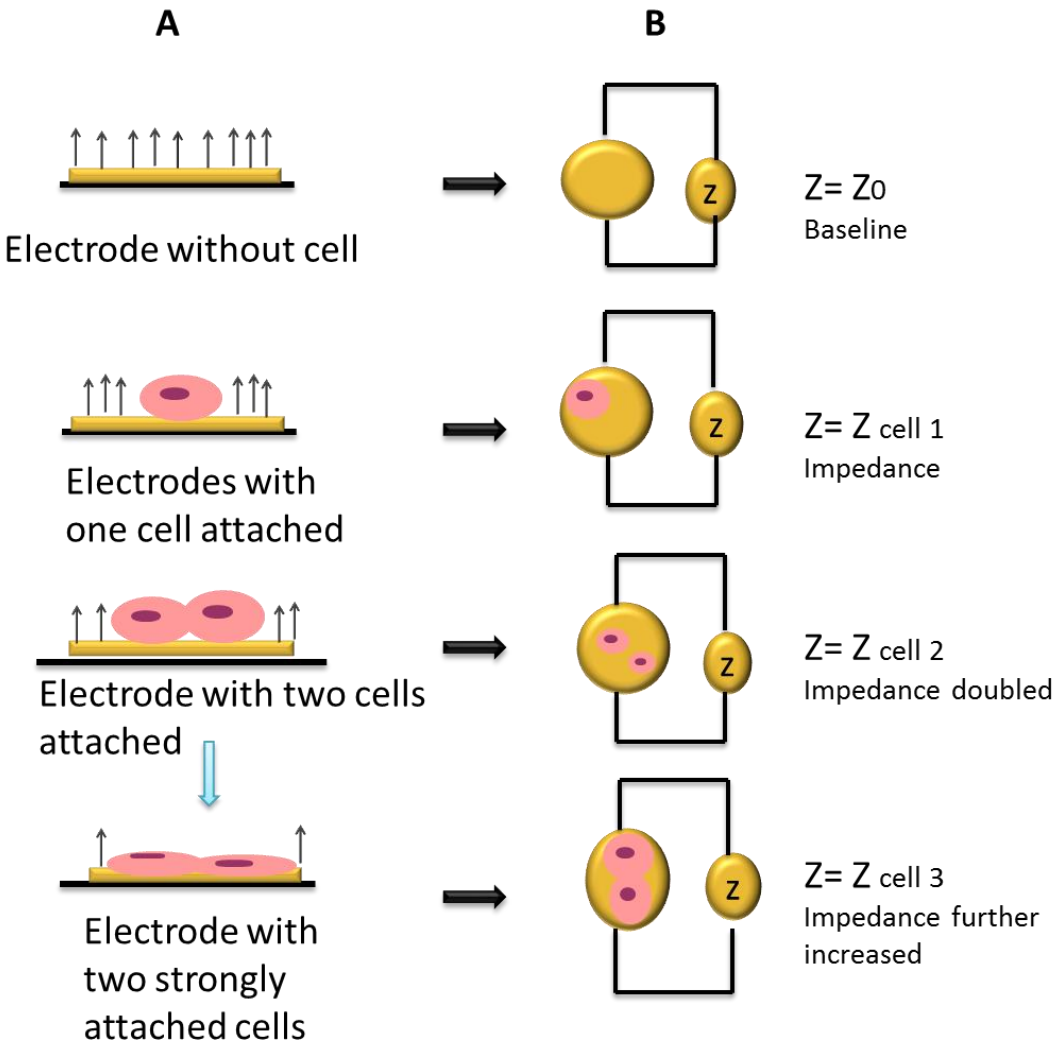


Figure 1.6 A diagrammatic representation of the cell-electrode interaction in an E-plate. Impedance increases as cells attach and divide. Panel **A)** as there are no cells attached to the gold electrode there is therefore no resistance to the electrical current (arrows) flowing through the electrode. As one cell attaches, the current decreases; and as two cells attach and spread there is a further decrease in current. Panel **B)** The impedance (resistance) equals zero as there are no cells attached to the electrode; as a cell attaches the resistance is increased and doubles when two cells attach. The impedance is further increased by the strength of cell attachment to the electrode. [Diagram was created on Microsoft Powerpoint, 2010; Msibi, 2014] and was adapted from *www.Roche.com*.

The TB exclusion assay is a simple and inexpensive test that is used to determine cell viability. TB is impermeable to live cell membranes, a property that is exploited by this assay. The live cells (viable) will exclude the dye, whereas dead cells (non-viable) take it in. Essentially, a cell suspension is produced and cells treated with TB are counted in a haemocytometer viewed under a microscope, allowing for the calculation of the percentage of viable (unstained cells) and non-viable (stained) cells. The TB assay thus provides for an effective test to assess drug concentration in relation to cell viability. A schematic representation of end-point versus real time assays is shown below (see Figure 1.7).

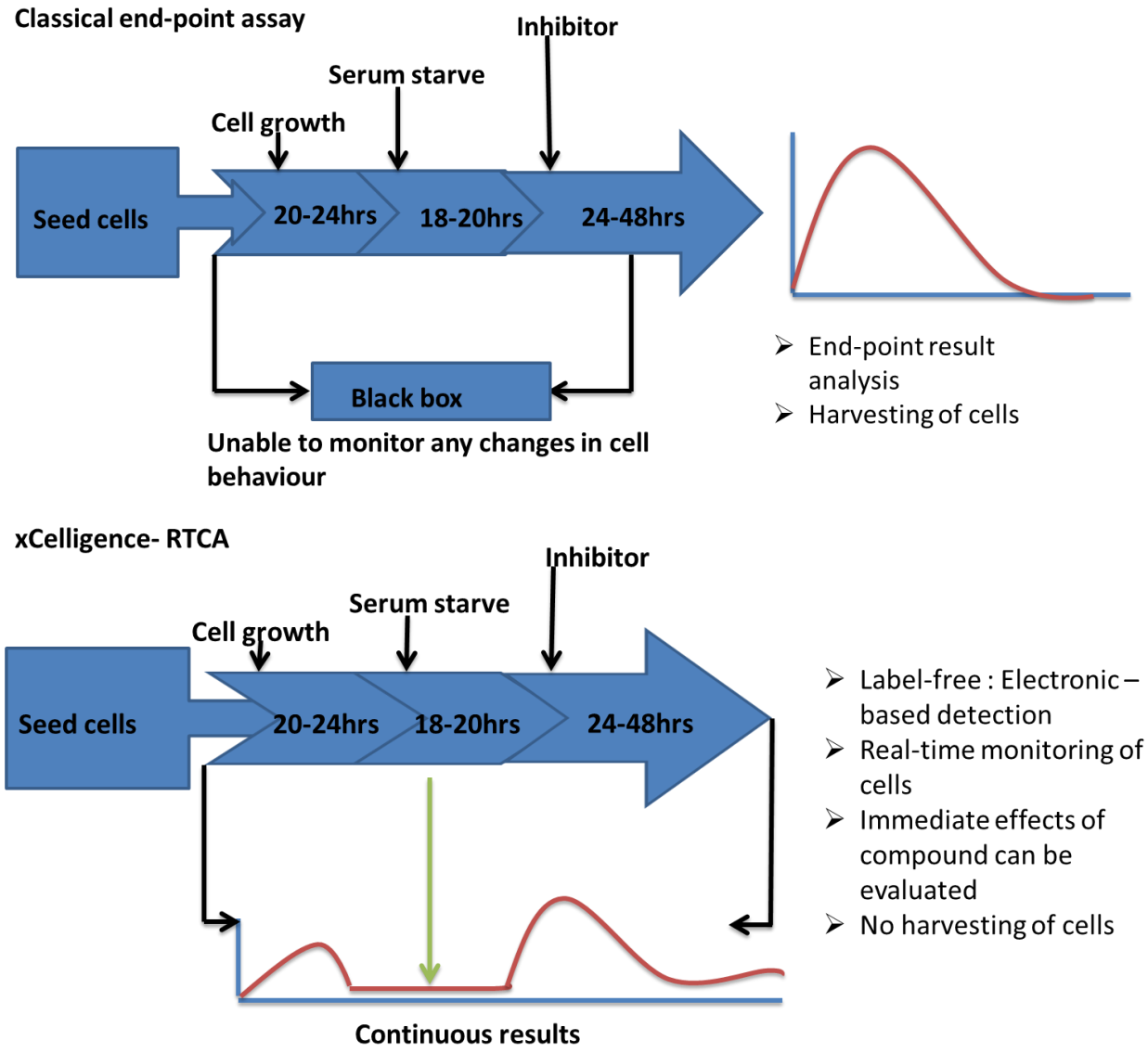


Figure 1.7 Schematic diagrams showing the difference between classical endpoint assay and the xCELLigence RTCA technology. In a classical end-point assay there is a period termed the "black box" in which the physiological effects of the inhibitor can't be monitored or collected. Data is only gathered after cell harvesting. In the xCelligence-RTCA system, there is no "black box", and cells may be monitored and data evaluated in real-time. [Diagrams were created on Microsoft Powerpoint, 2010; Msibi, 2014].

1.2.1.3 Evaluating cell morphology and migration

Morphology and migration will be assessed by fluorescence and immunofluorescence microscopy, specifically by monitoring alterations in the expression of the F-actin cytoskeleton and the cell adhesion protein, E-cadherin. The F-actin cytoskeleton is critical for cell motility, cell division, organelle movement, cell signaling and the establishment and maintenance of cell junctions and cell shape (Doherty and McMahon, 2008). As the cytoskeleton maintains the integrity of the cell its disruption can cause cellular arrest, as well changes in the cell shape can interrupt communication amongst cells (Heng and Koh, 2010). The result is that any pathway that is dependent on paracrine signaling may become aberrant.

E-cadherin is a homophilic cell-to-cell adhesion protein localized to the adherens junctions of all epithelial cells (Kalluri and Weinberg, 2009). Its cytoplasmic domain effectively creates a bridge between the cytoskeleton of adjacent cells by interacting with both cortical actin filaments and the microtubule network (Yilmaz and Christofori, 2009). Amongst its different functions it also serves as a tumor suppressor protein (Baranwal and Alahari, 2009).. Loss of E-cadherin results in invasion and migration therefore in this study the presence of the protein will be used as a marker for migration potential of the cells, that is cells that express the protein should be less invasive than those that do not.

The migration potential of each cell line will be assessed by employing the scratch assay.

1.2.2 Rationale

Determining the effects of Notch signalling on these aspects of cellular function, will provide an insight into the probable role that the signal plays in TNBC tumour progression. Additionally, while it has been shown that oestrogen inhibits Notch activity, there is however little evidence to support this. Investigating the role of Notch inhibition in TNBC versus ER positive BC, would improve our understanding of its functional role in TNBC development. This would allow for the development of novel therapeutics that specifically target the modulatory components of the Notch signalling pathway in patients with TNBC. Here, the potential role of Notch signalling is queried in TNBC and more specifically, its validity as a therapeutic target.

1.2.2.1 Aims and objectives

1.2.2.1.1 Aim

To evaluate the functional role of the Notch signalling pathway in triple negative (hormone insensitive) breast cancer cell lines.

1.2.2.1.2 Objectives

1. Profile the cellular growth of the hormone sensitive Michigan Cancer Foundation – 7 (MCF7) breast cancer cell line, relative to the hormone insensitive M.D Anderson- Metastatic Breast -231 (MDA-MB-231) and M.D Anderson-Metastatic Breast-436 (MDA-MB 436) cell lines, using cell impedance assays.
2. Determine the effects of pharmacological inhibition on cell growth patterns in the aforementioned cell lines, using cell impedance assays
3. Determine the protein expression of NIC and E-cadherin pre- and post-pharmacological inhibition of the Notch signal.
4. Determine the effects of Notch signal inhibition on cell migration using scratch assays.
5. Determine the effects of Notch signal inhibition on the F-actin cytoskeleton.

CHAPTER 2: MATERIALS AND METHODS

The overall summary of the experimental approach used here is presented in the diagram below (Figure 2.1).

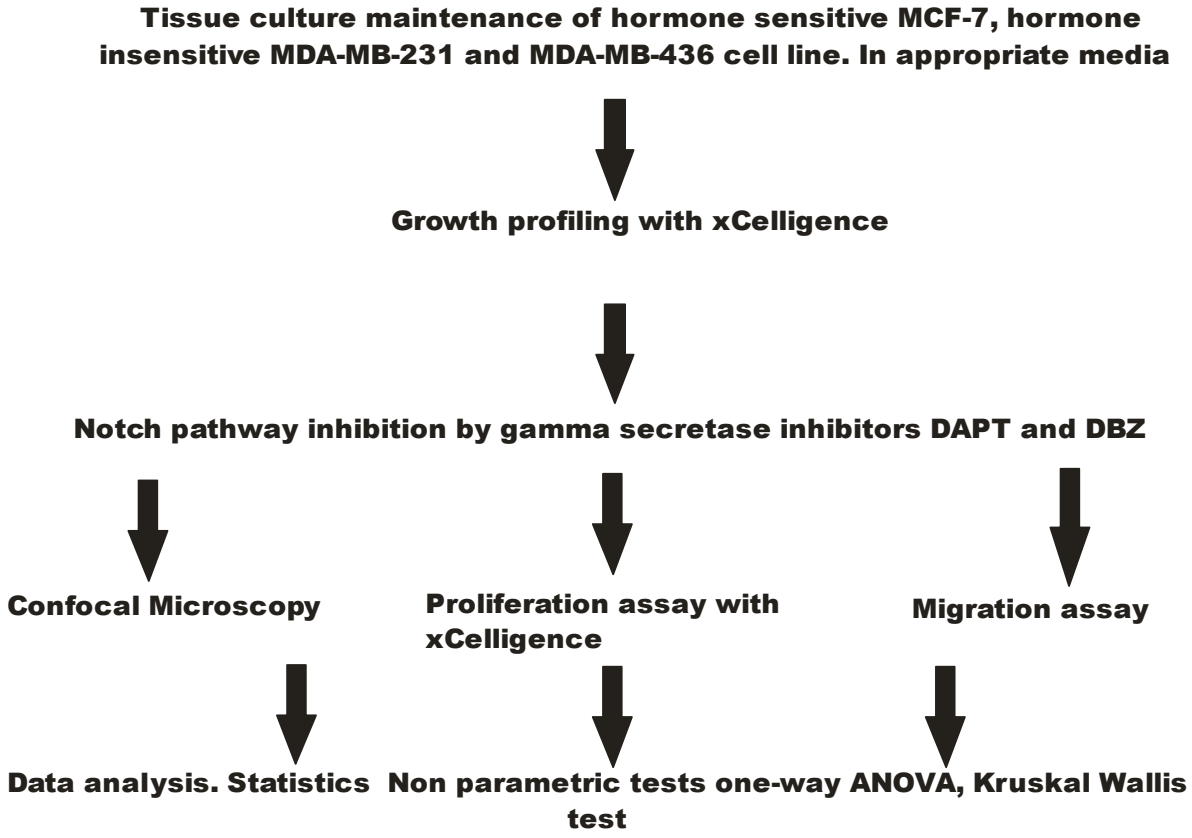


Figure 2.1. Flow diagram representation of methodology applied in this study. Cell lines were cultured and maintained in appropriate conditions. Thereafter their normal growth patterns were monitored in real time using cell impedance assays (xCELLigence, Roche). Cells were treated with the pharmacological gamma secretase inhibitors, N-[(1S)-2-[[(7S)-6,7-Dihydro-5-methyl-6-oxo-5H-dibenz[b,d]azepin-7-yl]amino]-1-methyl-2-oxoethyl]-3,difluorobenzeneacetamide (DBZ) and N-(N-3, 5-Diflurophenacetyl-L-alanyl))-S-phenyl glycine t-Butyl Ester (DAPT), respectively.
The subsequent pharmacological effects on cell proliferation, migration, and protein expression were assessed by each of xCelligence, scratch/migration assays and confocal microscopy, respectively. All data was analysed using Graph Pad Prism v5. Non-parametric tests, including One-way ANOVA and the Kruskal Wallis test were used for statistical analyses. Detailed protocols are in appendice A. [Diagram was created on Coreldraw version 12 (Msibi 2014)].

2.1 Mammalian cell lines and cell culture maintenance

As mammalian cell culture utilising commercially acquired cell lines were used to study the Notch pathway *in vitro*, human ethics clearance was not required (see ethics waiver-Appendix B.5).

2.1.1 Cell lines

All cell lines were procured from the American Type Cell Culture (ATCC, USA). A hormone sensitive BC cell line, MCF7 and two hormone insensitive BC cell lines, MDA-MB-231 and MDA-MB-436 were utilised in this study. These cell lines are described below and are summarised in Table 2.1:

- The MCF-7 cell line is an invasive ductal adenocarcinoma breast cell line, originally isolated from a metastatic site via pleural effusion in 1970 from a 69 year-old female Caucasian (Holliday and Spiers, 2011, Soule *et al*., 1973). In the present study it was used as the control group because it expresses ER, PR and HER-2 (which is not overexpressed)
- Both the MDA-MB-231 and MDA-MB-436 cells are invasive ductal adenocarcinoma breast cell lines, which were isolated from a metastatic site via pleural effusion from 51-year old and 43-year old female Caucasians, respectively (Brinkley et al., 1980, Chavez at al., 2010). Here they were used as the experimental group, since they lack ER, PR and HER-2 and thus represent TNBC.

Table 2.1: A summary of the characteristics of the breast cell lines.

Cell line	Hormone receptor status	Ethnicity	Age	Phenotype	Group
MCF-7	ER+ PR+ HER-2 + (not overexpressed)	Caucasian	69	Luminal epithelial	control
MDA-MB-231	ER-.PR-,HER-2-	Caucasian	51	Basal epithelial	experimental
MDA-MB-436	ER-,PR-,HER-2-	Caucasian	43	Basal epithelial	experimental

2.1.2 Cell culture maintenance

The cell lines mentioned above were grown and maintained in cell culture flasks (SPL-Life Sciences) and were incubated at 37℃ in 5% CO_2 (ThermoForm series ll water jacketed CO_2 Incubator [HEPA FILTER]). The MCF-7 and MDA-MB-231 cell lines were grown in DMEM-F12 (#BE12-719F, Biowhittaker® Lonza,USA) medium supplemented with 10% (v/v) foetal bovine serum (FBS) (#SV30160.03, HYCLONE®, USA) and 1% (v/v) antibiotic penicillin/streptomycin (#17-602E, Biowhittaker® Lonza, USA).

The MDA-MB-436 cell line was cultured in Leibovitz media (L-15) (#BE12-700F, Biowhittaker® Lonza,USA), supplemented with 10% (v/v) FBS, 0.1% (v/v) human insulin (#19278,Sigma Life Sciences, USA), 0.08% L-glutamine (#G7513, Sigma Life Sciences, USA) and 1% (v/v) antibiotic penicillin/streptomycin (#17-602E, Biowhittaker ® Lonza, USA). Cell growth media was changed every 3 days and confluency was monitored with an inverted phase contrast microscope (Carl Zeiss Axiovert 25).

2.2 Analysis of cellular proliferation

2.2.1 Normal growth curve profiling

As a first approach, normal growth signatures of each cell line were monitored with xCelligence-RTCA (Roche) both to assess individual differences in growth patterns and to compare the growth patterns of TNBC cell lines *versus* the hormone sensitive cell line.

Cells were grown in culture flasks until they reached 80% - 90% confluence. They were then trypsinized to create a single suspension and counted using an automated cell counter (Bio-Rad) (see Appendix B.1 and B.4). The cell count for each cell line was adjusted to an optimised seeding density (see Table 2.2 and optimisation in Appendix C.1).

Table 2.2: Optimised cell seeding density for xCelligence studies.

CELL LINE	SEEDING DENSITY cells/ml
MCF-7	10000
MDA-MB-231	5000
MDA-MB-436	5000

A volume of 100µl of culture medium, appropriate to the particular cell line, was added into each well of a 16–well E-plate (ACEA, San Diago). Prior to initiating an experiment, with the addition of cells, a reading of this complete drug-free medium was taken as a background scan; this was done for 1min. Thereafter 100µl of cell suspension was added to each well and mixed thoroughly with the medium to give a final volume of 200µl *per* well. The E-Plates were incubated at 37℃ and 5% CO_2 to allow cells to adhere to the bottom of the well surface for 45mins, as advised by Roche. Thereafter the plates were inserted on

the instrument's docking port and the monitoring system was set to record readings every 30mins for a total of 200hrs.

2.2.2 Cell viability and proliferation assays

To determine the effects of Notch pathway inhibition in BC cells, two γ-secretase inhibitors , DAPT (#D5942-5mg; Sigma Life Sciences) and DBZ (Tocris Biosciences, Bristol UK) were evaluated. Dimethyl Sulfoxide (DMSO) was used to dissolve the lyophilised form of the inhibitors and thus was included here as the vehicle control at 0.2%. The xCELLigence (Roche) instrument was employed to assess the effects of each inhibitor on the cell proliferation and viability. In addition the TB exclusion-dye assay was performed for the purposes of comparing it to xCelligence cell viability data and to optimise inhibitor concentrations.

2.2.2.1 xCelligence-proliferation and viability assay

All the steps of the normal growth profiling assay were followed, as described above. Cells were cultured in complete medium for 22-24 hours; and then wells of the E-plates were rinsed 3 times with 200µl of Phosphate Buffered Saline (PBS) (# P4417-100TAB; Sigma Life Sciences). Next 200µl of serum-free media was added to each well. The addition of serum-free media was done for the purpose of serum starvation, a process that arrests cells in G1/G0 phase of the cell cycle (Weinberg and Lundberg, 1999). Synchronizing the cells at the same phase of the cycle allows them to re-enter the cycle, once they are cultured again with serum containing medium.

Following serum starvation, wells were rinsed once with PBS and then 200ul of complete medium containing either 20µM of DAPT, 20µM DBZ, 20µl DMSO (vehicle control) or complete drug-free medium (untreated control) was added to the wells. The plates were incubated at 37℃ in 5% CO_2 in air for 48 hours, with impedance readings being recorded every 30mins.

2.2.2.2 Trypan blue exclusion cell viability assay

In the TB exclusion assay cells were grown in 12 well cell culture plates (SPL Life Sciences), at a seeding density of 2 x 10^3 cells/well. After 22-24 hours, the cells were rinsed 3 times with 1ml of sterile PBS. After this, 1ml of serum-free media was added to each well, to serum starve for 18-20 hours. Following serum starvation, wells were washed once with PBS, then 1ml of complete medium containing one of either 20µM of DAPT, 20µM DBZ, or 20µl DMSO (vehicle control) was added. In the case of untreated controls, complete drug-free media (untreated control) was added to wells. Then cells were incubated at 37℃ in 5% CO_2 in air for 48 hours. Thereafter the wells were rinsed 3 times with PBS, and the cells were trypsinized with 200µl of trypsin/EDTA for 3mins. After neutralizing the trypsin solution with complete medium, the cells were pelleted by centrifuging in 1ml Eppendorf tubes at 800rpm for 3mins; the supernatant was discarded and the cell pellet was re-suspended in 200µl of serum-free media to prepare for cell counting (TB binds to serum proteins, hence the use of serum-free media). Thereafter 10ul of TB was mixed with 10ul of cell suspension, making a 20ul mixture and 10ul of this mixture was loaded onto the haemocytometer. Cells were counted and viability was calculated by the formula: Percentage viability = [1.00 – (Number of non-viable cells ÷ Number of total cells)] × 100

2.3 Confocal immunofluorescence microscopy

The immunofluorescence staining technique makes use of antibodies to locate and identify the expression patterns of proteins in cells. A primary antibody will bind specifically to an antigen and a secondary antibody conjugated to a fluorochrome then binds to the primary antibody (Fritschy and Härtig, 2001). This binding allows for the detection of the target protein. When the fluorochrome absorbs high energy light it is excited and fluoresces at its characteristic emission wavelength, thus making it possible to detect the antibody-antigen complex (Fritschy and Härtig, 2001). The fluorescent proteins are viewed with a fluorescence microscope. There are different types of fluorescence microscopes and here a confocal scanning laser microscope was used. A confocal microscope (Figure 2.2) provides high resolution images and three dimensional reconstructions of specimens, and enables the co-localisation of two or more proteins on the same specimen.

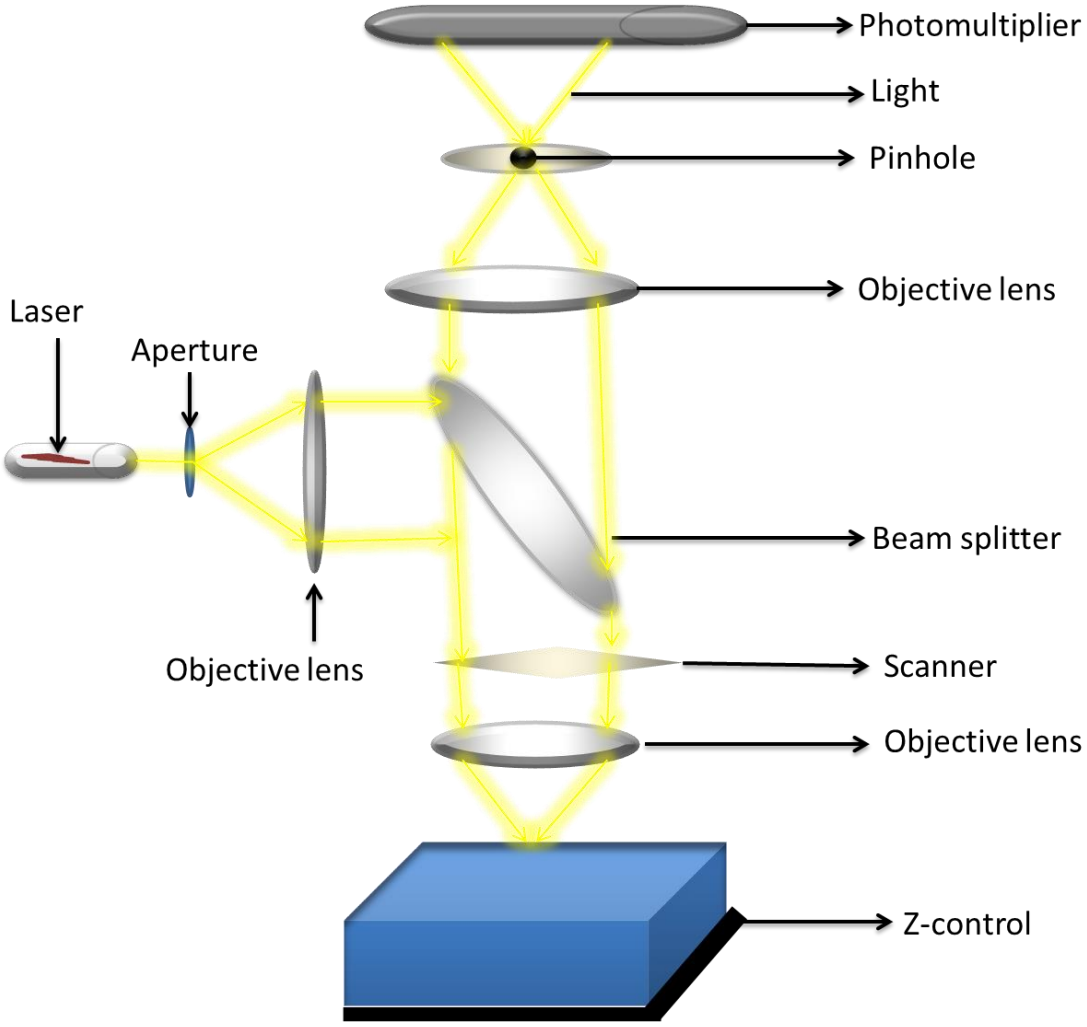


Figure 2.2. Principal of the confocal laser microscope. Light from a laser beam passes through the aperture, whereupon this light is then focused by the objective lens into the surface of a specimen. The reflection from the specimen passes back through the objective lens. The beam splitter separates a portion of the light. The light passes through the pinhole into the photomultiplier that then detects the intensity of the light. The light signal is transformed into an electrical signal that is read by the computer. [Diagrams were created on Microsoft Powerpoint 2010 (Msibi 2015)].

Here, the cellular expression and localisation of NIC and E-cadherin proteins within each cell line were assessed. Also, possible changes in cellular morphology were evaluated following treatment with the Notch inhibitors.

2.3.1 Immunofluorescence staining

2.3.1.1 Cell preparation

Cells were grown in appropriate media on sterile glass coverslips in 6 well culture plates (SPL Life Sciences) and were allowed to reach 50% confluence. Once the required cell confluence had been reached, cells were rinsed in PBS and medium was replenished with serum-free medium. This allowed for serum starvation which was done for 18-20hrs. Following this, cells were treated with complete medium containing 20µM DAPT, 20µM DBZ or 20µl of DMSO (vehicle control), or treated with complete medium alone (untreated control) and were incubated for 48 hours at 37℃ in 5% CO_2 in air.

After the 48 hour incubation period, the cells were rinsed 3 times with 1ml of PBS; then fixed for 15mins in an incubator at 37℃ in pre-warmed 3% PBS-formaldehyde solution (Appendices A.1.3) and were subsequently rinsed 3 times with 1ml of PBS.

In order to allow for intracellular staining and to block non-specific antibody binding, the cells were permeabilized with warm PBS-BSA (Santa Cruz Biotechnology) containing Triton X-100 (Appendix A.1.4) for 5mins at room temperature (RT). Triton X-100 is a detergent that permeabilizes cell membranes, whilst BSA binds antigenic sites and blocks non-specific antibody binding. After permeabilising, the cells were rinsed 3 times with PBS to remove excess Triton X-100.

2.3.1.2 Primary and Secondary antibody staining

The cells were incubated overnight at37℃ with 100µl of the following primary antibodies: rabbit-Anti-Notch-1 intracellular component domain (#07-1231; Merck Millipore) or purified mouse anti-E-cadherin (#610181; BD Transduction Laboratories ™) optimally diluted at 1:200 and 1:2500, respectively in warm PBS-BSA buffer. An additional negative control was to include the primary antibody incubation step, but to exclude the secondary antibody, substituting this with PBS-BSA.

The following morning the cells were rinsed with pre-warmed PBS-BSA 5 times with 1 min incubations. Next the cells were incubated in a dark cupboard for 1hr at RT with 100µl of one of the following secondary antibodies: donkey anti-rabbit IgG (H+L) Alexa Fluor® 488 (# A21203 Invitrogen) or donkey anti-mouse IgG (H+L) Alexa Fluor® 549 (#A21203 Invitrogen) diluted at 1:200 and 1:2500, respectively in 0.05% PBS-BSA. After 30mins into the secondary antibody incubation period, slides were further incubated with an additional 100µl of Cyto-painter Phalloidin iFluor 488 Reagent (# ab176753; ABCAM ®) to stain the F-actin cytoskeleton. Phalloidin is a heptapeptide that binds to F-actin. It stabilizes the filaments thereby preventing depolymerisation of actin fibers. An additional negative control was to include the secondary antibody incubation step, but to exclude the primary antibody, substituting this with PBS-BSA.

2.3.1.3 Nuclear staining

Subsequent to the secondary antibody and F-actin staining, the cells were rinsed 5 times with pre-warmed PBS-BSA at 1min incubations. The cells were then incubated in a dark cupboard for a further 5mins with a 100µl solution of 4', 6-diamidino-2-phenylindole

(DAPI) (#236276; Cell Biology Boehringer Mannheim, Germany) at RT. The cells were then rinsed 5 times at 1min incubations with PBS. Next, the coverslips were mounted onto glass slides with Fluorogel Mount (#17985-10, Electron Microscopy Sciences) and were left to dry in the dark for a few hours. These were then placed in a box and stored at 4℃, till viewing the next day on a Carl Zeiss LSM 780 Confocal Microscope (63 X Magnification).

2.3.1.4 Z-sectioning and 3 dimensional reconstruction analysis

The properties of the confocal laser scanning microscope allow for the optical sectioning in the Z- axis. The pinhole, a small, adjustable diaphram placed in front of the PMT (see Figure 2.2), eliminates unwanted light from out-of-focus areas. Capturing a series, or stack, of images focused at regularly placed intervals through the depth of an object of interest allows one to subsequently create renderings to visualise the entire sample in 3 dimensions (3D). Z-stacking of specimens was recorded using the Z-stack mode of the Carl Zeiss LSM 780 Confocal microscope (63X Magnification) (Appendix D).

2.4 Cell migration study

To assess cell migration the scratch assay technique was used. Here cells are seeded onto a sterile glass coverslip and grown to confluence. A cell-free area referred to as a "gap" was created by scoring through the cell monolayer with a sterile plastic pipette tip (Kramer *et al.*, 2013). The gap closure by cell migration is then monitored by microscopy over a specific period of time. This assay can directly reflect the cell dynamics and cell contacts that are involved in cellular migration (Liang *et al*., 2007, Kramer *et al*., 2013). Thus the

time it takes for the gap to close is an indication of the migration potential of the cell line (Liang *et al*., 2007).

2.4.1 Cell migration assay

Approximately 50000 cells/ml (in appropriate culture media) were seeded onto heat sterilised glass coverslips contained in each well of a 6 well cell culture plate (SPL Life Sciences) and were allowed to reach 100% confluence. The coverslips were then rinsed 3 times with PBS and 1ml of serum-free medium was then added, to facilitate 18-20 hours of serum starvation; subsequently the serum-free medium was removed and the wells were rinsed once with PBS. Next, the coverslip was scored or scratched through the confluent monolayer of cells with a sterile (200 µl) pipette tip to create a cell-free area. Following this, the coverslip was rinsed once with PBS to remove any cell remnants from the scored area. Thereafter 1 ml of complete medium containing either 20 µM DAPT, 20 µM DBZ, or 20 µl DMSO (vehicle control) or 1 ml of complete drug-free medium (untreated control) was added to each well. The gap closure was monitored every 2 hours for 48 hours to analyse the cell migration distance over time, this with an inverted microscope (Olympus IX71), and viewed under a 4X objective. The images were captured with an Olympus CKX41 camera. The extent of migration of cells into the gap was calculated at three points (Appendix E.1); the quantification of the relative closure of the gap was undertaken and compared with that of the control by using ImageJ software; pixels were converted to µm to obtain the value pixels/µm (Appendix E.1).

2.5 Data analysis

Experiments were performed in biological triplicates. All average and standard deviation (SDV) values were calculated in Microsoft Excel 2010 and were exported to Graph Pad PrismPad Prism, version 5. To evaluate the statistical difference between normal growth CI values of all three cell lines, non-parametric ANOVA analysis, followed by the Kruskal Wallis test were performed. To assess the effect of GSI between MCF-7 and MDA-MB-231 or MCF-7 and MDA-MB-436, an unpaired Student's *t*-test was calculated with 95% confidence. Finally, to evaluate the effects of the different GSIs on a cell line, a paired Student's *t*-test was calculated with 95% confidence. A *p*-value that was <0.05 was considered significant.

CHAPTER 3: RESULTS

3.1 Determination of the activity of Notch and the effect of gamma secretase inhibition

3.1.1 Notch signalling is active in breast cancer cells and NIC expression decreases post- inhibitor treatment

To determine the activity of Notch signalling in human BC cells and the expression and localisation of NIC within the cells, indirect immunofluorescence was used. BC cells were stained with an anti-NIC antibody, the cleaved product of γ-secretase which represents the activity of the pathway (Figure 1.4). This (NIC) was then localised using a secondary antibody conjugated to a fluorescent Alexa Fluor dye. In order to control for non-specific antibody binding, negative controls were carried out, wherein either the primary or the secondary antibody was omitted and substituted with PBS. These controls effectively showed a lack of non-specific primary or secondary antibody binding (see Appendix D.1).

Following serum starvation the cells were then treated with 20µM DAPT, 20µM DBZ, 20µl DMSO (vehicle control) or complete drug-free (untreated) medium , respectively, for 48hrs. The MCF-7 cell line demonstrated specific NIC (green) localisation, which appeared as discrete punctate areas on the nucleus (blue), being specifically associated with the nucleoli, the expression of which decreases when treated with each inhibitor (Figure 3.1-panel A- L arrows). In addition there is also some perinuclear staining that was observed.

In all the cell lines DAPT treatment results in a more drastic decrease of the NIC signal compared to DBZ and DMSO. The MDA-MB-436 cell lines show the same NIC-nucleoli localisation, but with a lower expression than in the MCF-7 drug treated cells (Figure 3.1-panel I) and untreated cells. DAPT in these cells also causes a marked decrease in NIC expression compared to treatment with each of DBZ and DMSO (Figure 3.1 panel J-L).

In the MDA-MB-231 cell line, NIC expression was raised, being concentrated both in a the perinuclear staining pattern and also being dispersed over the nucleus, largely masking the nucleoli that are visible in the nuclei of the other two cell lines (Figure 3.1 panel E-F). The nucleoli following NIC localisation are only faintly visible post-GSI treatment; and furthermore, both GSI's cause a dramatic decrease in nucleoli associated expression of NIC in the MDA-MB-231 cell line (Figure 3.1 panel G-H).

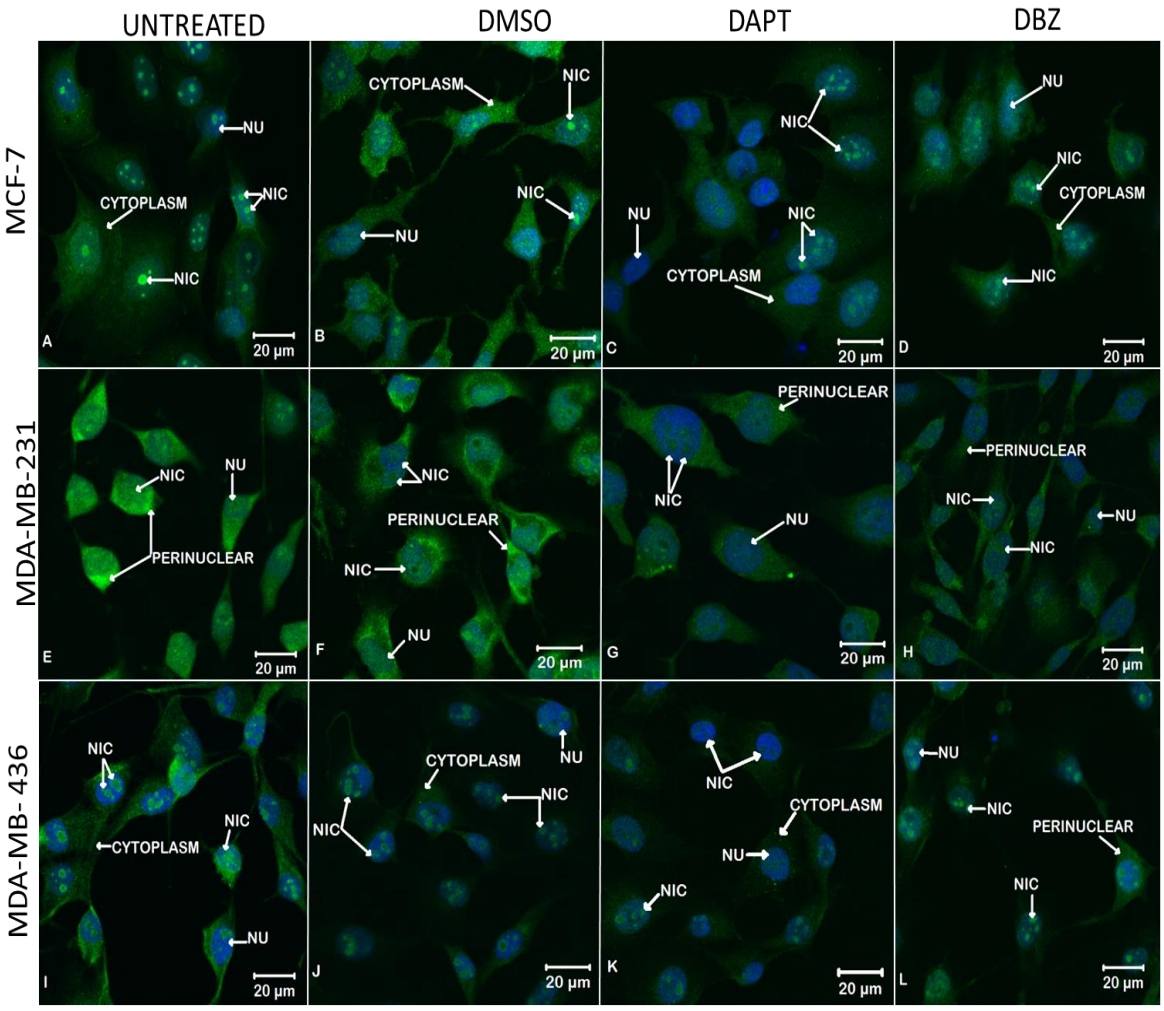


Figure 3.1. Notch signalling is active in breast cancer cells and its expression decreases post inhibitor treatment. Cells were treated with 20µM of either DAPT or DBZ. DMSO was used as a vehicle control. Each drug inhibits the pathway as the NIC signal represented by positively staining green nucleoli, decreases post-treatment. DAPT decreased the expression of NIC in MDA-MB-436 (Panel I-L) and MCF-7 (Panel A-D) cell lines, respectively. Both DAPT and DBZ decrease the expression of NIC in MDA-MB231 (Panel E-H). [Cells were stained with donkey anti-rabbit IgG (H+L) Alexa Fluo® 488 (# A21203 Invitrogen) to detect NIC (green) and DAPI for the nucleus(blue); and visualised using a Carl Zeiss LSM 780 Confocal Microscope, 63X objective.].
Key: A-D= MCF-7; E-H= MDA-MB231; I-L=MDA-MB436 NIC= Notch Intracellular Component NU=Nucleus

3.2 Effect of Notch on breast cancer cells

3.2.1 Oestrogen receptor positive cells grow more rapidly compared to TNBC cell lines

Following on the evaluation of Notch activity, through NIC expression in the hormone insensitive and hormone responsive BC cell lines, it was of interest to determine the potential effects of the pathway on cell proliferation.

Firstly, cell impedance assays using the xCelligence instrument (Roche) were used to evaluate the normal growth profiles of each cell line. The curves presented below (Figure 3.2) represent 3-repeats for each cell line. The MCF-7 cell line (blue) has a cell index (CI) of 6.9836 at 74.5hrs, which is the highest among the three cell lines. The MDA-MB-231(red) and MDA-MB-436 (green) cell lines have a CI of 1.9799 and 3.1712 respectively (Figure 3.2). The MCF-7 cells grow exponentially (log phase) for 20 hours before beginning to plateau. These cells grow significantly (p<0.001, ANOVA, Kruskal Wallis test) faster, compared to, the MDA-MB-231 and MDA-MB-436 cell lines, which grow exponentially for 22 hours, before they begin to plateau (Figure 3.2).

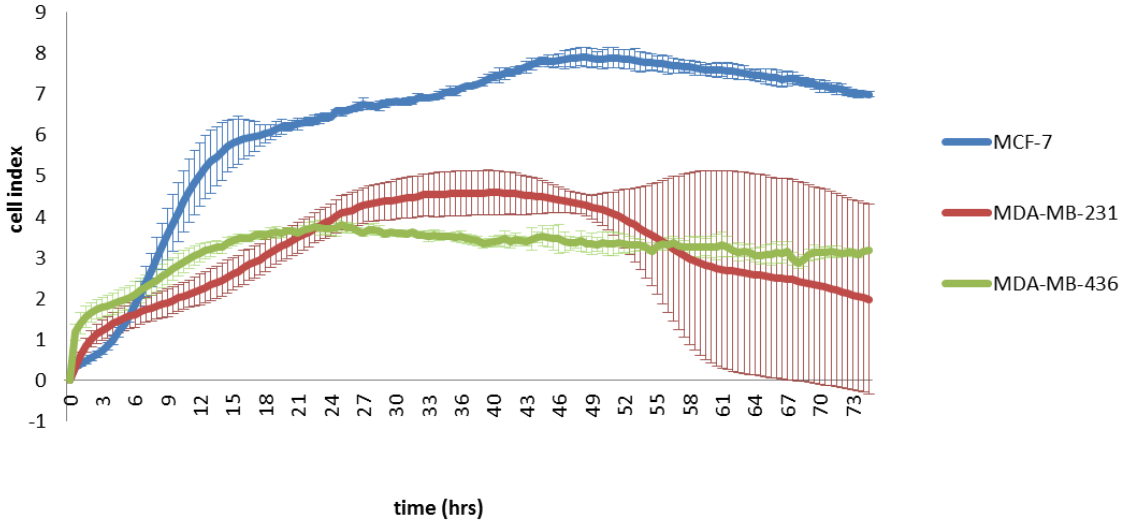


Figure 3.2 Normal cell growth profile of hormone receptor positive cell line (MCF-7) compared to hormone receptor negative positive cell line (MDA-MB-231 and MDA-MB-436). Cell impedance shows that MCF-7 (blue) has higher cell index compared to MDA-MB-231 (red) and MDA-MB-436 (green). The MCF-7 cell line has a significantly faster growth curve (p<0.001, ANOVA, Kruskal Wallis test) compared to MDA-MB-231 and MDA-MB-436 cell lines. Error bars represent standard deviation of N=3.

3.2.2 Notch signal pathway inhibition decreases cell proliferation and viability in breast cancer cells

To determine the effects of Notch signalling on cell proliferation and viability, GSI's were used. Prior to drug treatment, each of the cell lines were serum starved (Appendix C.3) and then treated with 20µM DAPT, 20µM DBZ, and 20µl DMSO (vehicle control) or complete drug-free medium (media control), respectively. As an initial assessment of the pharmacological activity of the GSI's on cell growth, the end-point TB cell viability assay was employed. This was then compared with the real-time measurements of cell viability measured with the xCelligence-RTCA instrument (Roche).

3.2.2.1 Trypan blue assay cell viability

The results of the TB assay show that cell viability decreases non-significantly with DBZ treatment in all cell lines, after 48hrs of treatment (Figure 3.3). Treatment with DAPT resulted in a 67% cell viability of the MDA-MB-231 cell line. The viability is less compared with the 87.68% and 96.67% of the MCF-7 and MDA-MB-436 cell lines, respectively.

All three cell lines were sensitive to DBZ, with a 29% , 27.67% and 22.22% decrease in cell viability of MCF-7, MDA-MB-231 and MDA-MB-436 cell lines respectively (Figure 3.3). Despite observing this trend of sensitivity, the effect of each treatment on each cell line was not statistically significant ($p > 0.05$, ANOVA, Kruskal Wallis test). Nevertheless a comparison between the DBZ and DAPT treatments shows that the effects of these drugs were significantly different ($p<0.05$, paired Student's *t*-test) in the MDA-MB-231cells. However, their pharmacological effects were indifferent in both of the MCF-7 and MDA-

MB-436 cell lines, respectively ($p > 0.05$, paired Student's *t*-test). There is no significant difference between the DMSO vehicle control and Media control, indicating that DMSO does not have anti-proliferative effects on each cell line.

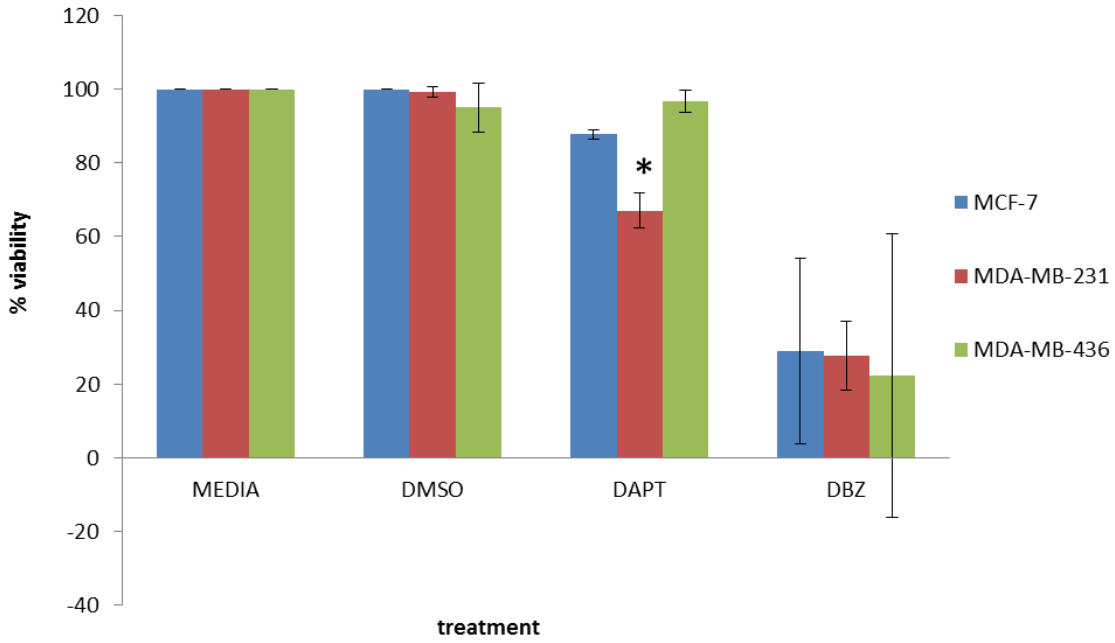


Figure 3.3 TB assay cell viability of breast cancer cells. TB assay following 48hrs of GSI treatment shows that DBZ decreased cell proliferation in MCF-7(blue), MDA-MB-231(red) and MDA-MB-436(green), cell lines although not significantly (p>0.05, paired Student's t-test). The proliferation of the MDA-MB-231 cell lines was significantly affected by DAPT (p<0.05, paired Student's t-test). Overall, GSI treatment did not cause a statistically significant decrease in cell viability (p> 0.05 ANOVA, Kruskal Wallis test) in all three cell lines. Error bars represent standard deviation of N=3.

3.2.2.2 xCelligence-RTCA cell proliferation and viability

In assessing cell viability and cell proliferation using xCelligence, at the end of 48hrs of drug treatment the CI for the MCF-7 cell line was 1.7920 when treated with DAPT which was significantly less, compared to a CI of 2.6847 than when treated with DBZ ($p < 0.05$ paired, Student's *t*-test). In comparison, the proliferation and viability of the MDA-MB-231 and MDA-MB-436 cell lines was significantly more decreased by DBZ, with CI's of 0.3704 and 0.4958 , respectively ($p< 0.05$ paired Student's *t*-test), when compared to the CI's of 0.4360 and 0.67503, after DAPT treatment.

With a CI of 3.3671, 0.4800 and 0.8200 for MCF-7, MDA-MB-231 and MDA-MB-436, respectively, the vehicle control DMSO decreases cell viability and proliferation. However, this was not as significant as the recorded effects of GSI's on each of the cell lines (Figure 3.4, 3.5 and 3.6). Overall the results show that decrease of both cell viability and proliferation following inhibition of Notch was statistically significant in the TNBC cell lines compared to the receptor positive cell line ($p<0.001$, ANOVA, Kruskal Wallis test).

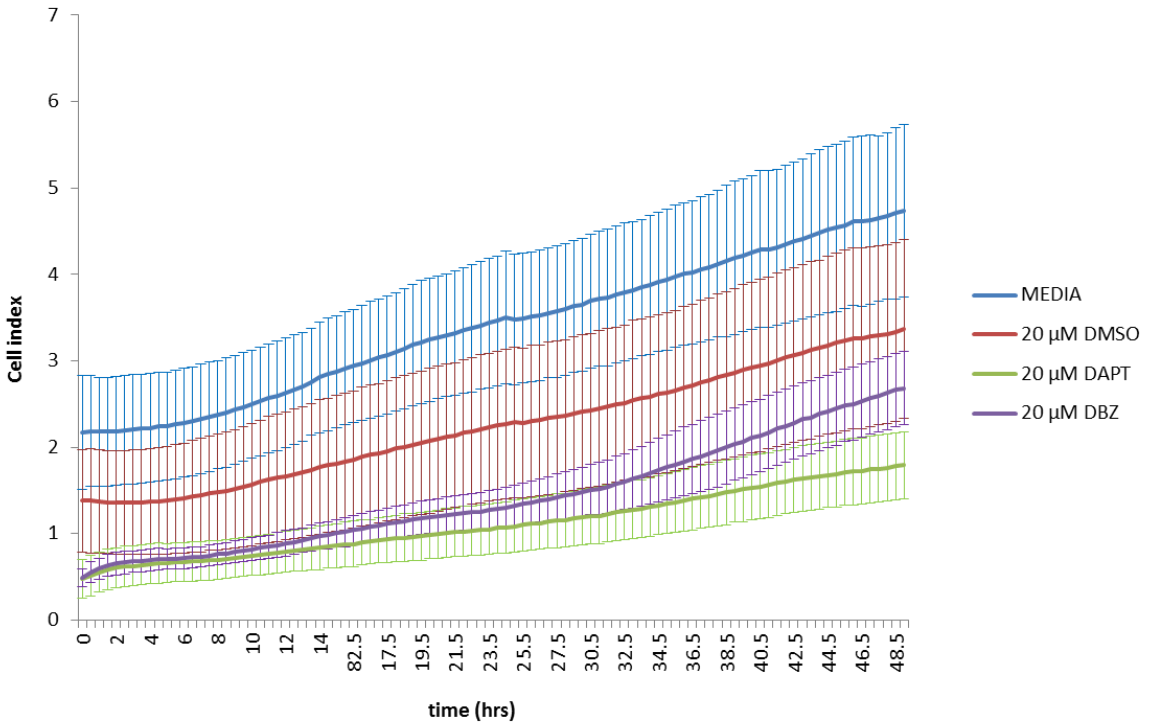


Figure 3.4 GSI treatment inhibits cell proliferation of MCF-7 breast cancer cell lines. DAPT (green) decreased the CI of the MCF-7cell line to 1.7920; this decrease was statistically significant compared to the decrease in CI of 2.684 produced by DBZ (purple) (p<0.001, paired Student's t-test). Overall both of the GSI's had a more significant effect on the cell proliferation and viability when compared to the CI's of the media control (blue) and DMSO (red) vehicle control, which were 4.7388 and 3.3671, respectively (p< 0.001, non-parametric unpaired Student's t-test). Error bars represent standard deviation of N=3.

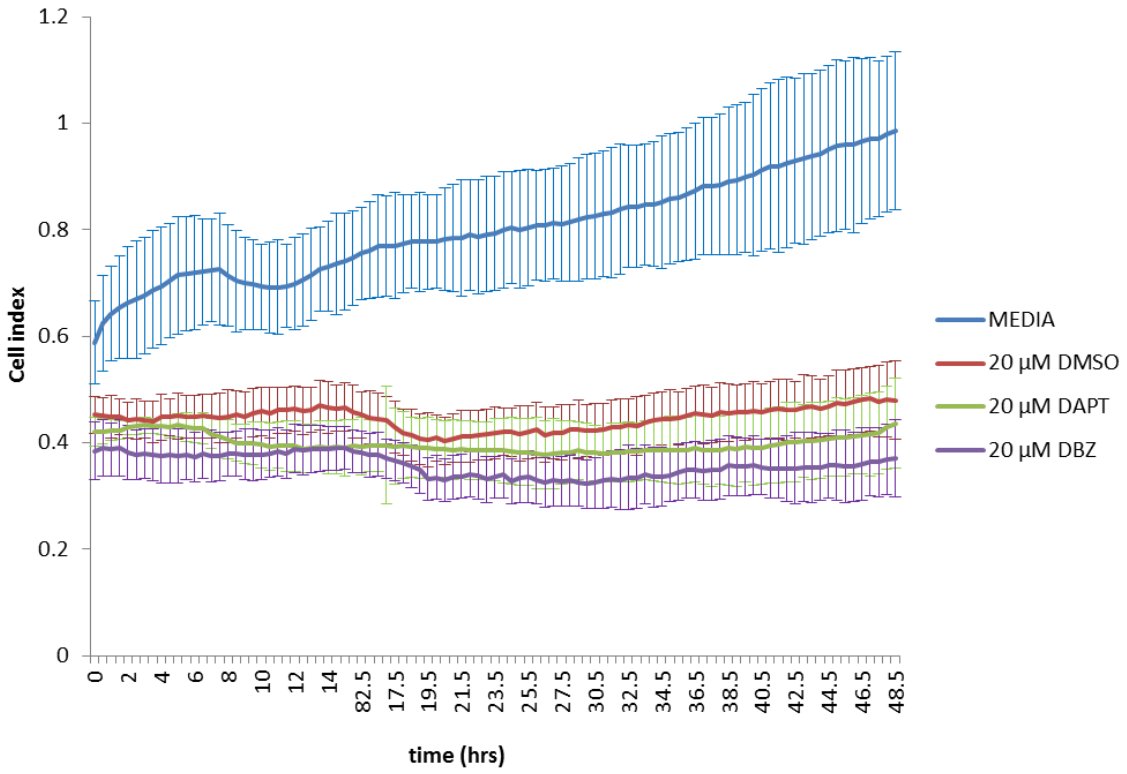


Figure 3.5 GSI treatment inhibits cell proliferation of MDA-MB-231 breast cancer cell lines. DBZ (purple) decreased the CI of the MDA-MB-231 cell line to 0.3704; this decrease was statistically significant compared to the decrease in CI of 0.4360 produced by DAPT (p<0.001, paired, Student's *t*-test). Overall both of the GSI's had a more significant effect on the cell proliferation and viability when compared to the CI's of the media control (blue) and DMSO (red) vehicle control, these were 0.9860 and 0.4800, respectively (p< 0.001, non-parametric unpaired, Student's *t*-test). Error bars represent standard deviation of N=3.

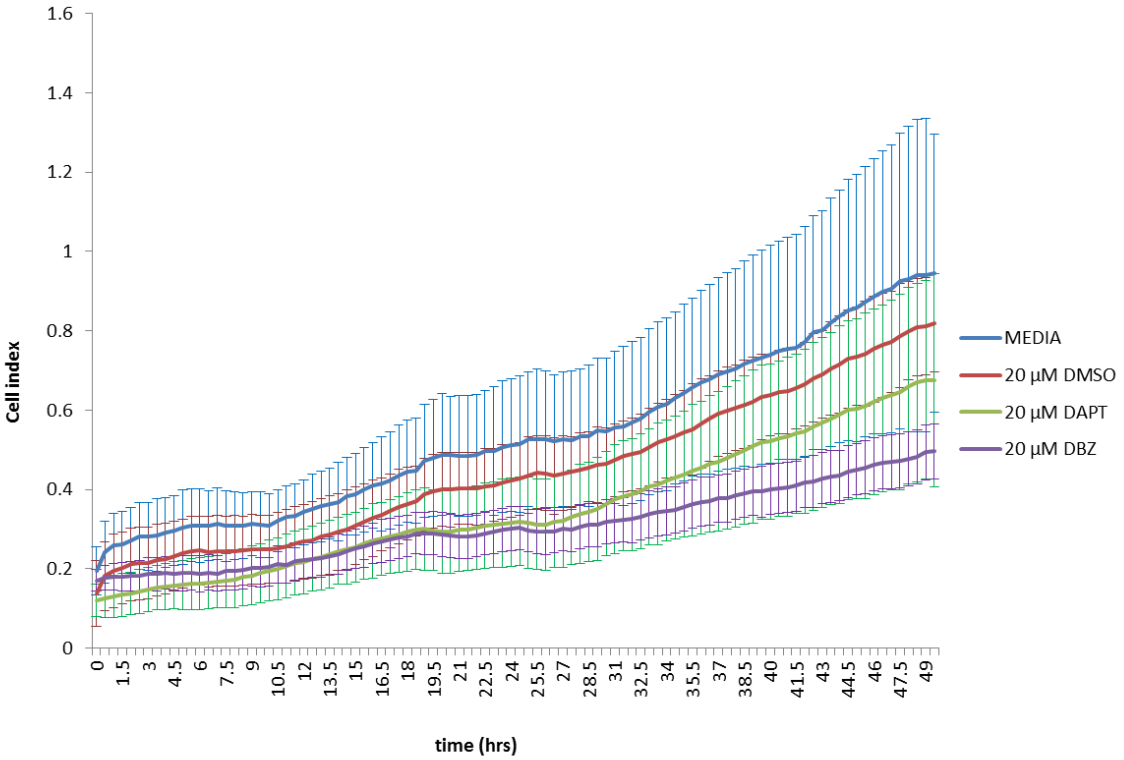


Figure 3.6 GSI treatment inhibits cell proliferation of MDA-MB-436 breast cancer cell line. DBZ (purple) decreased the CI of the MDA-MB-436 cell line to 0.4958; this decrease was statistically significant compared to the decrease in CI of 0.6750 produced by DAPT (green) (p<0.001, paired Student's t-test). Overall both of the GSI's had a more significant effect on the cell proliferation and viability when compared to the CI's of the media control (blue) and DMSO (red) vehicle control, which were 0.945 and 0.8200 respectively (p< 0.001, non-parametric unpaired Student's t-test). Error bars represent standard deviation of N=3.

3.3 Effect on cell morphology and cell migration

3.3.1 Notch inhibition decreases expression of E-cadherin in MCF-7 cells and alters cell morphology in MDA-MB-231 and MDA-MB-436 cell lines.

3.3.1.1 The expression of E-cadherin in human breast cancer cells

To evaluate the potential of Notch inhibition on a marker of cell adhesion and migration indirect immunofluorescence was used to detect the BC tumour invasion marker E-cadherin (Figure 3.7 and 3.8) (Singhai *et al*., 2011). This was done to assess whether there is a change in the expression and localisation of E-cadherin in BC cells post drug-treatment. The cell membranes were either permeabilized or not permeabilized, to assess intracellular localisation or cell surface localisation, respectively. To further assess the precise localisation of the markers of interest, Z-section sectioning and 3D surface projections of the cells were analysed.

In the permeabilised cell group, E-cadherin is highly expressed in the MCF-7 cell line within the cytoplasm, the nucleus and the cell membrane (supplementary image in Appendix D.3). Its expression decreases when treated with GSI, whereby DBZ causes a greater decrease compared to DAPT treatment (Figure 3.7-a panel A-D; Figure 3.7-b panel A-D; Figure 3.8-c panel A-D and Figure 3.8-d panel A-D).

The MDA-MB-231 cell line appeared not to express E-cadherin pre-treatment, indicating that it is a highly invasive cell line and that it has a high migration potential. Post GSI treatment, its expression was not up-regulated (Figure 3.7-a panel E-H; Figure 3.7-b panel E-H). Similarly the MDA-MB-436 cell line does not appear to express E-cadherin and

treatment with GSIs did not alter this status (Figure 3.7-a panel I-L; Figure 3.7-b panel I-L).

The non-permeabilised cell group shows a similar staining pattern for E-cadherin expression in all the cell lines, as recorded for the permeabilised breast cell group. The MDA-MB-231 and MDA-MB-436 cell lines lacked any E-cadherin expression at any intracellular location (Figure 3.8-a panel E-H; Figure 3.8-b panel E-H; Figure 3.8-a panel I-L; Figure 3.8-b panel I-L).

3.3.1.2 The morphology of human breast cancer cells

Next, to determine the effect of GSIs on the cytoskeleton, indirect immunofluorescence was used to visualize the F-actin cytoskeleton with fluorescently labelled phalloidin (Figure 3.7-a; Figure 3.7-b; Figure 3.8-a and Figure 3.8-b). Following drug treatment, the F-actin cytoskeleton of the MCF-7 cell line was apparently not adversely affected by the GSIs. Although the cells appear slightly detached from each other (Figure 3.7-a panel B, C), their shape remains the same, as in the untreated control (Figure 3.7-a panel A).

In MDA-MB-231 cells DBZ caused a change in the distribution of F-actin, as it appears aggregated around the nucleus (Figure 3.7-a and 3.7-b panel; Figure 3.8-a and 3.8-b panel H) which results in a change in cell shape from a fibroblast shape (Figure 3.7-a panel E and Figure 3.8-a panel E) when untreated to a more round shape post-treatment. With DAPT treatment the F-actin cytoskeleton aggregates adjacent to the nucleus (Figure 3.7-a panel G and Figure 3.7-b panel G) however, this was not observed in the non-permeabilised cells (Figure 3.8-a panel G and Figure 3.8-b panel G). The cytoplasmic stress fibers are lost as well as a result of DBZ and DAPT treatment (Figure 3.7-a panel E-H).

The F-actin cytoskeleton in the MDA-MB-436 cells is aggregated adjacent to the nucleus (Figure 3.7-a panel I-L; Figure 3.7-b panel I-L; Figure 3.8-a panel I-L and Figure 3.8-b), this is not affected by drug treatment. There is also nuclear localisation of F-actin observed, in DBZ treated non-permeabilised cells (Figure 3.8-a panel J, L and Figure 3.8-b panel J, L).The cytoplasmic stress fibers of these cells decrease post-treatment and there is in an increase in filapodia in the DAPT (Figure 3.7-a panel K) treated cells.

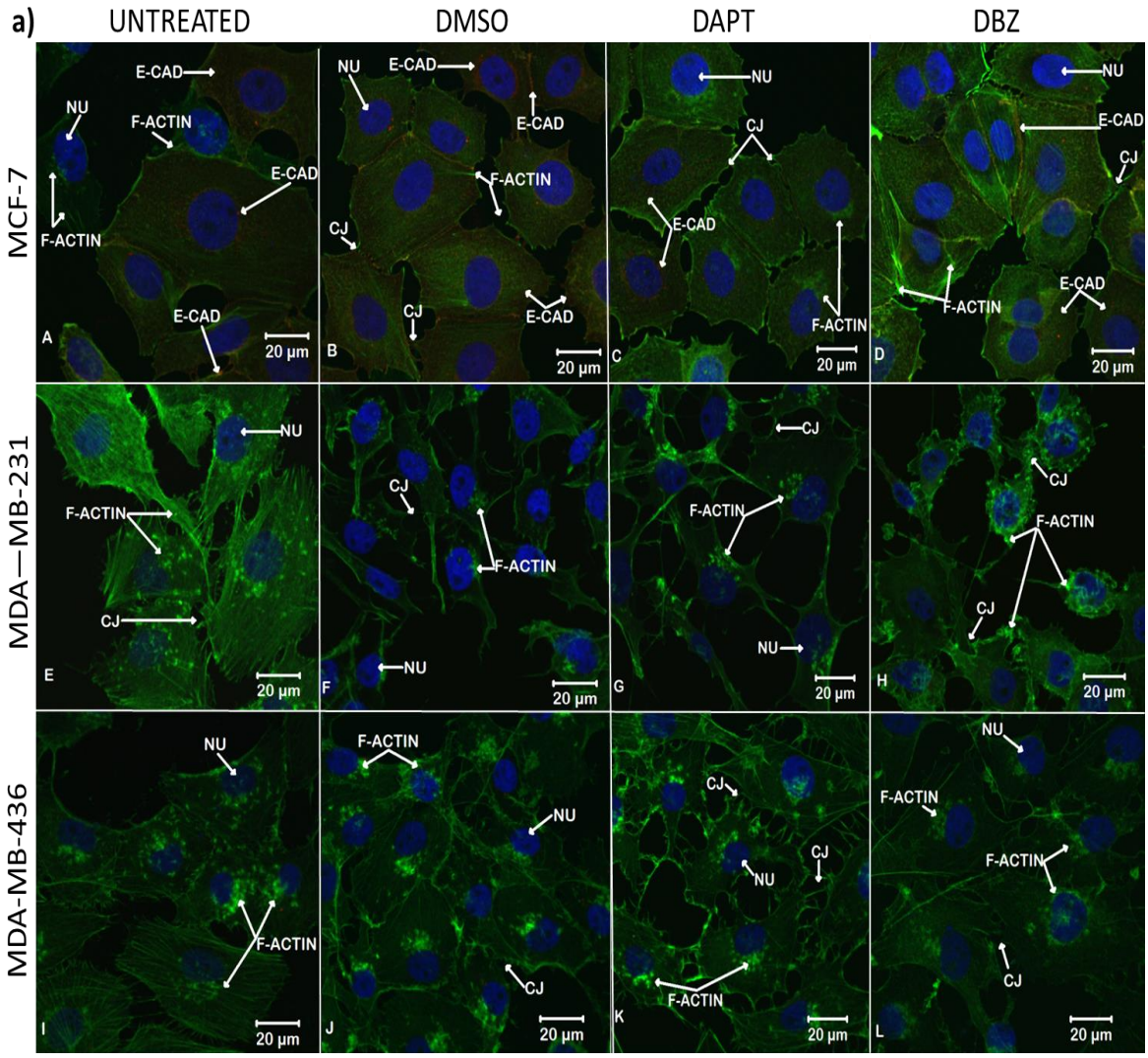


Figure 3.7 a) Effects of Notch inhibition on the expression of E-cadherin and cell morphology in permeabilised cells Permeabilised E-cadherin (red) expression decreases with inhibitor treatment (panel A-D). DBZ causes a decrease in E-cadherin expression in MCF-7 cells (panel D) whereas, F-actin (green) is relatively unaffected by either inhibitor (panel C and D). MDA-MB-231 cells lack E-cadherin signal post-treatment with DAPT/DBZ (panel E-H). Furthermore, the distribution of F-actin within these cells is altered post-treatment (panel G and H), indicating a change in cell morphology. F-actin appears punctate in MDA-MB-436 (panel I-L) and MDA-MB-231 (panel G).

Key: NU= nucleus; E-cad=E-cadherin; CJ= Cell Junction; A-F= MCF-7; E-H=MDA-MB231; I-L=MDA-MB436

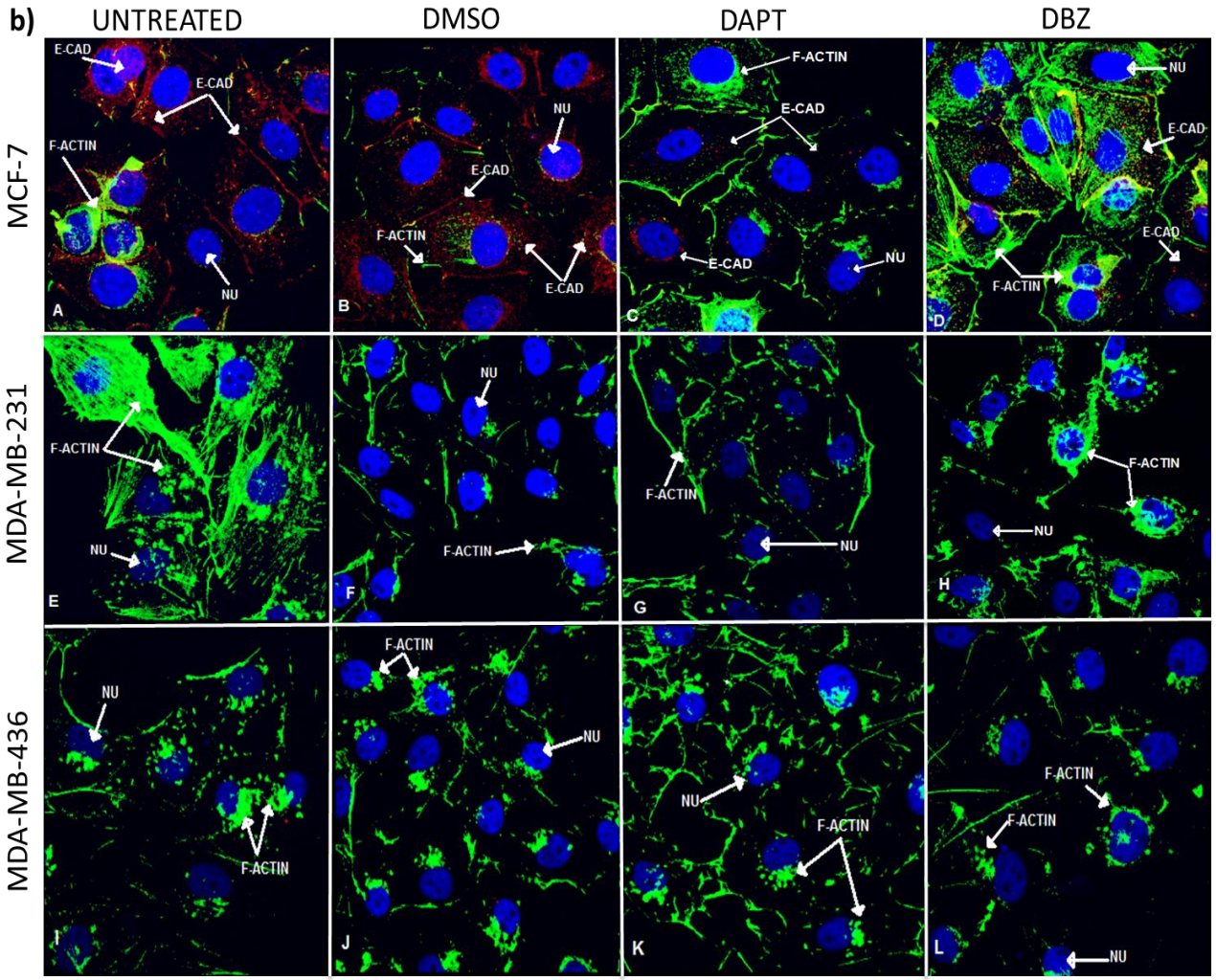


Figure 3.7 b) 3D projections, generated from Z-sectioning; Zeiss LSM 780 permeabilised cells. The YZ3 dimensional projection images of the cell lines seen which are represented in figure 3.7-**a.** Here membrane staining of E-cadherin in the MCF-7 cell line is clearly visible (panel A-D) and there is aggregation of F-actin adjacent to the nucleus visible in the MDA-MB-231 (panel E-H) and MDA-MB436 cell lines (panel I-L).
Key: NU= nucleus; E-cad=E-cadherin; CJ= Cell Junction; A-F= MCF-7; E-H=MDA-MB231; I-L=MDA-MB436

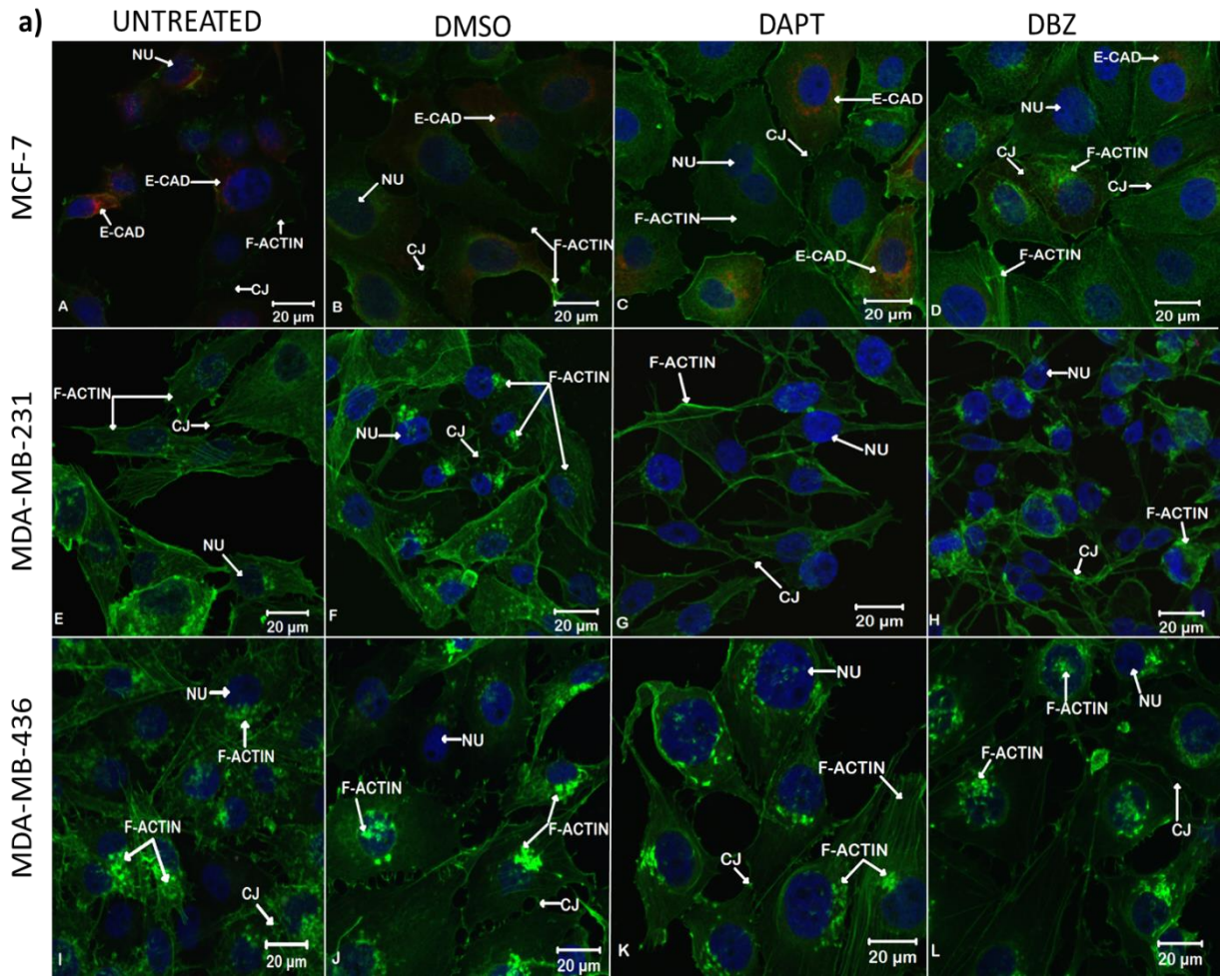


Figure 3.8 a) Effects of Notch inhibition on the expression of E-cadherin and cell morphology in non-permeabilised cells. Non-Permeabilised E-cadherin (red) expression decreases with inhibitor treatment (panel A-D). DBZ causes a decrease in E-cadherin expression in MCF-7 cells (panel D) whereas, F-actin (green) is relatively unaffected by either inhibitor (panel A-D). MDA-MB-231 cells lack E-cadherin signal post-treatment with DAPT/DBZ (panel E-H). Furthermore, the distribution of F-actin within these cells is altered post-treatment, indicating a change in cell morphology. F-actin appears punctate in MDA-MB-436 (panel I-L) and MDA-MB-231 (panel E, F).
Key: NU= nucleus; E-cad=E-cadherin; CJ= Cell Junction; A-F= MCF-7; E-H=MDA-MB231; I-L=MDA-MB436

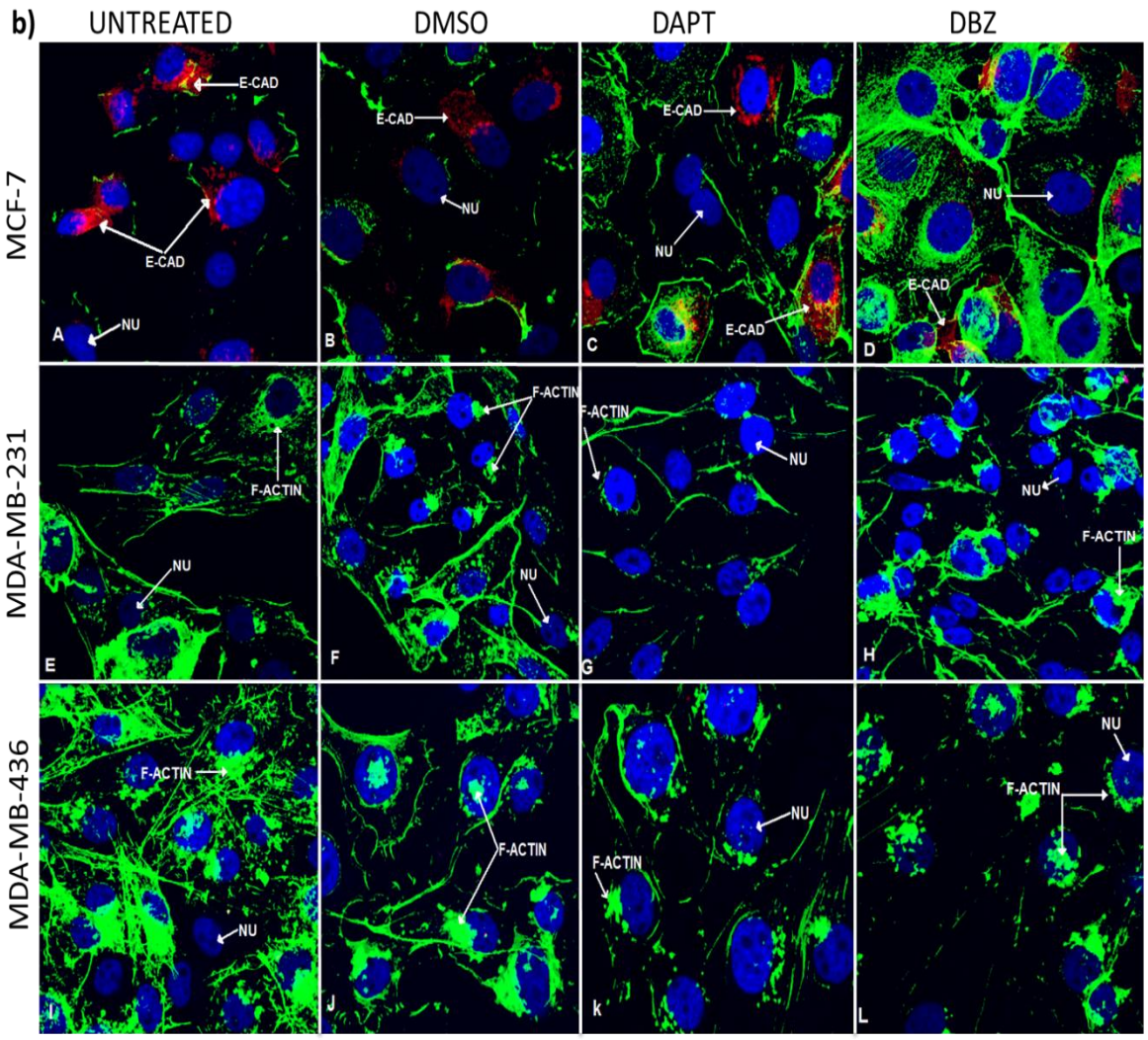


Figure 3.8 b) 3D projection, generated from Z-sectioning; Zeiss LSM 780 non-permebilised The YZ 3 dimensional projection images of the cell lines seen which are represented in Figure 3.8-**c**. Here perinuclear staining of E-cadherin in MCF-7 cells (panel A-D) is clearly visible. Perinuclear and nuclear actin is visible in the MDA-MB-436 cell line (panel I-L).
Key: NU= nucleus; E-cad=E-cadherin; CJ= Cell Junction; A-F= MCF-7; E-H=MDA-MB231; I-L=MDA-MB436

3.3.2 Notch inhibition does not affect cell migration in BC cell lines.

A scratch/migration assay was used to evaluate the effects of Notch signal pathway inhibition on cell migration. The distance the cells moved was recorded every 2hrs. This data is represented below by images of a scratch/migration assay and a plot of cell migration (gap closure) over time, for each respective treatment.

After 48 hours of treatment with GSI, cell migration of the MCF-7 hormone sensitive cell line is not significantly different from either the untreated or the vehicle control (Figure 3.9). Similarly the migration of MDA-MB-231 (Figure 3.10) and MDA-MB-436 (Figure 3.11) cell lines is not significantly different, when compared to their respective vehicle and untreated controls.

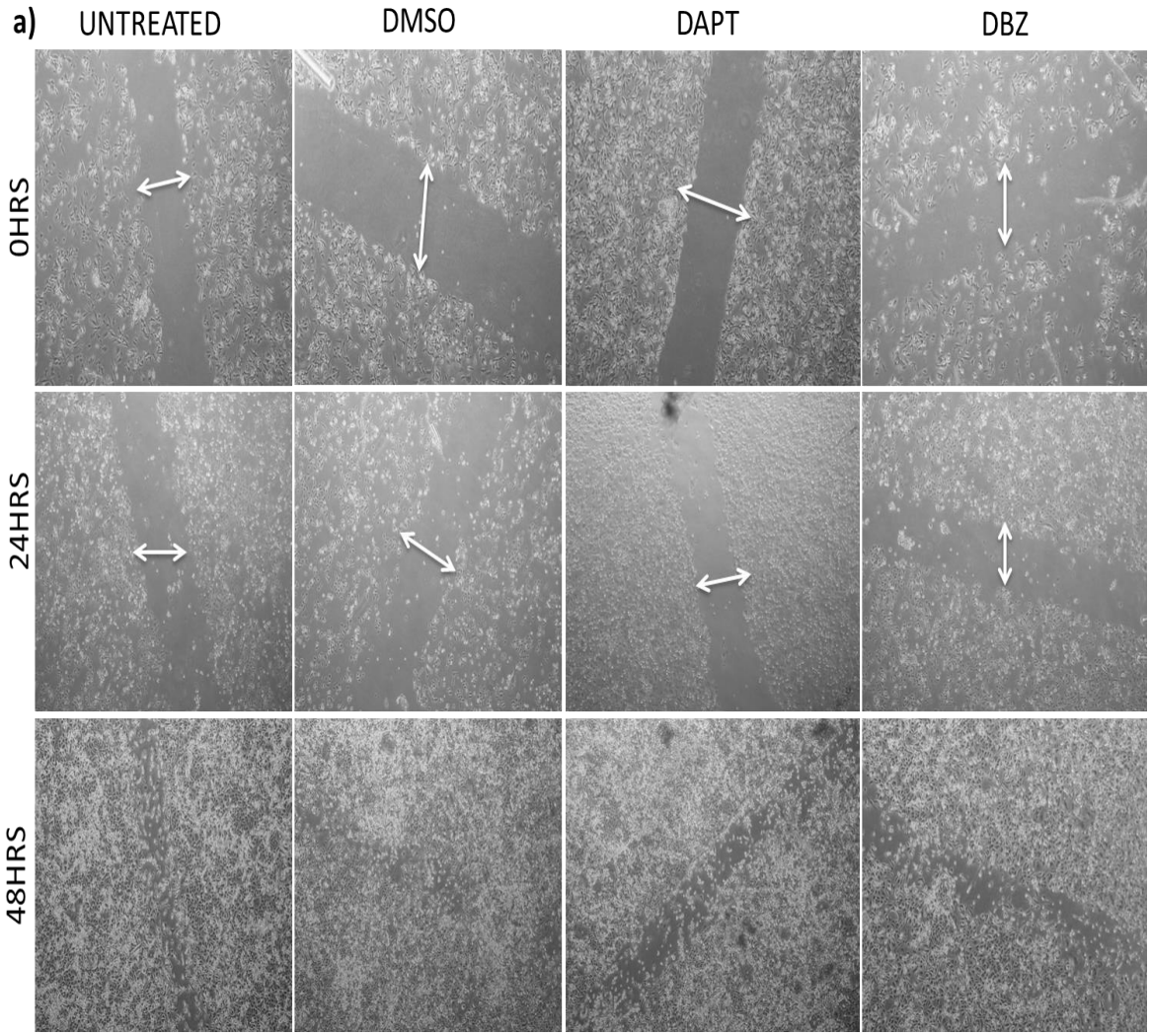


Figure 3.9.a) Notch inhibition does not affect cell migration in MCF-7 cell line. Scratch assay of MCF-7, gap closure was not significantly affected by the DMSO vehicle control and GSI treatment at 48hrs. The white arrow indicates the cell free area that was measured over time. The gap closure is represented in plots below. (4X magnification)

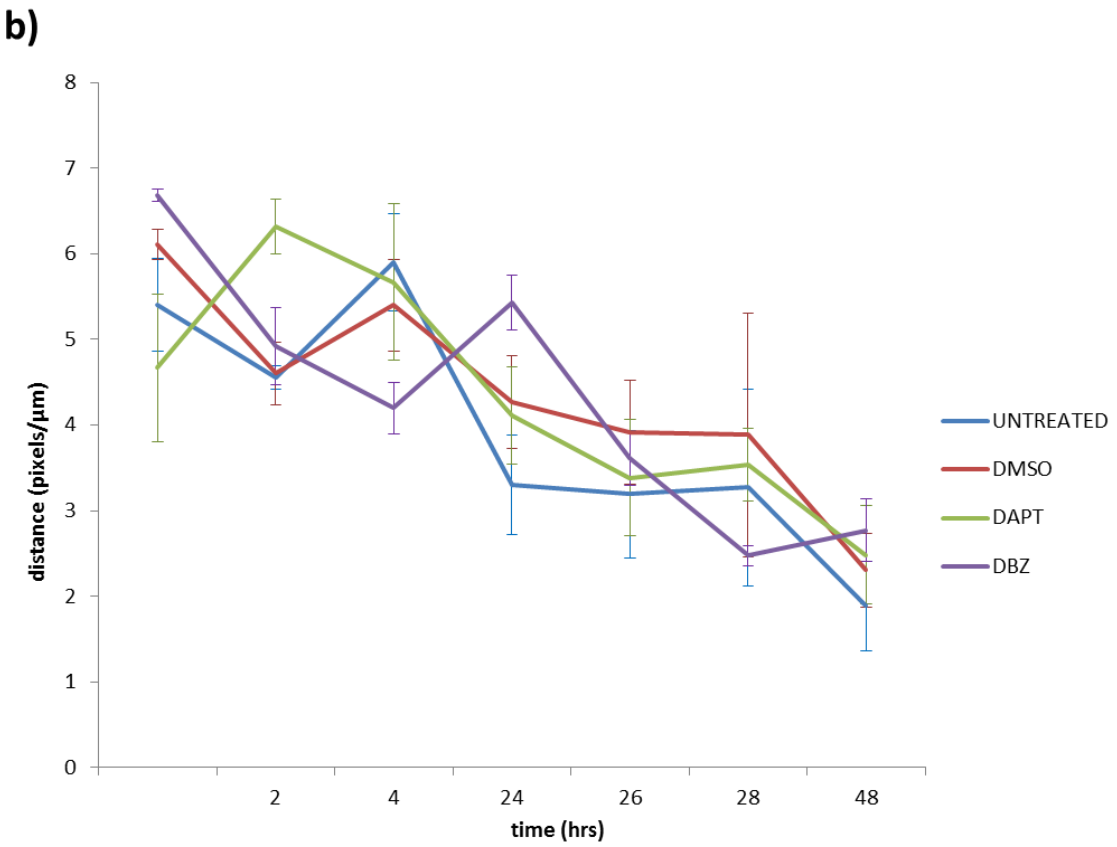


Figure 3.9 b) A plot representing the gap closure in Notch inhibited MCF7 cells. Gap closure was not significantly affected by either GSI treatment at 48hrs (p>0.05, paired Student's t-test) and was not significantly different from the controls (p>0.05, ANOVA, Kruskal Wallis test). Error Bars represent standard deviation of N=3

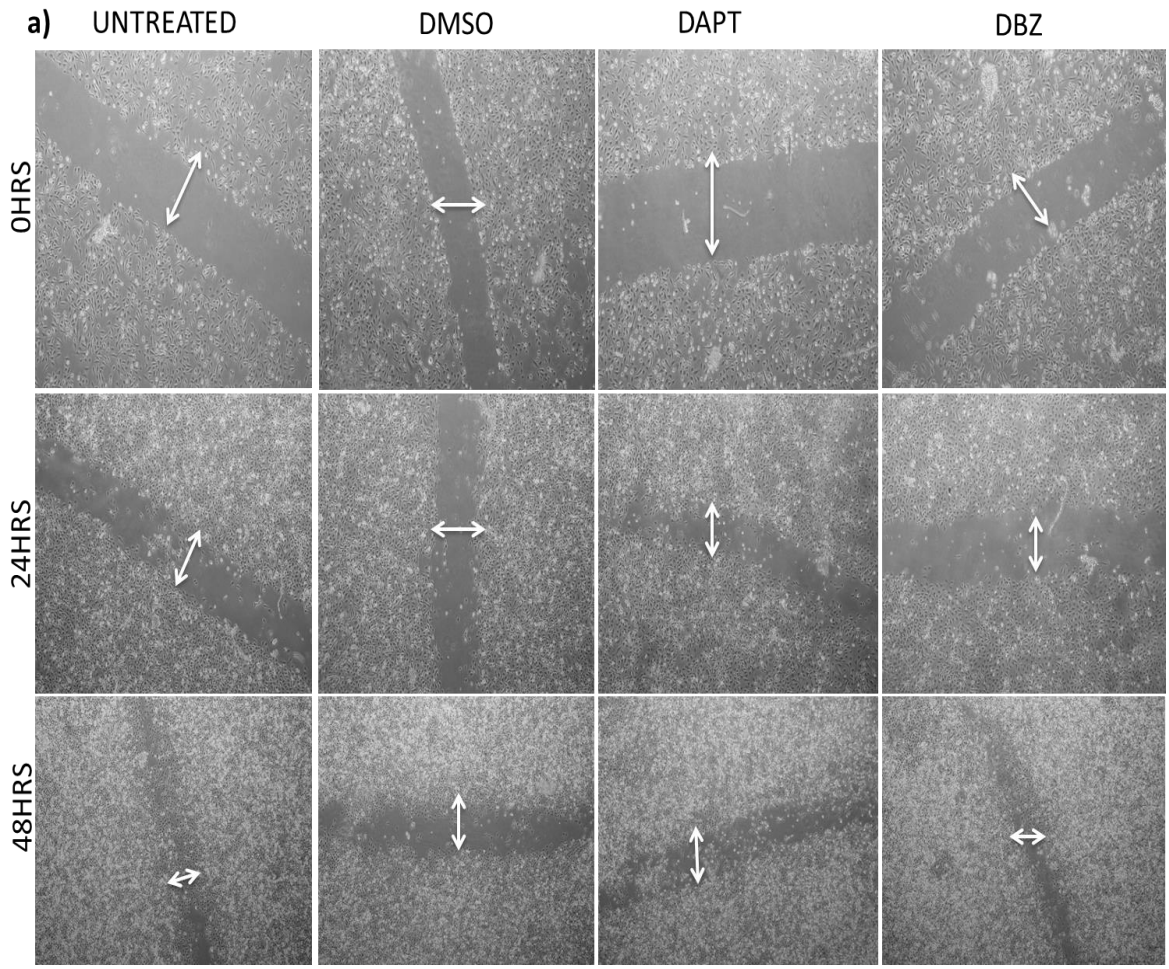


Figure 3.10.a) Notch inhibition does not affect cell migration in MDA-MB-231 cell line. Scratch assay of MDA-MB-231, gap closure appears to have been inhibited by the DMO vehicle control and DAPT at 48hrs. Treatment with DBZ appears to have little effect on the cell line. The white arrow indicates the cell free area that was measured over time. The gap closure is represented in plots below. (4X magnification)

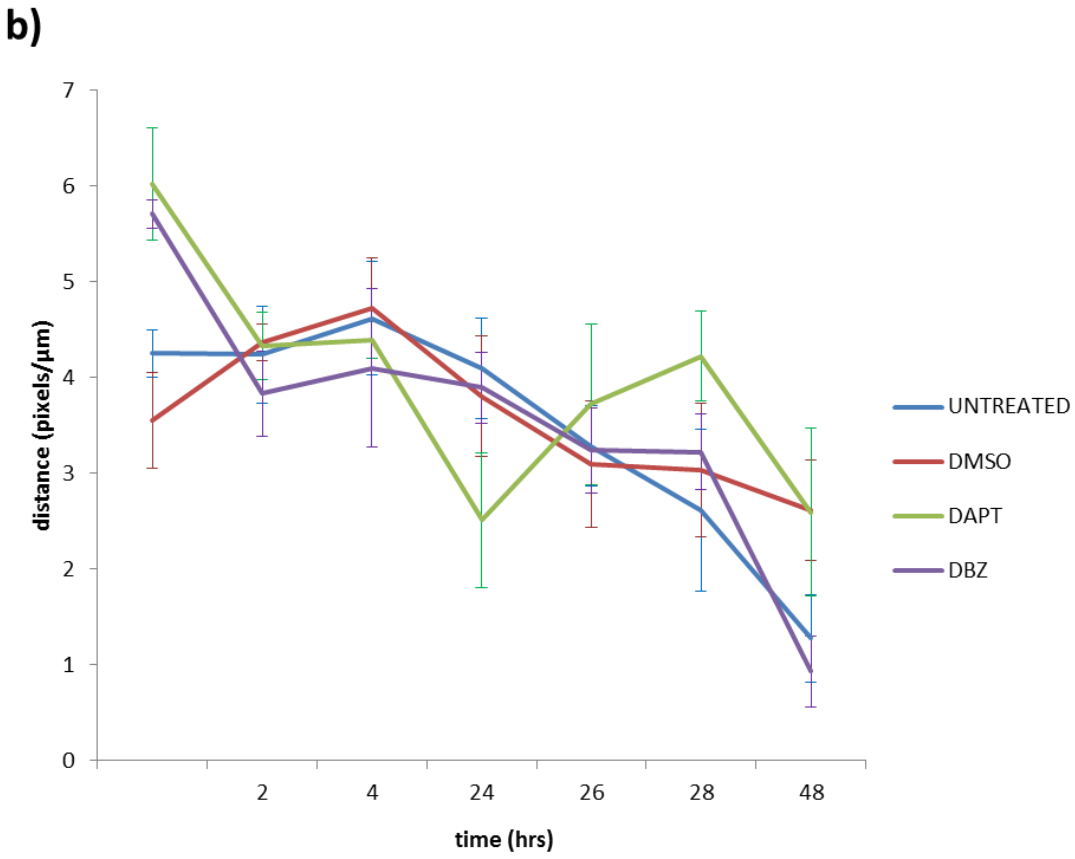


Figure 3.10 b) A plot representing the gap closure in Notch inhibited MDA-MB-231 cells.Gap closure was not significantly affected by either GSI treatment (p>0.05, paired, Student's t-test) and was not significantly different from the controls (p>0.05, ANOVA, Kruskal Wallis test) at 48hrs. Error Bars represent standard deviation of N=3

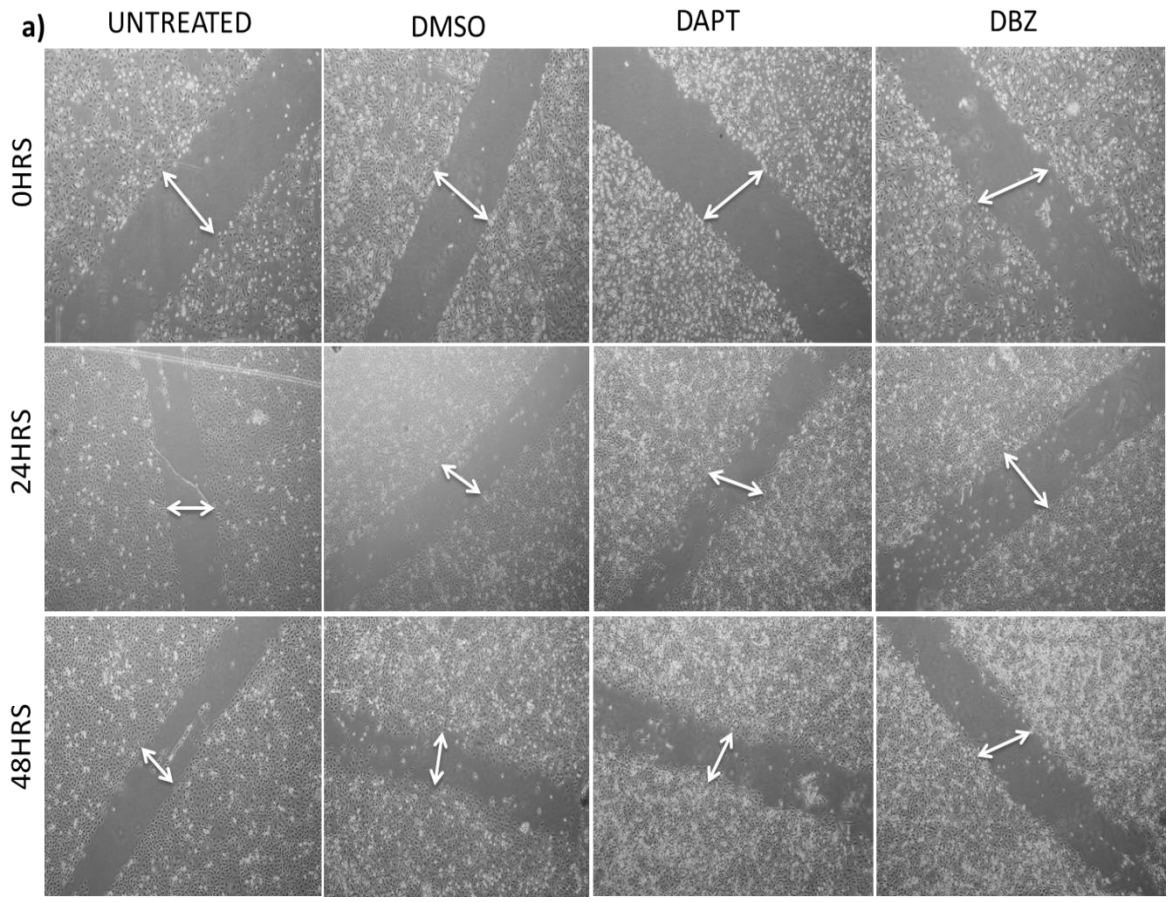


Figure 3.11.a) Notch inhibition does not affect cell migration in MDA-MB-436 cell line. Scratch assay of MDA-MB-436 cells. Gap closure was not significantly affected by the DMSO vehicle control and GSI treatment at 48hrs. The white arrow indicates the cell free area that was measured over time. The gap closure is represented in plots below. (4X magnification)

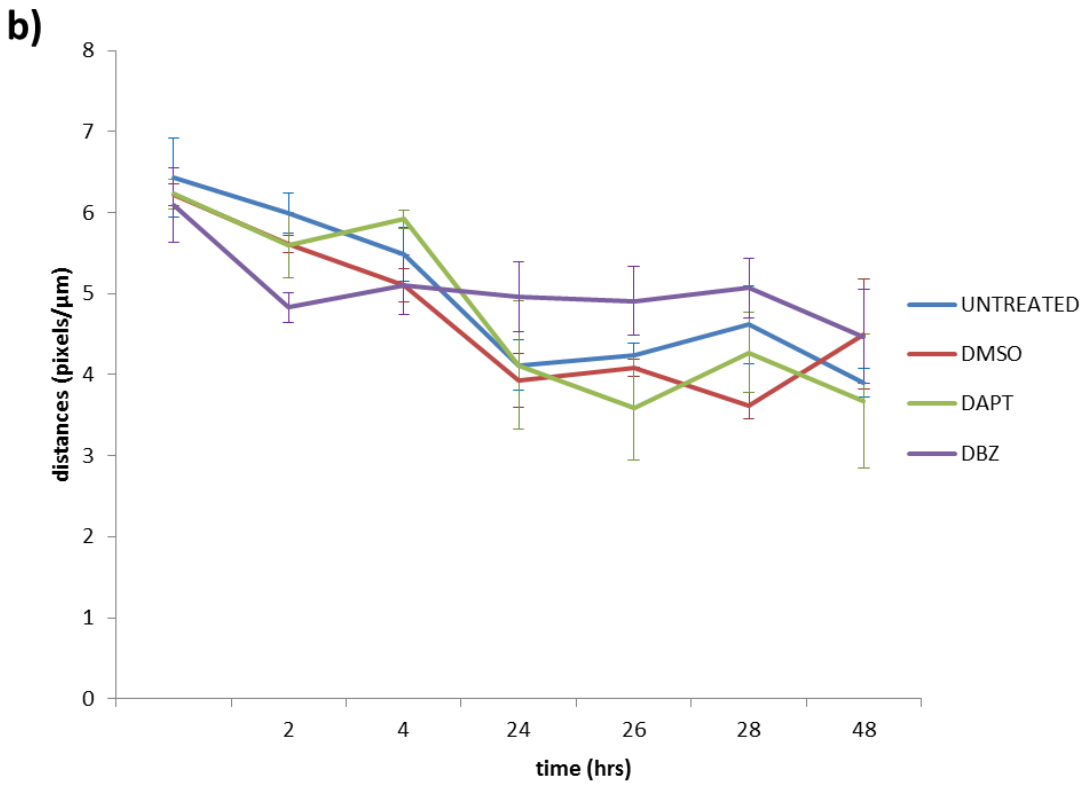


Figure 3.11 b) A plot representing the gap closure in Notch inhibited MDA-MB-436 cells. Gap closure was not significantly affected by either GSI treatment (p>0.05, paired, Student's t-test) and was not significantly different from the controls (p>0.05, ANOVA, Kruskal Wallis test). Error Bars represent standard deviation of N=3

CHAPTER 4: DISCUSSION

It has been reported by Rizzo and colleagues that, the Notch signalling pathway is deregulated in BC and that it is activated in the absence of oestrogen (Rizzo *et al*., 2009). . However to- date studies that confirm or challenge this have been few and far between. Moreover, studies that explore the relationship between Notch signalling and cell migration are sparse. In general research on the functional role of the Notch signalling pathway in TNBC is limited. The pertinent findings relating to Notch signalling in TNBC are discussed below.

4.1 Notch expression and activity

The subcellular localisation of NIC may be a morphological illustration of the functional activity of notch in the cell (Speiser *et al*., 2013). NIC is released into the cytoplasm once it has been cleaved by γ-secretase. Whilst it is in the cytoplasm, NIC is inactive and thus the signal has yet to exert its effects on gene expression. However, once translocated to the nucleus subsequent binding to DNA binding factors then allows for Notch target gene activation. Therefore accumulation of NIC in the cytoplasm indicates an inactive Notch signal, whilst an accumulation of NIC in the nucleus represents the active form.

When comparing the expression and localisation of NIC1 in hormone receptor positive cell lines to that of hormone insensitive cells, prior to γ-secretase inhibition, there was a similarity between the localisation of NIC1 in both the MCF-7 and MDA-MB-436 cell lines; as this factor is present within the nucleus and it is specifically associated with the nucleoli (Figure 3.1). This may be a good indication of the formation of the transcriptional

complex together with the DNA binding factors. While NIC1 was localised to the nucleoli of both cell lines, it differed in expression intensity; the MCF-7 cell line displayed more densely stained nucleoli compared to the MDA-MB-436 cell line, suggesting that Notch is more active in hormone receptor positive cells and less active in the hormone insensitive cells.

The localisation and expression of NIC1 in the MDA-MB-231 cell line was quite different to the above-mentioned cell lines; in these, NIC1 was both concentrated in a perinuclear aggregation on one side of the nucleus, suggestive of a Golgi/endoplasmic reticulum association, and was also densely scattered over the nuclear membrane, effectively masking the nucleoli. The observation suggests that the pathway is hyperactive in those cells.

Interestingly, though both the MB-MDA-231 and the MDA-MB-436 cell lines are TNBC models (Chavez *et al*., 2010), they express NIC differently. This may be seen as supporting evidence that there may indeed be subtypes of TNBC; this however is still quite controversial. It may also indicate that Notch activity is different within each subtype. This could indicate that oestrogen may not be an inhibitor of Notch, but rather that there may be crosstalk between Notch and other pathways that influence its activity. One such candidate may be the Wnt pathway; and, the MDA-MB-231 cell line possesses the WNT7B oncogene that is part of a large family of genes that regulate the WNT pathway (Huguet *et al*., 1994). Moreover, the deregulation of WNT is associated with BC, and it has been proposed that is involved in crosstalk with Notch signalling (Guo *et al*., 2011, Ayyanan *et al*., 2006, Yamaguchi *et al*., 2014, Visvader, 2009).

It is suggested here that the presence of the WNT oncogene in the MDA-MB-231 cell lines may be a factor influencing the up-regulation of Notch. In contrast the MDA-MB-436 cell line does not possess this gene, but Notch is down-regulated in these cells, which may indicate that in this instance a lack of oestrogen, may be causing deregulation in Notch activity in these cells. However, the MDA-MB-436 data obtained in the present study challenges the hypothesis that a lack of oestrogen increases Notch activity proposed by Rizzo *et. al* (2009) (Rizzo *et al*., 2009) , who based this notion on the observed increase in Notch activity when MCF-7 cell lines were deprived of oestrogen, or when oestrogen is antagonized by selective ER modulators. In contrast, however the findings observed here from the MDA-MB-231 cell lines agree with their data in experimentally oestrogen deprived MCF-7 cells, where NOTCH-1 could be detected in both the cytoplasm and nucleus. To date there is no report in the literature referring to the distribution of NIC1 in MDA-MB-436 cell lines (Bolos *et al*., 2007).

It is important to note here that the distribution of NIC1 alone is evaluated. Neither the distribution of NOTCH-2 intracellular component, NOTCH-3 intracellular component nor NOTCH-4 intracellular components were assessed. The expression and localisation of each of these could be remarkably different in each of the cell lines, since BC cells have been reported to co-express Notch receptors .

4.2 The cellular growth, proliferation and viability of human breast cancer cells

As recorded here, the hormone and growth receptor positive cells grow significantly faster than their receptor negative counterparts. This is somewhat expected as hormones and

growth factors are known to promote growth and proliferation of breast cells *in vivo* (Tarulli *et al*., 2014, Yarden, 2001, Sibilia *et al*., 2007). Although receptor positive BC grows much faster than TNBC, the latter is reportedly a more aggressive cancer (Dent *et al*., 2007). Therefore it is apparent that there are factors other than the presence of key breast cell receptors that are perpetuating TNBC tumours.

From this it was hypothesised that deregulated Notch signalling may be a key factor in TNBC cell proliferation and the cell lines were thus treated with GSIs. Notably the TNBC cell lines were more sensitive to GSI treatment when compared with receptor positive cell lines. These data corroborate the results presented by Lee *et.al* (2008) who found that GSI treatment of the MCF-7 and MDA-MB-231 cell lines decreased cell proliferation, to a greater effect in the MDA-MB-231 cell line (Lee *et al*., 2008a) . Also in the same study they found that GSI treatment abolished colony formation of MDA-MB-231 cells on soft agar, at the magnitude of three orders more than the MCF-7 cell line. In another study by Rizzo *et .al* (2009) GSI treatment of MDA-MB-231cells had strong anti-proliferative effects and when combined with Tamoxifen, GSI caused significant growth inhibitory effects (Rizzo *et al*., 2009). Additionally the combination of the GSI, PF-03084014 with docetaxel resulted in a decrease in tumour size and a reversal of chemo-resistance in TNBC xenograft models (Zhang *et al*., 2013). A preclinical study on breast tumours from 30 patients with advanced BC of an unspecified subtype showed that a combination of the GSI, MK-0725 and docetaxel reduced the numbers of BC CSCs (Schott et al., 2013).

Currently, there are three on going GSI/Notch pathway based clinical studies, two of which are specifically on TNBC (www.clinicaltrials.gov). One study is investigating the effects and the best dose of the GSI inhibitor, R04929097 when combined with paclitaxel and

carboplatin in patients with stage II and stage III TNBC (www.clinicaltrials.gov). The other investigates how well the same inhibitor will fair in treating patients with metastatic or recurrent TNBC. Overall, the findings reported on here concur with the literature having shown that GSI is effective in reducing TNBC cell proliferation and viability

4.2.1 Classical end-point assay versus real-time cell analysis assay

The TB classical end-point assay revealed that the GSIs do not affect cell viability of the MCF-7 and MDA-MB-436 cell lines, while the cell viability of MDA-MB-231 cell lines was significantly affected. These results differ from those produced by the RTCA system; this assay reveals that all cell lines are significantly affected by the GSI, demonstrating the sensitivity of evaluating cellular responses in real time. As well because it monitors cell behavior over time it is able to detect both cell viability and cell proliferation.

4.3 Notch and cell migration and morphology

In order to investigate the effect of inhibiting Notch on cell migration, the expression of the invasion and metastasis suppressor protein E-cadherin (Baranwal and Alahari, 2009) was assessed. Its normal physiologic process includes tissue morphology and epithelial-to-mesenchymal transition (EMT), wherein cells lose their epithelial characteristics and acquire mesenchymal features (Abdulla *et al*., 2013). Since the activation of invasion and metastasis are a particular hallmark of cancer, E-cadherin expression is thus considered a good marker for BC malignancy (Hanahan and Weinberg, 2011).

The receptor positive BC cells displayed a greater E-cadherin expression, which decreases when cells are treated with GSIs. The TNBC cell lines did not exhibit E-cadherin

expression and upon treatment with GSI it is not up-regulated in TNBC cells. The data observed here corroborate Chen *et al*. (2010) who report that an overexpression of NIC1 inhibits E-cadherin, in MDA-MB-231 because prior experiments show that MDA-MB-231 cell line overexpress NIC1 (Figure 3.1) (Chen *et al*., 2010) . However, in contrast, when tumour xenografts from MDA-MB-231 cell lines were treated with GSI, immunohistochemical evaluation demonstrated an increase in E-cadherin expression, due to the GSI preventing its proteolysis (Leong *et al*., 2007).

While in the present study it may then be hypothesised that a decrease in Notch could result in E-cadherin up-regulation, this however was not apparent in the MDA-MB-436 cell line; instead E-cadherin expression was not detected. This suggests that possibly in some types of TNBC cell lines Notch and E-cadherin expression are independent or dependant on each other. This is a further example of the different behaviours of TNBC cell types and also provides evidence that the deregulation of the signal is different in TNBC tumours.

Furthermore it is shown here that GSI treatment causes a disruption in the F-actin cytoskeleton in the TNBC cell lines, with DBZ affecting the F-actin cytoskeleton of the MDA-MB-231 cell line more so than DAPT treatment. This may be an indication that Notch deregulation may have adverse effects on the integrity of the F-actin cytoskeleton. Disruption of the cytoskeleton could disturb proper cellular function, such as cell motility and cell signalling. This in turn may possibly affect the ability of the cells to migrate as well as their ability to effectively communicate with neighbouring cells. As the cellular junctions are disturbed it's most likely that activation of the Notch signal is aberrant. From

the literature it still unclear as to what effect Notch inhibition has on the F-actin cytoskeleton.

The migration/scratch assay showed that pre-GSI treatment, MCF-7 cells had a far greater gap closure after 48hrs, when compared to TNBC cell lines, which showed less migration, especially the MDA-MB-436 cells. Post-treatment, the results were similar, wherein MCF-7 cell migration was greater after 48hrs, compared to cell migration of the TNBC's. Within each cell line regardless of treatment, however, the difference in cell migration was not statistically significant. A possible explanation for this result is that migration was studied under normoxic cell culture conditions. Other studies however have concluded that hypoxia activates Notch signal induced migration (Chen *et al*., 2010). The data obtained here also contradicts another study which reported that Notch inhibition of MDA-MB-231 cells by DAPT and R04929097 GSIs increases E-cadherin expression together with a reduction in their invasive capacity (Bolos *et al*., 2013). It has been reported that knockdown of Notch-1 exhibited limited wound closure activity even after 48hrs (Zhao et al., 2014).

4.4 Conclusion

The data presented here show that Notch activity is more stable in hormone receptor positive MCF-7 cell line compared to TNBC cell lines. Moreover, while GSIs are effective in decreasing the cell proliferation of both subtypes of BC, TNBC were however the most sensitive to them.

Sensitivity to ER status does not seem to be a strict regulator of Notch activity as each TNBC cell model seemed to express Notch in a different manner. Although not statistically

significant, cell migration did decrease with Notch inhibition and further work is required to reach a definitive conclusion relating to Notch and migration.

CHAPTER 5: PERSPECTIVES AND FUTURE WORK

Although we demonstrate here that the Notch signal may be dysfunctional in TNBC, the effects of neither NOTCH-1 upregulation nor NOTCH- receptor knockdown were assessed, as this was beyond the scope of the study. In particular the modulation of the NOTCH-1 gene will allow for the testing of the hypothesis that NOTCH-1 expression regulates for cell proliferation in TNBCs. Moreover, it may be important to replicate the present studies under hypoxic conditions, since it is reported in the literature that this activates Notch, causing an increased BC cell migration. Such an approach may be of some consequence since hypoxia rather than normoxia may be indicative of the *in vivo* tumour environment.

5.1 Proposed approach for future work

To further elucidate the role of the Notch pathway, it is proposed that further *in vitro* studies be carried out with MCF-7 and T47D cell line as the receptor positive BC representative cell line and MDA-MB-231 and MDA-MB-436 cell lines as the TNBC representative cell line. To assess the effects of Notch-1 down-regulation on cell proliferation and migration, siRNA knockdown of the NOTCH-1 gene should be carried out and monitored using the RTCA system. Moreover, an effective means to determine more precisely the effects of NOTCH-1 activity would be an inducible system of NOTCH-1 expression. In association with this, it may be important to evaluate further changes in cell adhesion proteins, such as integrins and other EMT markers, for example Vimentin

Each experiment would be performed under both normoxic and hypoxic conditions to further understand the relationship between Notch and BC cell migration. Below is a diagram of the proposed scheme for future work (Figure 5.1). In summary fine control of Notch gene expression will provide for a better understanding of Notch expression in breast cancer.

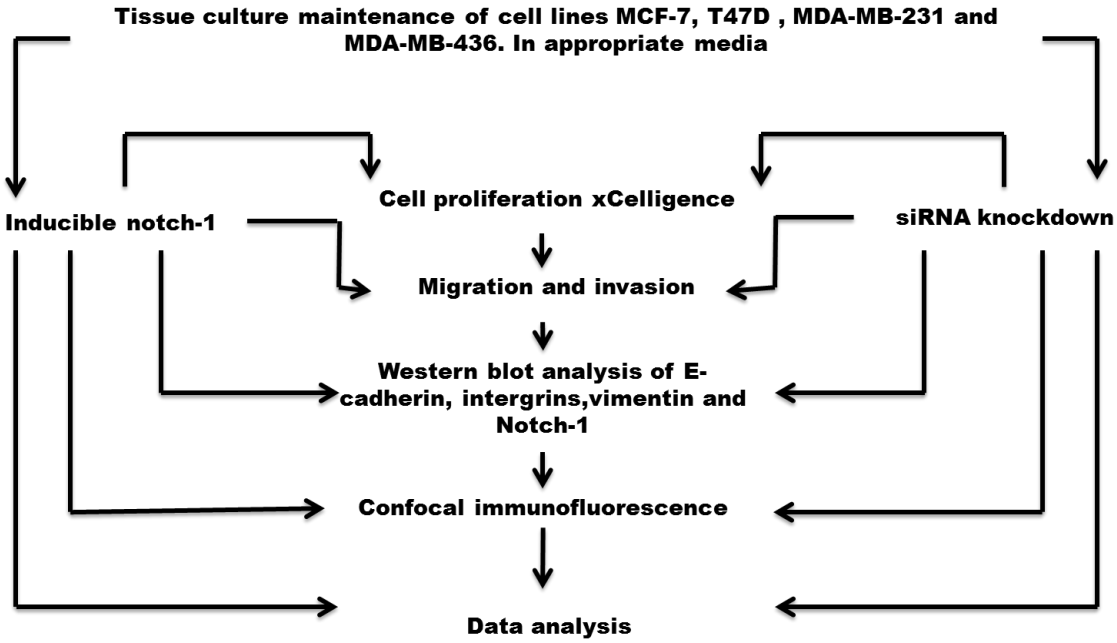


Figure 5.1. Diagram representing the methodology for future work. BC cell lines will maintained in appropriate media.Notch-1 expression induced using a NIC1 inducible clone. Knockdown of NOTCH-1 may be done using siRNA and the effects thereafter, can be evaluated using xCelligence, Western-blot and confocal immunofluorescence.

CHAPTER 6: REFERENCES

6.1. Journal articles

1. ABDULLA, T., LUNA-ZURITA, L., DE LA POMPA, J. L., SCHLEICH, J. M. & SUMMERS, R. 2013. Epithelial to mesenchymal transition-the roles of cell morphology, labile adhesion and junctional coupling. *Computer Methods Programs Biomedicine,* 111**,** 435-46.
2. ANDRE, F. & ZIELINSKI, C. C. 2012. Optimal strategies for the treatment of metastatic triple-negative breast cancer with currently approved agents. *Annals of Oncology,* 23**,** vi46-51.
3. ASTER, J. C., BLACKLOW, S. C. & PEAR, W. S. 2011. Notch signalling in T-cell lymphoblastic leukaemia/lymphoma and other haematological malignancies. *The Journal of Pathology,* 223**,** 262-73.
4. AULMANN, S., WALDBURGER, N., PENZEL, R., ANDRULIS, M., SCHIRMACHER, P. & SINN, H. P. 2010. Reduction of CD44(+)/CD24(-) breast cancer cells by conventional cytotoxic chemotherapy. *Human Pathology,* 41**,** 574-81.
5. AYYANAN, A., CIVENNI, G., CIARLONI, L., MOREL, C., MUELLER, N., LEFORT, K., MANDINOVA, A., RAFFOUL, W., FICHE, M., DOTTO, G. P. & BRISKEN, C. 2006. Increased Wnt signaling triggers oncogenic conversion of human breast epithelial cells by a Notch-dependent mechanism. *Proceeding of the National Academy of Science U S A,* 103**,** 3799-804.
6. BADVE, S., DABBS, D. J., SCHNITT, S. J., BAEHNER, F. L., DECKER, T., EUSEBI, V., FOX, S. B., ICHIHARA, S., JACQUEMIER, J., LAKHANI, S. R., PALACIOS, J., RAKHA, E. A., RICHARDSON, A. L., SCHMITT, F. C., TAN, P. H., TSE, G. M., WEIGELT, B., ELLIS, I. O. & REIS-FILHO, J. S. 2011. Basal-like and triple-negative breast cancers: a critical review with an emphasis on the implications for pathologists and oncologists. *Modern Pathology,* 24**,** 157-67.

7. BARANWAL, S. & ALAHARI, S. K. 2009. Molecular mechanisms controlling E-cadherin expression in breast cancer. *Biochemical and Biophysical Research Communications,* 384**,** 6-11.
8. BAYOUMI, Y., ABDELSAMIE, A., ABDELSAID, A. & RADWAN, A. 2014. Locoregional recurrence of triple-negative breast cancer: effect of type of surgery and adjuvant postoperative radiotherapy. *Breast Cancer,* 6**,** 151-8.
9. BEABER, E. F., MALONE, K. E., TANG, M. T., BARLOW, W. E., PORTER, P. L., DALING, J. R. & LI, C. I. 2014. Oral contraceptives and breast cancer risk overall and by molecular subtype among young women. *Cancer Epidemiology Biomarkers and Prevention,* 23**,** 755-64.
10. BOLOS, V., GREGO-BESSA, J. & DE LA POMPA, J. L. 2007. Notch signaling in development and cancer. *Endocrine Reviews,* 28**,** 339-63.
11. BOLOS, V., MIRA, E., MARTINEZ-POVEDA, B., LUXAN, G., CANAMERO, M., MARTINEZ, A. C., MANES, S. & DE LA POMPA, J. L. 2013. Notch activation stimulates migration of breast cancer cells and promotes tumor growth. *Breast Cancer Research,* 15.
12. BREWSTER, A. M., CHAVEZ-MACGREGOR, M. & BROWN, P. Epidemiology, biology, and treatment of triple-negative breast cancer in women of African ancestry, *Lancet Oncology*. 2014 Dec;15(13):e625-e634. doi: 10.1016/S1470-2045(14)70364-X. Epub 2014 Nov 24.
13. BRINKLEY, B. R., BEALL, P. T., WIBLE, L. J., MACE, M. L., TURNER, D. S. & CAILLEAU, R. M. 1980. Variations in cell form and cytoskeleton in human breast carcinoma cells in vitro. *Cancer Research,* 40**,** 3118-29.
14. CAPACCIONE, K. M. & PINE, S. R. 2013. The Notch signaling pathway as a mediator of tumor survival. *Carcinogenesis,* 34**,** 1420-30.
15. CAREY, L., WINER, E., VIALE, G., CAMERON, D. & GIANNI, L. 2010. Triple-negative breast cancer: disease entity or title of convenience? *Nature Reviews Clinical Oncology,* 7**,** 683-92.
16. CHAVEZ, K. J., GARIMELLA, S. V. & LIPKOWITZ, S. 2010. Triple negative breast cancer cell lines: one tool in the search for better treatment of triple negative breast cancer. *Breast Disease,* 32**,** 35-48.

17. CHEN, J., IMANAKA, N., CHEN, J. & GRIFFIN, J. D. 2010. Hypoxia potentiates Notch signaling in breast cancer leading to decreased E-cadherin expression and increased cell migration and invasion. *British Journal of Cancer,* 102**,** 351-60.
18. CHILLAKURI, C. R., SHEPPARD, D., LEA, S. M. & HANDFORD, P. A. 2012. Notch receptor-ligand binding and activation: insights from molecular studies. *Seminars in Cell and Developmental Biology,* 23**,** 421-8.
19. CORTAZAR, P., ZHANG, L., UNTCH, M., MEHTA, K., COSTANTINO, J. P., WOLMARK, N., BONNEFOI, H., CAMERON, D., GIANNI, L., VALAGUSSA, P., SWAIN, S. M., PROWELL, T., LOIBL, S., WICKERHAM, D. L., BOGAERTS, J., BASELGA, J., PEROU, C., BLUMENTHAL, G., BLOHMER, J., MAMOUNAS, E. P., BERGH, J., SEMIGLAZOV, V., JUSTICE, R., EIDTMANN, H., PAIK, S., PICCART, M., SRIDHARA, R., FASCHING, P. A., SLAETS, L., TANG, S., GERBER, B., GEYER, C. E., JR., PAZDUR, R., DITSCH, N., RASTOGI, P., EIERMANN, W. & VON MINCKWITZ, G. 2014. Pathological complete response and long-term clinical benefit in breast cancer: the CTNeoBC pooled analysis. *Lancet,* 384**,** 164-72.
20. COUCH, F. J., HART, S. N., SHARMA, P., TOLAND, A. E., WANG, X., MIRON, P., OLSON, J. E., GODWIN, A. K., PANKRATZ, V. S., OLSWOLD, C., SLETTEDAHL, S., HALLBERG, E., GUIDUGLI, L., DAVILA, J. I., BECKMANN, M. W., JANNI, W., RACK, B., EKICI, A. B., SLAMON, D. J., KONSTANTOPOULOU, I., FOSTIRA, F., VRATIMOS, A., FOUNTZILAS, G., PELTTARI, L. M., TAPPER, W. J., DURCAN, L., CROSS, S. S., PILARSKI, R., SHAPIRO, C. L., KLEMP, J., YAO, S., GARBER, J., COX, A., BRAUCH, H., AMBROSONE, C., NEVANLINNA, H., YANNOUKAKOS, D., SLAGER, S. L., VACHON, C. M., ECCLES, D. M. & FASCHING, P. A. 2015. Inherited mutations in 17 breast cancer susceptibility genes among a large triple-negative breast cancer cohort unselected for family history of breast cancer. *Journal of Clinical Oncology,* 33**,** 304-11.
21. DAVIES, E. A., RENSHAW, C., DIXON, S., MOLLER, H. & COUPLAND, V. H. 2013. Socioeconomic and ethnic inequalities in screen-detected breast cancer in London. *Journal of Public Health,* 35**,** 607-15.

22. DAWOOD, S., LEI, X., LITTON, J. K., BUCHHOLZ, T. A., HORTOBAGYI, G. N. & GONZALEZ-ANGULO, A. M. 2012. Impact of body mass index on survival outcome among women with early stage triple-negative breast cancer. *Clinical Breast Cancer,* 12**,** 364-72.
23. DENT, R., TRUDEAU, M., PRITCHARD, K. I., HANNA, W. M., KAHN, H. K., SAWKA, C. A., LICKLEY, L. A., RAWLINSON, E., SUN, P. & NAROD, S. A. 2007. Triple-negative breast cancer: clinical features and patterns of recurrence. *Clinical Cancer Research,* 13**,** 4429-34.
24. DEXTER, J. S. 1914. The Analysis of a Case of Continuous Variation in Drosophila by a Study of Its Linkage Relations. *The American Naturalist,* 48**,** 712-758.
25. DICKENS, C., DUARTE, R., ZIETSMAN, A., CUBASCH, H., KELLETT, P., SCHUZ, J., KIELKOWSKI, D. & MCCORMACK, V. 2014a. Racial comparison of receptor-defined breast cancer in southern african women: subtype prevalence and age-incidence analysis of nationwide cancer registry data. *Cancer Epidemiology Biomarkers and Prevention,* 23**,** 2311-21.
26. DICKENS, C., JOFFE, M., JACOBSON, J., VENTER, F., SCHUZ, J., CUBASCH, H. & MCCORMACK, V. 2014b. Stage at breast cancer diagnosis and distance from diagnostic hospital in a periurban setting: a South African public hospital case series of over 1,000 women. *International Journal of Cancer,* 135**,** 2173-82.
27. DICKSON, B. C., MULLIGAN, A. M., ZHANG, H., LOCKWOOD, G., O'MALLEY, F. P., EGAN, S. E. & REEDIJK, M. 2007. High-level JAG1 mRNA and protein predict poor outcome in breast cancer. *Modern Pathology,* 20**,** 685-93.
28. DOHERTY, G. J. & MCMAHON, H. T. 2008. Mediation, modulation, and consequences of membrane-cytoskeleton interactions. *Annual Reviews of Biophysics,* 37**,** 65-95.
29. DOLLE, J. M., DALING, J. R., WHITE, E., BRINTON, L. A., DOODY, D. R., PORTER, P. L. & MALONE, K. E. 2009. Risk factors for triple-negative breast cancer in women under the age of 45 years. *Cancer Epidemiology Biomarkers and Prevention,* 18**,** 1157-66.

30. DU, R., SUN, W., XIA, L., ZHAO, A., YU, Y., ZHAO, L., WANG, H., HUANG, C. & SUN, S. 2012. Hypoxia-induced down-regulation of microRNA-34a promotes EMT by targeting the Notch signaling pathway in tubular epithelial cells. *PLoS One,* 7**,** 17.
31. DUNN, B. K., AGURS-COLLINS, T., BROWNE, D., LUBET, R. & JOHNSON, K. A. 2010. Health disparities in breast cancer: biology meets socioeconomic status. *Breast Cancer Research and Treatment,* 121**,** 281-92.
32. EIERMANN, W., BERGH, J., CARDOSO, F., CONTE, P., CROWN, J., CURTIN, N. J., GLIGOROV, J., GUSTERSON, B., JOENSUU, H., LINDERHOLM, B. K., MARTIN, M., PENAULT-LLORCA, F., PESTALOZZI, B. C., RAZIS, E., SOTIRIOU, C., TJULANDIN, S. & VIALE, G. 2012. Triple negative breast cancer: Proposals for a pragmatic definition and implications for patient management and trial design. *The Breast,* 21**,** 20-26.
33. ELLISEN, L. W., BIRD, J., WEST, D. C., SORENG, A. L., REYNOLDS, T. C., SMITH, S. D. & SKLAR, J. 1991. TAN-1, the human homolog of the Drosophila notch gene, is broken by chromosomal translocations in T lymphoblastic neoplasms. *Cell,* 66**,** 649-61.
34. ELSAWAF, Z., SINN, H. P., ROM, J., BERMEJO, J. L., SCHNEEWEISS, A. & AULMANN, S. 2013. Biological subtypes of triple-negative breast cancer are associated with distinct morphological changes and clinical behaviour. *Breast,* 22**,** 986-92.
35. ENG, A., MCCORMACK, V. & DOS-SANTOS-SILVA, I. 2014. Receptor-defined subtypes of breast cancer in indigenous populations in Africa: a systematic review and meta-analysis. *PLoS Medicine,* 11.
36. ESCUDERO-ESPARZA, A., JIANG, W. G. & MARTIN, T. A. 2011. The Claudin family and its role in cancer and metastasis. *Front Biosciences,* 16**,** 1069-83.
37. ESPINOZA, I. & MIELE, L. 2013. Notch inhibitors for cancer treatment. *Pharmacology & Therapeutics,* 139**,** 95-110.
38. FARNIE, G. & CLARKE, R. 2007. Mammary Stem Cells and Breast Cancer—Role of Notch Signalling. *Stem Cell Reviews,* 3**,** 169-175.

39. FERLAY, J., SOERJOMATARAM, I., DIKSHIT, R., ESER, S., MATHERS, C., REBELO, M., PARKIN, D. M., FORMAN, D. & BRAY, F. 2015. Cancer incidence and mortality worldwide: Sources, methods and major patterns in GLOBOCAN 2012. *International Journal of Cancer,* 136**,** 9.
40. FIRE, A., XU, S., MONTGOMERY, M. K., KOSTAS, S. A., DRIVER, S. E. & MELLO, C. C. 1998. Potent and specific genetic interference by double-stranded RNA in Caenorhabditis elegans. *Nature,* 391**,** 806-11.
41. FOSTIRA, F., TSITLAIDOU, M., PAPADIMITRIOU, C., PERTESI, M., TIMOTHEADOU, E., STAVROPOULOU, A. V., GLENTIS, S., BOURNAKIS, E., BOBOS, M., PECTASIDES, D., PAPAKOSTAS, P., PENTHEROUDAKIS, G., GOGAS, H., SKARLOS, P., SAMANTAS, E., BAFALOUKOS, D., KOSMIDIS, P. A., KOUTRAS, A., YANNOUKAKOS, D., KONSTANTOPOULOU, I. & FOUNTZILAS, G. 2012. Prevalence of BRCA1 mutations among 403 women with triple-negative breast cancer: implications for genetic screening selection criteria: a Hellenic Cooperative Oncology Group Study. *Breast Cancer Research and Treatment,* 134**,** 353-62.
42. FRITSCHY, J.-M. & HÄRTIG, W. 2001. Immunofluorescence. *eLS.* John Wiley & Sons, Ltd.
43. GALUKANDE, M., WABINGA, H., MIREMBE, F., KARAMAGI, C. & ASEA, A. 2014. Molecular breast cancer subtypes prevalence in an indigenous Sub Saharan African population. *Pan African Medical Journal,* 17.
44. GAO, J., SARKAR, F. H., MIELE, L. & WANG, Z. 2014. Chapter 4 - The Role of Notch Signaling Pathway in the Progression of Pancreatic Cancer. *In:* AZMI, A. S. (ed.) *Molecular Diagnostics and Treatment of Pancreatic Cancer.* Oxford: Academic Press.
45. GLUZ, O., LIEDTKE, C., GOTTSCHALK, N., PUSZTAI, L., NITZ, U. & HARBECK, N. 2009. Triple-negative breast cancer--current status and future directions. *Annals of Oncology,* 20**,** 1913-27.
46. GOLDE, T. E., KOO, E. H., FELSENSTEIN, K. M., OSBORNE, B. A. & MIELE, L. 2013. γ-Secretase inhibitors and modulators. *Biochimica et Biophysica Acta (BBA) - Biomembranes,* 1828**,** 2898-2907.

47. GRAHAM, J. D., MOTE, P. A., SALAGAME, U., VAN DIJK, J. H., BALLEINE, R. L., HUSCHTSCHA, L. I., REDDEL, R. R. & CLARKE, C. L. 2009. DNA replication licensing and progenitor numbers are increased by progesterone in normal human breast. *Endocrinology,* 150**,** 3318-26.
48. GREENUP, R., BUCHANAN, A., LORIZIO, W., RHOADS, K., CHAN, S., LEEDOM, T., KING, R., MCLENNAN, J., CRAWFORD, B., KELLY MARCOM, P. & SHELLEY HWANG, E. 2013. Prevalence of BRCA mutations among women with triple-negative breast cancer (TNBC) in a genetic counseling cohort. *Annals of Surgical Oncology,* 20**,** 3254-8.
49. GUO, S., LIU, M. & GONZALEZ-PEREZ, R. R. 2011. Role of Notch and its oncogenic signaling crosstalk in breast cancer. *Biochim Biophys Acta-Review on Cancer,* 2**,** 197-213.
50. HAIMAN, C. A., CHEN, G. K., VACHON, C. M., CANZIAN, F., DUNNING, A., MILLIKAN, R. C., WANG, X., ADEMUYIWA, F., AHMED, S., AMBROSONE, C. B., BAGLIETTO, L., BALLEINE, R., BANDERA, E. V., BECKMANN, M. W., BERG, C. D., BERNSTEIN, L., BLOMQVIST, C., BLOT, W. J., BRAUCH, H., BURING, J. E., CAREY, L. A., CARPENTER, J. E., CHANG-CLAUDE, J., CHANOCK, S. J., CHASMAN, D. I., CLARKE, C. L., COX, A., CROSS, S. S., DEMING, S. L., DIASIO, R. B., DIMOPOULOS, A. M., DRIVER, W. R., DUNNEBIER, T., DURCAN, L., ECCLES, D., EDLUND, C. K., EKICI, A. B., FASCHING, P. A., FEIGELSON, H. S., FLESCH-JANYS, D., FOSTIRA, F., FORSTI, A., FOUNTZILAS, G., GERTY, S. M., GILES, G. G., GODWIN, A. K., GOODFELLOW, P., GRAHAM, N., GRECO, D., HAMANN, U., HANKINSON, S. E., HARTMANN, A., HEIN, R., HEINZ, J., HOLBROOK, A., HOOVER, R. N., HU, J. J., HUNTER, D. J., INGLES, S. A., IRWANTO, A., IVANOVICH, J., JOHN, E. M., JOHNSON, N., JUKKOLA-VUORINEN, A., KAAKS, R., KO, Y. D., KOLONEL, L. N., KONSTANTOPOULOU, I., KOSMA, V. M., KULKARNI, S., LAMBRECHTS, D., LEE, A. M., MARCHAND, L. L., LESNICK, T., LIU, J., LINDSTROM, S., MANNERMAA, A., MARGOLIN, S., MARTIN, N. G., MIRON, P., MONTGOMERY, G. W., NEVANLINNA, H., NICKELS, S., NYANTE, S., OLSWOLD, C., PALMER, J., PATHAK, H., PECTASIDES, D.,

PEROU, C. M., PETO, J., PHAROAH, P. D., POOLER, L. C., PRESS, M. F., PYLKAS, K., REBBECK, T. R., RODRIGUEZ-GIL, J. L., ROSENBERG, L., ROSS, E., RUDIGER, T., SILVA IDOS, S., et al. 2011. A common variant at the TERT-CLPTM1L locus is associated with estrogen receptor-negative breast cancer. *Nature Genetics,* 43**,** 1210-4.

51. HAN, J., MA, I., HENDZEL, M. J. & ALLALUNIS-TURNER, J. 2009. The cytotoxicity of gamma-secretase inhibitor I to breast cancer cells is mediated by proteasome inhibition, not by gamma-secretase inhibition. *Breast Cancer Research,* 11**,** 6.
52. HAN, S., DZIEDZIC, N., GADUE, P., KELLER, G. M. & GOUON-EVANS, V. 2011. An endothelial cell niche induces hepatic specification through dual repression of Wnt and Notch signaling. *Stem Cells,* 29**,** 217-28.
53. HANAHAN, D. & WEINBERG, ROBERT A. 2011. Hallmarks of Cancer: The Next Generation. *Cell,* 144**,** 646-674.
54. HENG, Y.-W. & KOH, C.-G. 2010. Actin cytoskeleton dynamics and the cell division cycle. *The International Journal of Biochemistry & Cell Biology,* 42**,** 1622-1633.
55. HOLLIDAY, D. L. & SPEIRS, V. 2011. Choosing the right cell line for breast cancer research. *Breast Cancer Research,* 13.
56. HUGUET, E. L., MCMAHON, J. A., MCMAHON, A. P., BICKNELL, R. & HARRIS, A. L. 1994. Differential expression of human Wnt genes 2, 3, 4, and 7B in human breast cell lines and normal and disease states of human breast tissue. *Cancer Res,* 54**,** 2615-21.
57. IGNATIADIS, M. & SOTIRIOU, C. 2013. Luminal breast cancer: from biology to treatment. *Nature Reviews Clinical Oncology,* 10**,** 494-506.
58. KALLURI, R. & WEINBERG, R. A. 2009. The basics of epithelial-mesenchymal transition. *The Journal of Clinical Investigation* 119**,** 1420-8.
59. KARAGIANNIS, T. C. & EL-OSTA, A. 2005. RNA interference and potential therapeutic applications of short interfering RNAs. *Cancer Gene Therapy,* 12**,** 787-95.

60. KAWAI, M., MALONE, K. E., TANG, M. T. & LI, C. I. 2014. Height, body mass index (BMI), BMI change, and the risk of estrogen receptor-positive, HER2-positive, and triple-negative breast cancer among women ages 20 to 44 years. *Cancer,* 120**,** 1548-56.
61. KIDD, S., KELLEY, M. R. & YOUNG, M. W. 1986. Sequence of the notch locus of Drosophila melanogaster: relationship of the encoded protein to mammalian clotting and growth factors. *Molecular and Cell Biology,* 6**,** 3094-108.
62. KIKUCHI, A., YAMAMOTO, H., SATO, A. & MATSUMOTO, S. 2011. New insights into the mechanism of Wnt signaling pathway activation. *International Review of Cell and Molecular Biology,* 291**,** 21-71.
63. KIM, S. H., YIN, Y. I., LI, Y. M. & SISODIA, S. S. 2004. Evidence that assembly of an active gamma-secretase complex occurs in the early compartments of the secretory pathway. *The Journal of Biological Chemistry,* 279**,** 48615-9.
64. KOPAN, R. & ILAGAN, M. X. 2009. The canonical Notch signaling pathway: unfolding the activation mechanism. *Cell,* 137**,** 216-33.
65. KORKAYA, H. & WICHA, M. S. 2009. HER-2, notch, and breast cancer stem cells: targeting an axis of evil. *Clinical Cancer Research,* 15**,** 1845-7.
66. KOZIOL, M., PUSKULLUOGLU, M. & ZYGULSKA, A. 2012. PARP inhibitors and their role in the therapy of triple-negative metastatic breast cancer. *Przegl Lek,* 69**,** 265-70.
67. KRAMER, N., WALZL, A., UNGER, C., ROSNER, M., KRUPITZA, G., HENGSTSCHLÄGER, M. & DOLZNIG, H. 2013. In vitro cell migration and invasion assays. *Mutation Research/Reviews in Mutation Research,* 752**,** 10-24.
68. LEE, C. W., RASKETT, C. M., PRUDOVSKY, I. & ALTIERI, D. C. 2008a. Molecular dependence of estrogen receptor-negative breast cancer on a notch-survivin signaling axis. *Cancer Research,* 68**,** 5273-81.
69. LEE, C. W., SIMIN, K., LIU, Q., PLESCIA, J., GUHA, M., KHAN, A., HSIEH, C. C. & ALTIERI, D. C. 2008b. A functional Notch-survivin gene signature in basal breast cancer. *Breast Cancer Research,* 10**,** 24.
70. LEE, H. J., SONG, I. H., SEO, A. N., LIM, B., KIM, J. Y., LEE, J. J., PARK, I. A., SHIN, J., YU, J. H., AHN, J. H. & GONG, G. 2014. Correlations Between

Molecular Subtypes and Pathologic Response Patterns of Breast Cancers After Neoadjuvant Chemotherapy. *Annals of Surgical Oncology,* 6**,** 6.

71. LEHMANN, B. D., BAUER, J. A., CHEN, X., SANDERS, M. E., CHAKRAVARTHY, A. B., SHYR, Y. & PIETENPOL, J. A. 2011. Identification of human triple-negative breast cancer subtypes and preclinical models for selection of targeted therapies. *The Journal of Clinical Investigation,* 121**,** 2750-2767.
72. LEONG, K. G., NIESSEN, K., KULIC, I., RAOUF, A., EAVES, C., POLLET, I. & KARSAN, A. 2007. Jagged1-mediated Notch activation induces epithelial-to-mesenchymal transition through Slug-induced repression of E-cadherin. *The Journal of Experimental Medicine,* 204**,** 2935-48.
73. LEWIS, H. D., PEREZ REVUELTA, B. I., NADIN, A., NEDUVELIL, J. G., HARRISON, T., POLLACK, S. J. & SHEARMAN, M. S. 2003. Catalytic site-directed gamma-secretase complex inhibitors do not discriminate pharmacologically between Notch S3 and beta-APP cleavages. *Biochemistry,* 42**,** 7580-6.
74. LI, C. I., BEABER, E. F., TANG, M. T., PORTER, P. L., DALING, J. R. & MALONE, K. E. 2013. Reproductive factors and risk of estrogen receptor positive, triple-negative, and HER2-neu overexpressing breast cancer among women 20-44 years of age. *Breast Cancer Research and Treatment,* 137**,** 579-87.
75. LIANG, C. C., PARK, A. Y. & GUAN, J. L. 2007. In vitro scratch assay: a convenient and inexpensive method for analysis of cell migration in vitro. *Nature Protocol,* 2**,** 329-33.
76. LIU, Z., ZHANG, X. S. & ZHANG, S. 2014. Breast tumor subgroups reveal diverse clinical prognostic power. *Scientific Reports,* 4.
77. LOBRY, C., OH, P., MANSOUR, M. R., LOOK, A. T. & AIFANTIS, I. 2014. Notch signaling: switching an oncogene to a tumor suppressor. *Blood,* 123**,** 2451-9.
78. LU, P., BAI, X. C., MA, D., XIE, T., YAN, C., SUN, L., YANG, G., ZHAO, Y., ZHOU, R., SCHERES, S. H. & SHI, Y. 2014. Three-dimensional structure of human gamma-secretase. *Nature,* 512**,** 166-70.

79. MA, H., WANG, Y., SULLIVAN-HALLEY, J., WEISS, L., MARCHBANKS, P. A., SPIRTAS, R., URSIN, G., BURKMAN, R. T., SIMON, M. S., MALONE, K. E., STROM, B. L., MCDONALD, J. A., PRESS, M. F. & BERNSTEIN, L. 2010. Use of four biomarkers to evaluate the risk of breast cancer subtypes in the women's contraceptive and reproductive experiences study. *Cancer Research,* 70**,** 575-87.
80. MCCLEMENTS, L., YAKKUNDI, A., PAPASPYROPOULOS, A., HARRISON, H., ABLETT, M. P., JITHESH, P. V., MCKEEN, H. D., BENNETT, R., DONLEY, C., KISSENPFENNIG, A., MCINTOSH, S., MCCARTHY, H. O., O'NEILL, E., CLARKE, R. B. & ROBSON, T. 2013. Targeting treatment-resistant breast cancer stem cells with FKBPL and its peptide derivative, AD-01, via the CD44 pathway. *Clinical Cancer Research,* 19**,** 3881-93.
81. MCCORMACK, V. A., JOFFE, M., VAN DEN BERG, E., BROEZE, N., DOS SANTOS SILVA, I., ROMIEU, I., JACOBSON, J. S., NEUGUT, A. I., SCHUZ, J. & CUBASCH, H. 2013. Breast cancer receptor status and stage at diagnosis in over 1,200 consecutive public hospital patients in Soweto, South Africa: a case series. *Breast Cancer Research,* 15.
82. MIKI, M., MATSUO, Y., YOSHIDA, S., TANE, K., HIROKAGA, K., MAEKAWA, Y. & TAKAO, S. 2014. [A case of locally advanced and metastatic breast cancer successfully treated with combination therapy of paclitaxel and bevacizumab]. *Gan To Kagaku Ryoho,* 41**,** 1027-9.
83. MOWAD, R., CHU, Q. D., LI, B. D., BURTON, G. V., AMPIL, F. L. & KIM, R. H. 2013. Does obesity have an effect on outcomes in triple-negative breast cancer? *Journal of Surgical Research,* 184**,** 253-9.
84. NETWORK, C. G. A. 2012. Comprehensive molecular portraits of human breast tumours. *Nature,* 490**,** 61-70.
85. NEWMAN, L. A., GRIFFITH, K. A., JATOI, I., SIMON, M. S., CROWE, J. P. & COLDITZ, G. A. 2006. Meta-analysis of survival in African American and white American patients with breast cancer: ethnicity compared with socioeconomic status. *Journal of Clinical Oncology,* 24**,** 1342-9.

86. NIELSEN, T. O., HSU, F. D., JENSEN, K., CHEANG, M., KARACA, G., HU, Z., HERNANDEZ-BOUSSARD, T., LIVASY, C., COWAN, D., DRESSLER, L., AKSLEN, L. A., RAGAZ, J., GOWN, A. M., GILKS, C. B., VAN DE RIJN, M. & PEROU, C. M. 2004. Immunohistochemical and clinical characterization of the basal-like subtype of invasive breast carcinoma. *Clinical Cancer Research,* 10**,** 5367-74.
87. NTZIACHRISTOS, P., LIM, J. S., SAGE, J. & AIFANTIS, I. 2014. From fly wings to targeted cancer therapies: a centennial for notch signaling. *Cancer Cell,* 25**,** 318-34.
88. O'NEILL, C. F., URS, S., CINELLI, C., LINCOLN, A., NADEAU, R. J., LEON, R., TOHER, J., MOUTA-BELLUM, C., FRIESEL, R. E. & LIAW, L. 2007. Notch2 signaling induces apoptosis and inhibits human MDA-MB-231 xenograft growth. *The American Journal of Pathology,* 171**,** 1023-36.
89. OLSAUSKAS-KUPRYS, R., ZLOBIN, A. & OSIPO, C. 2013. Gamma secretase inhibitors of Notch signaling. *OncoTargets and Therapy,* 6**,** 943-55.
90. OSIPO, C., PATEL, P., RIZZO, P., CLEMENTZ, A. G., HAO, L., GOLDE, T. E. & MIELE, L. 2008. ErbB-2 inhibition activates Notch-1 and sensitizes breast cancer cells to a gamma-secretase inhibitor. *Oncogene,* 27**,** 5019-32.
91. PALMER, J. R., RUIZ-NARVAEZ, E. A., ROTIMI, C. N., CUPPLES, L. A., COZIER, Y. C., ADAMS-CAMPBELL, L. L. & ROSENBERG, L. 2013. Genetic susceptibility loci for subtypes of breast cancer in an African American population. *Cancer Epidemiology Biomarkers and Prevention,* 22**,** 127-34.
92. PARISE, C. A. & CAGGIANO, V. 2013. Disparities in race/ethnicity and socioeconomic status: risk of mortality of breast cancer patients in the California Cancer Registry, 2000-2010. *BMC Cancer,* 13**,** 1471-2407.
93. PARR, C., WATKINS, G. & JIANG, W. G. 2004. The possible correlation of Notch-1 and Notch-2 with clinical outcome and tumour clinicopathological parameters in human breast cancer. *International Journal of Molecular Medicine,* 14**,** 779-86.
94. PEROU, C. M. 2011. Molecular stratification of triple-negative breast cancers. *Oncologist,* 1**,** 61-70.

95. PEROU, C. M., SORLIE, T., EISEN, M. B., VAN DE RIJN, M., JEFFREY, S. S., REES, C. A., POLLACK, J. R., ROSS, D. T., JOHNSEN, H., AKSLEN, L. A., FLUGE, O., PERGAMENSCHIKOV, A., WILLIAMS, C., ZHU, S. X., LONNING, P. E., BORRESEN-DALE, A. L., BROWN, P. O. & BOTSTEIN, D. 2000. Molecular portraits of human breast tumours. *Nature,* 406**,** 747-52.
96. PIEROBON, M. & FRANKENFELD, C. L. 2013. Obesity as a risk factor for triple-negative breast cancers: a systematic review and meta-analysis. *Breast Cancer Research and Treatment,* 137**,** 307-14.
97. PODO, F., BUYDENS, L. M., DEGANI, H., HILHORST, R., KLIPP, E., GRIBBESTAD, I. S., VAN HUFFEL, S., VAN LAARHOVEN, H. W., LUTS, J., MONLEON, D., POSTMA, G. J., SCHNEIDERHAN-MARRA, N., SANTORO, F., WOUTERS, H., RUSSNES, H. G., SORLIE, T., TAGLIABUE, E. & BORRESEN-DALE, A. L. 2010. Triple-negative breast cancer: present challenges and new perspectives. *Molecular Oncology,* 4**,** 209-29.
98. POGODA, K., NIWINSKA, A., MURAWSKA, M. & PIENKOWSKI, T. 2013. Analysis of pattern, time and risk factors influencing recurrence in triple-negative breast cancer patients. *Medicaal Oncology,* 30**,** 012-0388.
99. PRAT, A., ADAMO, B., CHEANG, M. C., ANDERS, C. K., CAREY, L. A. & PEROU, C. M. 2013. Molecular characterization of basal-like and non-basal-like triple-negative breast cancer. *Oncologist,* 18**,** 123-33.
100. PRAT, A., PARKER, J. S., KARGINOVA, O., FAN, C., LIVASY, C., HERSCHKOWITZ, J. I., HE, X. & PEROU, C. M. 2010. Phenotypic and molecular characterization of the claudin-low intrinsic subtype of breast cancer. *Breast Cancer Research,* 12**,** 2.
101. PRAT, A. & PEROU, C. M. 2011. Deconstructing the molecular portraits of breast cancer. *Molecular Oncology,* 5**,** 5-23.
102. QIU, M., PENG, Q., JIANG, I., CARROLL, C., HAN, G., RYMER, I., LIPPINCOTT, J., ZACHWIEJA, J., GAJIWALA, K., KRAYNOV, E., THIBAULT, S., STONE, D., GAO, Y., SOFIA, S., GALLO, J., LI, G., YANG, J., LI, K. & WEI, P. 2013. Specific inhibition of Notch1 signaling enhances the

antitumor efficacy of chemotherapy in triple negative breast cancer through reduction of cancer stem cells. *Cancer Letters,* 328**,** 261-70.

103. RAKHA, E., ELLIS, I. & REIS-FILHO, J. Are triple-negative and basal-like breast cancer synonymous?, *Clinical Cancer Research*. 2008 Jan 15;14(2):618; author reply 618-9. doi: 10.1158/1078-0432.CCR-07-1943.

104. RAKHA, E. A. & ELLIS, I. O. 2011. Modern classification of breast cancer: should we stick with morphology or convert to molecular profile characteristics. *Advances in Anatomical Pathology,* 18**,** 255-67.

105. RAKHA, E. A., ELSHEIKH, S. E., ALESKANDARANY, M. A., HABASHI, H. O., GREEN, A. R., POWE, D. G., EL-SAYED, M. E., BENHASOUNA, A., BRUNET, J. S., AKSLEN, L. A., EVANS, A. J., BLAMEY, R., REIS-FILHO, J. S., FOULKES, W. D. & ELLIS, I. O. 2009. Triple-negative breast cancer: distinguishing between basal and nonbasal subtypes. *Clinical Cancer Research,* 15**,** 2302-10.

106. REEDIJK, M., ODORCIC, S., CHANG, L., ZHANG, H., MILLER, N., MCCREADY, D. R., LOCKWOOD, G. & EGAN, S. E. 2005. High-level coexpression of JAG1 and NOTCH1 is observed in human breast cancer and is associated with poor overall survival. *Cancer Research,* 65**,** 8530-7.

107. RIZZO, P., MIAO, H., D'SOUZA, G., OSIPO, C., SONG, L. L., YUN, J., ZHAO, H., MASCARENHAS, J., WYATT, D., ANTICO, G., HAO, L., YAO, K., RAJAN, P., HICKS, C., SIZIOPIKOU, K., SELVAGGI, S., BASHIR, A., BHANDARI, D., MARCHESE, A., LENDAHL, U., QIN, J. Z., TONETTI, D. A., ALBAIN, K., NICKOLOFF, B. J. & MIELE, L. 2008a. Cross-talk between notch and the estrogen receptor in breast cancer suggests novel therapeutic approaches. *Cancer Research,* 68**,** 5226-35.

108. RIZZO, P., OSIPO, C., FOREMAN, K., GOLDE, T., OSBORNE, B. & MIELE, L. 2008b. Rational targeting of Notch signaling in cancer. *Oncogene,* 27**,** 5124-31.

109. RIZZO, P., OSIPO, C., PANNUTI, A., GOLDE, T., OSBORNE, B. & MIELE, L. 2009. Targeting Notch signaling cross-talk with estrogen receptor and ErbB-2 in breast cancer. *Advances Enzyme Regulation,* 49**,** 134-41.

110. ROSE, D. P. & VONA-DAVIS, L. 2009. Influence of obesity on breast cancer receptor status and prognosis. *Expert Review Anticancer Therapy,* 9**,** 1091-101.

111. ROSE, D. P. & VONA-DAVIS, L. 2010. Interaction between menopausal status and obesity in affecting breast cancer risk. *Maturitas,* 66**,** 33-8.

112. ROSE, S. L., KUNNIMALAIYAAN, M., DRENZEK, J. & SEILER, N. 2010. Notch 1 signaling is active in ovarian cancer. *Gynecologic Oncology,* 117**,** 130-133.

113. ROSENBERG, L., BOGGS, D. A., WISE, L. A., ADAMS-CAMPBELL, L. L. & PALMER, J. R. 2010. Oral contraceptive use and estrogen/progesterone receptor-negative breast cancer among African American women. *Cancer Epidemiology Biomarkers and Prevention,* 19**,** 2073-9.

114. ROY, M., PEAR, W. S. & ASTER, J. C. 2007. The multifaceted role of Notch in cancer. *Current Opinion in Genetics Development,* 17**,** 52-9.

115. SAYED, S., MOLOO, Z., WASIKE, R., BIRD, P., OIGARA, R., GOVENDER, D., KIBERA, J., CARRARA, H. & SALEH, M. 2014. Is breast cancer from Sub Saharan Africa truly receptor poor? Prevalence of ER/PR/HER2 in breast cancer from Kenya. *Breast,* 23**,** 591-6.

116. SCHOTT, A. F., LANDIS, M. D., DONTU, G., GRIFFITH, K. A., LAYMAN, R. M., KROP, I., PASKETT, L. A., WONG, H., DOBROLECKI, L. E., LEWIS, M. T., FROEHLICH, A. M., PARANILAM, J., HAYES, D. F., WICHA, M. S. & CHANG, J. C. 2013. Preclinical and clinical studies of gamma secretase inhibitors with docetaxel on human breast tumors. *Clinical Cancer Research,* 19**,** 1512-24.

117. SENEVIRATNE, S., CAMPBELL, I., SCOTT, N., SHIRLEY, R. & LAWRENSON, R. 2015. Impact of mammographic screening on ethnic and socioeconomic inequities in breast cancer stage at diagnosis and survival in New Zealand: a cohort study. *BMC Public Health,* 15**,** 46.

118. SHAO, H., HUANG, Q. & LIU, Z.-J. 2012. Chapter Seven - Targeting Notch Signaling for Cancer Therapeutic Intervention. *In:* KEIRAN, S. M. S. (ed.) *Advances in Pharmacology.* Academic Press.

119. SHARIFF-MARCO, S., YANG, J., JOHN, E. M., SANGARAMOORTHY, M., HERTZ, A., KOO, J., NELSON, D. O., SCHUPP, C. W., SHEMA, S. J., COCKBURN, M., SATARIANO, W. A., YEN, I. H., PONCE, N. A., WINKLEBY, M., KEEGAN, T. H. & GOMEZ, S. L. 2014. Impact of neighborhood and individual socioeconomic status on survival after breast cancer varies by race/ethnicity: the Neighborhood and Breast Cancer Study. *Cancer Epidemiology Biomarkers and Prevention,* 23**,** 793-811.

120. SHARMA, A., PARANJAPE, A. N., RANGARAJAN, A. & DIGHE, R. R. 2012. A monoclonal antibody against human Notch1 ligand-binding domain depletes subpopulation of putative breast cancer stem-like cells. *Molecular Cancer Therapeutics,* 11**,** 77-86.

121. SHUPTRINE, C. W., SURANA, R. & WEINER, L. M. 2012. Monoclonal antibodies for the treatment of cancer. *Seminars in Cancer Biology,* 22**,** 3-13.

122. SIBILIA, M., KROISMAYR, R., LICHTENBERGER, B. M., NATARAJAN, A., HECKING, M. & HOLCMANN, M. 2007. The epidermal growth factor receptor: from development to tumorigenesis. *Differentiation,* 75**,** 770-787.

123. SINESHAW, H. M., GAUDET, M., WARD, E. M., FLANDERS, W. D., DESANTIS, C., LIN, C. C. & JEMAL, A. 2014. Association of race/ethnicity, socioeconomic status, and breast cancer subtypes in the National Cancer Data Base (2010-2011). *Breast Cancer Research and Treatment,* 145**,** 753-63.

124. SINGHAI, R., PATIL, V. W., JAISWAL, S. R., PATIL, S. D., TAYADE, M. B. & PATIL, A. V. 2011. E-Cadherin as a diagnostic biomarker in breast cancer. *North American Journal of Medical Sciences,* 3**,** 227-33.

125. SOLIN, L. J., HWANG, W. T. & VAPIWALA, N. 2009. Outcome after breast conservation treatment with radiation for women with triple-negative early-stage invasive breast carcinoma. *Clinical Breast Cancer,* 9**,** 96-100.

126. SORLIE, T., PEROU, C. M., TIBSHIRANI, R., AAS, T., GEISLER, S., JOHNSEN, H., HASTIE, T., EISEN, M. B., VAN DE RIJN, M., JEFFREY, S. S., THORSEN, T., QUIST, H., MATESE, J. C., BROWN, P. O., BOTSTEIN, D., LONNING, P. E. & BORRESEN-DALE, A. L. 2001. Gene expression patterns of

breast carcinomas distinguish tumor subclasses with clinical implications. *Proceedings of the National Academy of Science U S A,* 98**,** 10869-74.

127. SORLIE, T., TIBSHIRANI, R., PARKER, J., HASTIE, T., MARRON, J. S., NOBEL, A., DENG, S., JOHNSEN, H., PESICH, R., GEISLER, S., DEMETER, J., PEROU, C. M., LONNING, P. E., BROWN, P. O., BORRESEN-DALE, A. L. & BOTSTEIN, D. 2003. Repeated observation of breast tumor subtypes in independent gene expression data sets. *Proceedings of the National Academy of Science U S A,* 100**,** 8418-23.

128. SOTIRIOU, C. & PUSZTAI, L. 2009. Gene-expression signatures in breast cancer. *The New England Journal of Medicine,* 360**,** 790-800.

129. SOULE, H. D., VAZGUEZ, J., LONG, A., ALBERT, S. & BRENNAN, M. 1973. A human cell line from a pleural effusion derived from a breast carcinoma. *Journal of the National Cancer Institute,* 51**,** 1409-16.

130. SPEISER, J., FOREMAN, K., DRINKA, E., GODELLAS, C., PEREZ, C., SALHADAR, A., ERSAHIN, C. & RAJAN, P. 2012. Notch-1 and Notch-4 biomarker expression in triple-negative breast cancer. *International Journal of Surgical Pathology,* 20**,** 139-45.

131. SPEISER, J. J., ERSAHIN, C. & OSIPO, C. 2013. The functional role of Notch signaling in triple-negative breast cancer. *Vitamins and Hormones,* 93**,** 277-306.

132. STANLEY, P. & OKAJIMA, T. 2010. Roles of glycosylation in Notch signaling. *Current Topics in Development Biology,* 92**,** 131-64.

133. STEAD, L. A., LASH, T. L., SOBIERAJ, J. E., CHI, D. D., WESTRUP, J. L., CHARLOT, M., BLANCHARD, R. A., LEE, J. C., KING, T. C. & ROSENBERG, C. L. 2009. Triple-negative breast cancers are increased in black women regardless of age or body mass index. *Breast Cancer Research,* 11**,** 25.

134. STURTZ, L. A., MELLEY, J., MAMULA, K., SHRIVER, C. D. & ELLSWORTH, R. E. 2014. Outcome disparities in African American women with triple negative breast cancer: a comparison of epidemiological and molecular factors between African American and Caucasian women with triple negative breast cancer. *BMC Cancer,* 14**,** 1471-2407.

135. SWEDE, H., GREGORIO, D. I., TANNENBAUM, S. H., BROCKMEYER, J. A., AMBROSONE, C., WILSON, L. L., PENSA, M. A., GONSALVES, L., STEVENS, R. G. & RUNOWICZ, C. D. 2011. Prevalence and Prognostic Role of Triple-Negative Breast Cancer by Race: A Surveillance Study. *Clinical Breast Cancer,* 11**,** 332-341.

136. TAIT, S., PACHECO, J. M., GAO, F., BUMB, C., ELLIS, M. J. & MA, C. X. 2014. Body mass index, diabetes, and triple-negative breast cancer prognosis. *Breast Cancer Research and Treatment,* 146**,** 189-97.

137. TAKEBE, N., NGUYEN, D. & YANG, S. X. 2014. Targeting Notch signaling pathway in cancer: Clinical development advances and challenges. *Pharmacology & Therapeutics,* 141**,** 140-149.

138. TARULLI, G. A., BUTLER, L. M., TILLEY, W. D. & HICKEY, T. E. 2014. Bringing androgens up a NOTCH in breast cancer. *Endocrine Related Cancer,* 21**,** 14-0248.

139. THEYS, J., YAHYANEJAD, S., HABETS, R., SPAN, P., DUBOIS, L., PAESMANS, K., KATTENBELD, B., CLEUTJENS, J., GROOT, A. J., SCHUURBIERS, O. C. J., LAMBIN, P., BUSSINK, J. & VOOIJS, M. 2013. High NOTCH activity induces radiation resistance in non small cell lung cancer. *Radiotherapy and Oncology,* 108**,** 440-445.

140. TOLIA, A. & DE STROOPER, B. 2009. Structure and function of γ-secretase. *Seminars in Cell & Developmental Biology,* 20**,** 211-218.

141. TURKOZ, F. P., SOLAK, M., PETEKKAYA, I., KESKIN, O., KERTMEN, N., SARICI, F., ARIK, Z., BABACAN, T., OZISIK, Y. & ALTUNDAG, K. 2013. Association between common risk factors and molecular subtypes in breast cancer patients. *Breast,* 22**,** 344-50.

142. VISVADER, J. E. 2009. Keeping abreast of the mammary epithelial hierarchy and breast tumorigenesis. *Genes and Development,* 23**,** 2563-77.

143. VUONG, D., SIMPSON, P. T., GREEN, B., CUMMINGS, M. C. & LAKHANI, S. R. 2014. Molecular classification of breast cancer. *Virchows Arch,* 465**,** 1-14.

144. WANG, M., WU, L., WANG, L. & XIN, X. 2010. Down-regulation of Notch1 by gamma-secretase inhibition contributes to cell growth inhibition and apoptosis in ovarian cancer cells A2780. *Biochemical and Biophysical Research Communications,* 393**,** 144-149.

145. WEI, P., WALLS, M., QIU, M., DING, R., DENLINGER, R. H., WONG, A., TSAPARIKOS, K., JANI, J. P., HOSEA, N., SANDS, M., RANDOLPH, S. & SMEAL, T. 2010. Evaluation of selective gamma-secretase inhibitor PF-03084014 for its antitumor efficacy and gastrointestinal safety to guide optimal clinical trial design. *Molecular Cancer Therapetics,* 9**,** 1618-28.

146. WEIGELT, B., MACKAY, A., A'HERN, R., NATRAJAN, R., TAN, D. S. P., DOWSETT, M., ASHWORTH, A. & REIS-FILHO, J. S. 2010. Breast cancer molecular profiling with single sample predictors: a retrospective analysis. *The Lancet Oncology,* 11**,** 339-349.

147. WEINBERG, R. A. & LUNDBERG, A. S. 1999. Control of the cell cycle and apoptosis. *European Journal of Cancer,* 35**,** 531-539.

148. WHARTON, K. A., JOHANSEN, K. M., XU, T. & ARTAVANIS-TSAKONAS, S. 1985. Nucleotide sequence from the neurogenic locus notch implies a gene product that shares homology with proteins containing EGF-like repeats. *Cell,* 43**,** 567-81.

149. WOLFE, M. S. 2009. γ-Secretase in biology and medicine. *Seminars in Cell & Developmental Biology,* 20**,** 219-224.

150. YAGATA, H., KAJIURA, Y. & YAMAUCHI, H. 2011. Current strategy for triple-negative breast cancer: appropriate combination of surgery, radiation, and chemotherapy. *Breast Cancer,* 18**,** 165-73.

151. YAMAGUCHI, H., CHANG, S. S., HSU, J. L. & HUNG, M. C. 2014. Signaling cross-talk in the resistance to HER family receptor targeted therapy. *Oncogene,* 33**,** 1073-81.

152. YAMAGUCHI, N., OYAMA, T., ITO, E., SATOH, H., AZUMA, S., HAYASHI, M., SHIMIZU, K., HONMA, R., YANAGISAWA, Y., NISHIKAWA, A., KAWAMURA, M., IMAI, J., OHWADA, S., TATSUTA, K., INOUE, J., SEMBA, K. & WATANABE, S. 2008. NOTCH3 signaling pathway plays crucial

roles in the proliferation of ErbB2-negative human breast cancer cells. *Cancer Research,* 68**,** 1881-8.

153. YARDEN, Y. 2001. The EGFR family and its ligands in human cancer: signalling mechanisms and therapeutic opportunities. *European Journal of Cancer,* 37, Supplement 4**,** 3-8.

154. YERSAL, O. & BARUTCA, S. 2014. Biological subtypes of breast cancer: Prognostic and therapeutic implications. *World Journal Clinical Oncology,* 5**,** 412-24.

155. YILMAZ, M. & CHRISTOFORI, G. 2009. EMT, the cytoskeleton, and cancer cell invasion. *Cancer Metastasis Reviews,* 28**,** 15-33.

156. YONG, T., SUN, A., HENRY, M. D., MEYERS, S. & DAVIS, J. N. 2011. Down regulation of CSL activity inhibits cell proliferation in prostate and breast cancer cells. *Journal of Cell Biochemistry,* 112**,** 2340-51.

157. ZANG, S., CHEN, F., DAI, J., GUO, D., TSE, W., QU, X., MA, D. & JI, C. 2010. RNAi-mediated knockdown of Notch-1 leads to cell growth inhibition and enhanced chemosensitivity in human breast cancer. *Oncology Reports,* 23**,** 893-9.

158. ZHANG, C. C., YAN, Z., ZONG, Q., FANG, D. D., PAINTER, C., ZHANG, Q., CHEN, E., LIRA, M. E., JOHN-BAPTISTE, A. & CHRISTENSEN, J. G. 2013. Synergistic effect of the gamma-secretase inhibitor PF-03084014 and docetaxel in breast cancer models. *Stem Cells Transational Medicine,* 2**,** 233-42.

159. ZHANG, J., FACKENTHAL, J. D., ZHENG, Y., HUO, D., HOU, N., NIU, Q., ZVOSEC, C., OGUNDIRAN, T. O., HENNIS, A. J., LESKE, M. C., NEMESURE, B., WU, S. Y. & OLOPADE, O. I. 2012. Recurrent BRCA1 and BRCA2 mutations in breast cancer patients of African ancestry. *Breast Cancer Research and Treatment,* 134**,** 889-94.

160. ZHANG, M. H., MAN, H. T., ZHAO, X. D., DONG, N. & MA, S. L. 2014. Estrogen receptor-positive breast cancer molecular signatures and therapeutic potentials (Review). *Biomedical Reports,* 2**,** 41-52.

161. ZHAO, C., QIAO, Y., JONSSON, P., WANG, J., XU, L., ROUHI, P., SINHA, I., CAO, Y., WILLIAMS, C. & DAHLMAN-WRIGHT, K. 2014.

Genome-wide profiling of AP-1 regulated transcription provides insights into the invasiveness of triple-negative breast cancer. *Cancer Research*, 15.

6.2 E-references

1. www.Roche.com
2. www.sigmaaldrich.com
3. www.tocris.com
4. www.clinicaltrials.gov
5. www.cansa.org.za

Appendix A: Protocols

A.1 Preparation of solutions and reagents

A.1.1 1X Phosphate Buffered Solution (PBS)

1 PBS tablet (# P4417-100TAB; Sigma Life Sciences, USA) was dissolved in 200ml of distilled water to make a 1X PBS solution and was sterilised by autoclaving it.

A.1.2 Blocking buffer

0.5% of bovine serum albumin (BSA) (# CAS9048-46-8, Santa Cruz Biotechnology, USA) was mixed with PBS (PBS/BSA).

A.1.3 Fixing Solution/Buffer

3% of formaldehyde (#104003, Merk, SA) in 1X PBS solution

A.1.4 Permeabilisation solution/Buffer

0.25% (v/v) of t-Octylphenoxypoly ethoxyethanol (TritonX-100) (#T-9289; Sigma Life Sciences, USA) was dissolved in PBS/BSA.

A.1.5 F-actin cytoskeleton staining solution

To prepare 1X Phalloidin conjugate working solution. Add 1µl of 1000X Cyto-painter Phalloidin iFluor 488 Reagent (# ab176753; ABCAM ®, USA) conjugate DMSO solutions into 1ml PBS/BSA.

A.1.6 Nuclear stain

4',6-diamidino-2-phenylindole (DAPI) (#236276 ; Cell Biology Boehringer Mannheim , Germany) was received in a 10mg crystalized form and was dissolved in N,N-Dimethylformamide (DMF) to make up a stock solution of 5mg/ml.

The working solution of DAPI was prepared by re-suspending 1µl of stock solution in 10ml PBS. It was aliqouted in 2ml Eppendorf tubes and kept frozen at -20 C˚until use.

A.1.7 Cell culture media

Table A1: Media preparation for MCF-7, MDA-MB-231 and MDA-MB-436 cell lines.

Cell line	Growth medium
MCF-7	DMEM-F12 (#BE12-719F, Biowhittaker® Lonza,USA) was supplemented with 5ml FBS (#SV30160.03, HYCLONE®,USA) and 100µl of 100µg/ml pen/strep solution (#17-602E, Biowhittaker® Lonza,USA)
MDA-MB-231	DMEM-F12(#BE12-719F, Biowhittaker® Lonza,USA) was supplemented with 5ml FBS(#SV30160.03, HYCLONE® ,USA) and 100µl of 100µg/ml pen/strep solution(#17-602E, Biowhittaker® Lonza,USA)
MDA-MB-436	Leibovitz (#BE12-700F, Biowhittaker® Lonza,USA) media was supplemented with 50µl of human insulin (#1927,Sigma Life Sciences, USA), 5ml FBS(#SV30160.03, HYCLONE®, USA) , 100µg/ml pen/strep solution (#17-602E, Biowhittaker® Lonza,USA) and 40µl of L-glutamine (#G7513, Sigma,USA)

A.1.8 Freezing media and thawing media

Freezing media contained 15% Dimethyl Sulfoxide (#D2650; Sigma Life sciences, USA) (DMSO) and 20% FBS in media appropriate for each cell line. DMSO is used as a cryo-preserving agent.

Thawing media contained 20% FBS in media appropriate for each cell line. The additional FBS is added to aid cell recovery from DMSO as well as cell adherence.

A.2 Pharmacological inhibitor concentration calculations

A.2.1 DAPT stock solution

N-(N-3, 5-Diflurophenacetyl-L-alanyl))-S-phenyl glycine t-Butyl Ester (DAPT) (#D5942-5mg; Sigma Life Sciences,USA) is in a lyophilized form and must be dissolved in DMSO to make a 10mM stock solution. The concentration was calculated:

Mass = Concentration x Volume x Molecular Weight

5mg = (10mM) (x) (432.46)

X = 1.1562

Therefore the volume of DMSO required making a 10mM stock solution from 5mg DAPT powder is 1.1562ml.

A.2.2 DBZ stock solution

N-[(1S)-2-[[(7S)-6,7-Dihydro-5-methyl-6-oxo-5H-dibenz[b,d]azepin-7-yl]amino]-1-methyl-2-oxoethyl]-3,5-difluorobenzeneacetamide (DBZ) (#CAS209984-56-5,Tocris Biosciences, Bristol UK) is a lyophilized and must be dissolved in DMSO to make a 10mM stock solution. The concentration was calculated as:

Mass = Concentration x Volume x Molecular Weight

10mg = (10mM) (x) (467.98)

X = 2.1368ml

Therefore the volume of DMSO required making a 10mM stock solution from 10mg DBZ powder is 2.1368ml.

DAPT and DBZ working solution calculation was given by (stock solution calculation in appendices 1.3.1 and 1.3.2):

C1V1=C2V2

(10mM)(x)= (10µM) (100µl)

x = 0.1µl

C1V1=C2V2

(10mM)(x)= (10µM) (1ml)

x = 1µl

Therefore 0.1µl of DAPT/DBZ in 99µl of cell culture media makes 10µM and 20µM solution would mean adding 0.2µl of DAPT/DBZ in 98µl in cell culture media and 1µl of DAPT/DBZ in 999µl of cell culture media makes 10µM and 2µl in 998µl of cell culture media makes 20µM.

Appendix B: Cell culture maintenance and ethics

B.1 Cell sub-culture

Cells were passaged once they had reached 90% confluence. The cell culture medium was poured out of the flasks and thereafter the cells rinsed thrice with 2ml of 1X PBS, then 1ml of trypsin/EDTA (#BE17-161E, Biowhittaker ® Lonza, USA) was poured onto the cells and was left to incubate for 3mins at 37℃ in 5% CO2 (ThermoForm series ll water jacketed CO2 Incubator [HEPA FILTER]). After 3mins, 1ml of culture media that was appropriate to the cell line being sub-cultured was poured onto the cells to deactivate trypsin/EDTA. The cells were triturated gently and 2ml of the cell suspension was transferred into a 15ml tube (SPL Lifesciences, Korea) and centrifuged at 1000 rpm for 3mins. The supernatant was discarded and cells were re-suspended in 1ml of media (appropriate for the cell line being that was being sub-cultured). The cell suspension was split in a 1:2 ratio and then added into 4ml of pre-warmed cell culture media in a culture flask.

B.2 Cell Freezing

Sub-culturing procedures were followed until the centrifugation step. The supernatant was discarded and cells were re-suspended in 1ml of cold freezing media. The cell suspension was diluted in a 1:5 ratio to obtain an ideal freezing density , 1ml of the suspension was aliquoted into cryo-vials (Greiner Bio-one®, Germany) and transferred to a polystyrene tube rack to freeze slowly overnight at -70℃ the following day the cryo-vials were transferred to a -80℃ freezer.

B.3 Cell thawing

Prior to thawing, 1ml of thawing medium was aliquoted into a 15ml tube and another 4ml was aliquoted into a cell culture flask (SPL-Lifesciences, Korea) and placed in the incubator to warm up. The cryo-vials were removed from the -80oC freezer and sprayed down with 70% ethanol. The cells were thawed by rubbing the vials in-between gloved hands- this was done to avoid possible contamination from the water bath. Once cells had thawed they were immediately transferred into the 1ml of pre-warmed medium. The suspension of cells was centrifuged at 1000 rpm for 3mins to wash out the DMSO from the cells. The supernatant was discarded and the cells were re-suspended in 1ml of warm thawing media and suspension was transferred into 4ml of pre-warmed thawing media.

B.4 Cell counting

Once the cells had been re-suspended in media after centrifugation (from 1.2.2 or 1.2.3), the cell suspension was mixed with Trypan Blue dye solution (#17-942E; Biowhitattaker® Lonza,USA) in a 1:1 ratio and 10µl of that mixture was pipetted into a disposable cell counting slide (#1450011; Bio-rad,USA) which was then inserted into a TC10 automated cell counter (Bio-rad,USA) or was counted manually with a disposable haemocytomer fastread counting slide (#BVS100; Immune systems, UK). The heamocytomer was viewed under an inverted phase contrast microscope (Carl Zeiss 426126 Axiovert 25) and 2 grids were counted. Concentration (count/ml) was calculated by:

Counts/ml = (total counts/number of complete 4x4 grids counts) x104 x sample dilution

Cell seeding densities were adjusted to the optimal cell concentration by calculating:

C1V1=C2V2

B.5 Ethic waiver

Attached below is the ethics approval letter from the Human research committee (medical).

Human Research Ethics Committee (Medical)

Research Office Secretariat: Senate House Room SH 10005, 10th floor. Tel +27 (0)11-717-1252
Medical School Secretariat: Medical School Room 10M07, 10th Floor. Tel +27 (0)11-717-2700
Private Bag 3, Wits 2050, www.wits.ac.za. Fax +27 (0)11-717-1265

Ref: W-AW-140721-1

21/07/2014

TO WHOM IT MAY CONCERN:

Waiver: This certifies that the following research does not require clearance from the Human Research Ethics Committee (Medical).

Investigator: Dr CB Penny and Ms T Msibi (Student number 0605815F)

Project title: Investigating the notch signaling pathway in triple negative breast cancer.

Reason: This research involves the culturing of breast cancer cell lines obtained from the American Type Culture Collection (ATCC), including the "MCF7", "MDA-MB-231" and "MDA-MB-436" cell lines. As such this research will not involve any human or animal participants.

Professor Angela Woodiwiss

Co-Chair: Human Research Ethics Committee (Medical)

Copy: Anisa Keshav and Zanele Ndlovu, Research Office, Senate House, Wits

APPENDIX C: Cell growth, proliferation and viability raw Data

C.1 Normal growth profile cell number optimisation

Table C.1: Dilution series for cell seeding densities for growth signature optimization.

CELL LINES	**MCF-7**	**MDA-MB-231**	**MDA-MB-436**
SERIES 1	**10000**	**10000**	**20000**
SERIES 2	**5000**	**5000**	**10000**
SERIES 3	**2500**	**2500**	**5000**
SERIES 4	**1250**	**1250**	**2500**
SERIES 5			**1250**

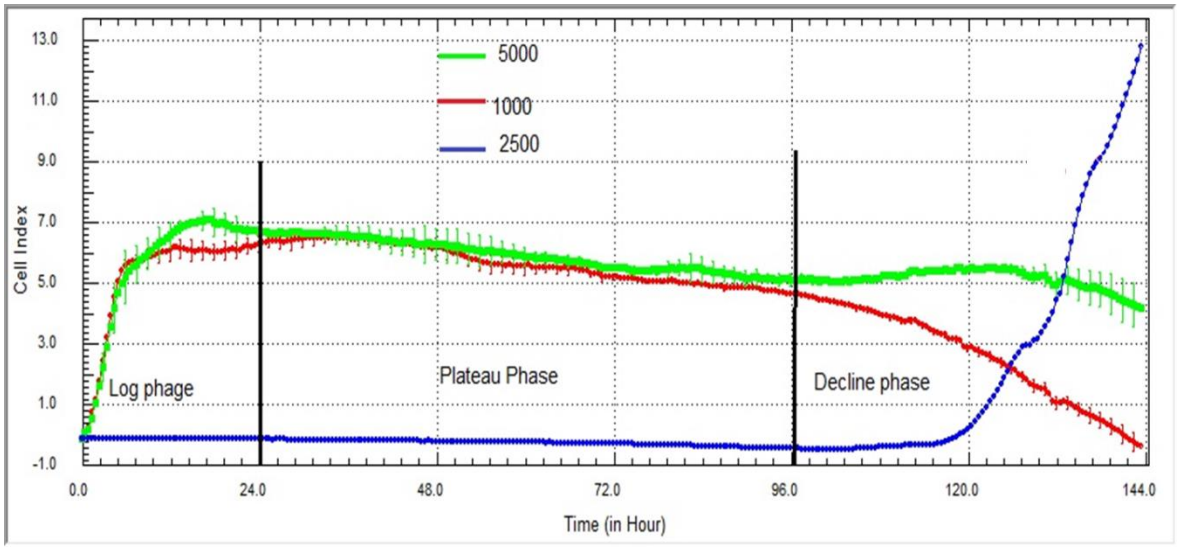


Figure C.1 Optimising cell seeding density of MCF-7 cell line. Effect of cell density on CI, Cell growth signature for MCF-7 cell line over a period of 77 hours, cells were seeded at 10000 cell (red) ; 5000 cells(green) and 2500cells (blue). The Error bars represent the CI at ± standard deviation. Optimisation of seeding density was repeated in triplicate.

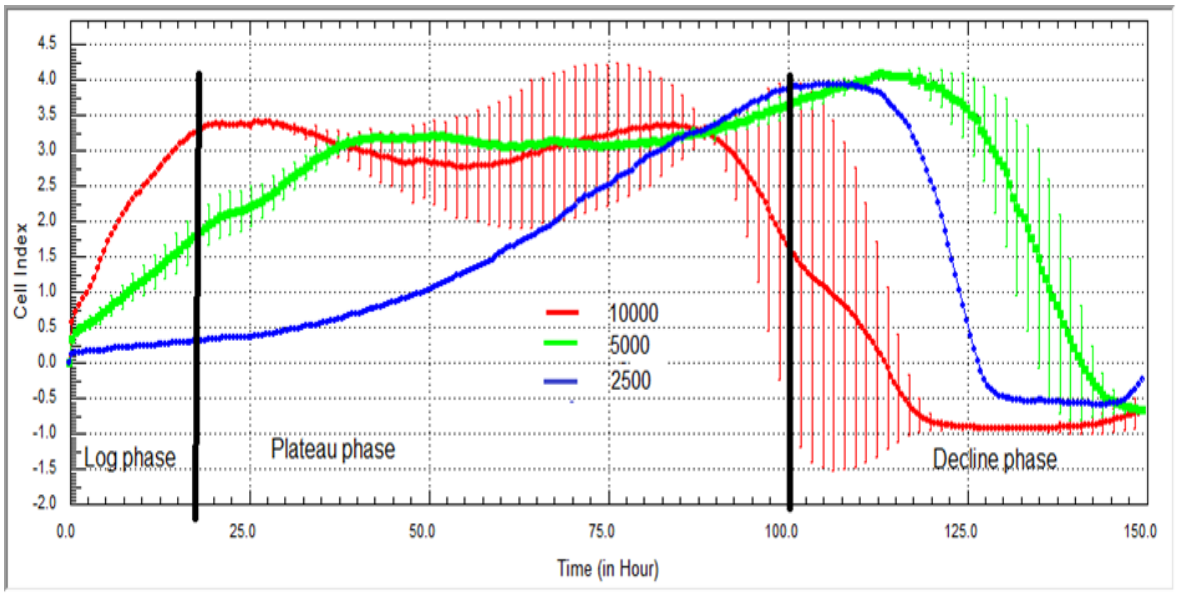


Figure C.2 Optimising cell seeding density of MDA-MB-231cell line. Effect of cell density on CI, Cell growth signature for MDA-MB-231 cell line over a period of 150.0 hours, cells were seeded at 10000 cell (red) ; 5000 cells(green) and 2500cells (blue). The Error bars represent the CI at ± standard deviation. Optimisation of seeding density was repeated in triplicate

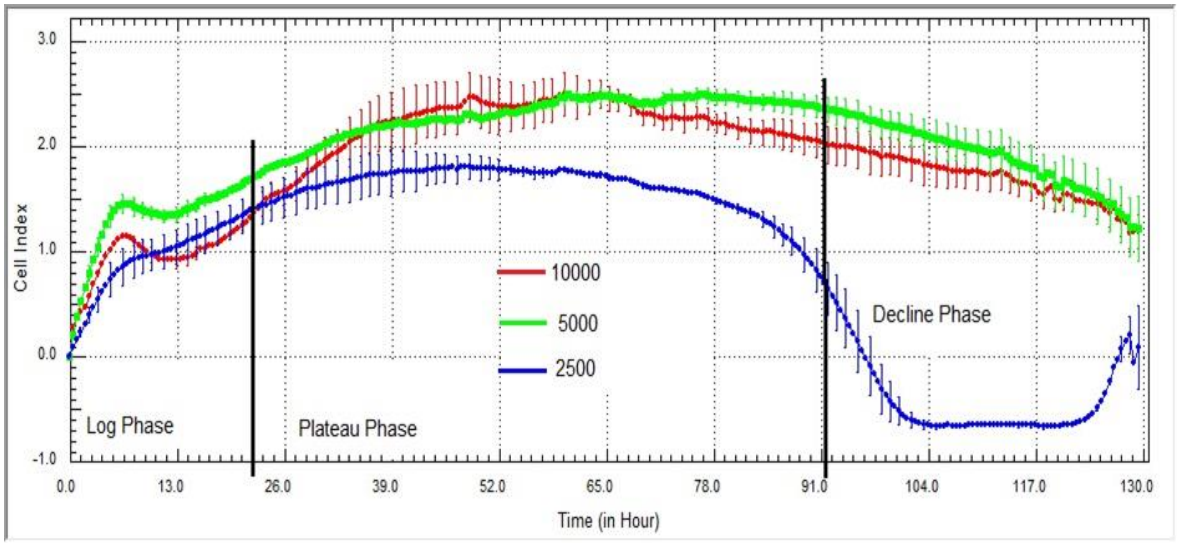


Figure C.3 Optimising cell seeding density of MDA-MB-436 cell line. Effect of cell density on CI, Cell growth signature for MDA-MB-436 cell line over a period of 77 hours, cells were seeded at 10000 cell (red) ; 5000 cells(green) and 2500cells (blue). The Error bars represent the CI at ± standard deviation. Optimisation of seeding density was repeated in triplicate.

C.2 Trypan blue assay and cell viability drug concentration optimisation

C.2.2 Trypan Blue viability assay

Table C.2: Average percentage values of MCF-7 cell viability.

Concentration	10µM	20µM	30µM	40µM	50µM
DBZ	89.6667	29	44.4433	73	87.6667
DAPT	95.8333	87.68	81	55.6667	100
DMSO	98.8333	100	77.7767	66.64	67.7733
MEDIA	99	100	95.3333	94.4433	100

Table C.3: Standard deviation values of MCF-7 cell viability.

Concentration	10µM	20µM	30µM	40µM	50µM
DBZ	3.2146	25.1197	41.942	12.1244	21.362
DAPT	3.7072	1.12089	5.2915	5.1316	0
DMSO	2.0207	0	4.80933	0.03464	1.92835
MEDIA	0	0	8.0829	9.62443	0

Table C.4: Average percentage values of MDA-MB-231 viability.

Concentration	10µM	20µM	30µM	40µM	50µM
DBZ	88.5	27.6666667	41.6667	46.6667	86.9867
DAPT	89	67.0533333	87	9.66667	88.8867
DMSO	94.6667	99.1666667	38		100
MEDIA	100	100	96		59.6667

Table C.5: Standard deviation values of MDA-MB-231 cell viability.

Concentration	10µM	20µM	30µM	40µM	50µM
DBZ	10.037	9.2376	14.4338	50.3322	4.95
DAPT	9.777	4.7622	11.2694	16.7432	19.2489
DMSO	9.2376	1.44338	33.6452		0
MEDIA	0	0	6.9282		52.7289

Table C.6: Average percentage values of MDA-MB-436 cell viability.

Concentration	10µM	20µM	30µM	40µM	50µM
DBZ	89.0833	22.22	87.7767	29	100
DAPT	92.4167	96.6666667	97.2	91.6667	100
DMSO	96.75	95.0666667	100	100	100
MEDIA	97	100	87.6667	33.3333	100

Table C.7: Standard deviation values of MDA-MB-436 cell viability.

Concentration	10µM	20µM	30µM	40µM	50µM
DBZ	3.3292	38.4862	10.7159	34.3948	0
DAPT	1.59478	3.05505	4.84974	14.4338	0
DMSO	2.20681	6.65307	0	0	0
MEDIA	0	0	2.88675	57.735	0

C.2.3 Cell proliferation raw data

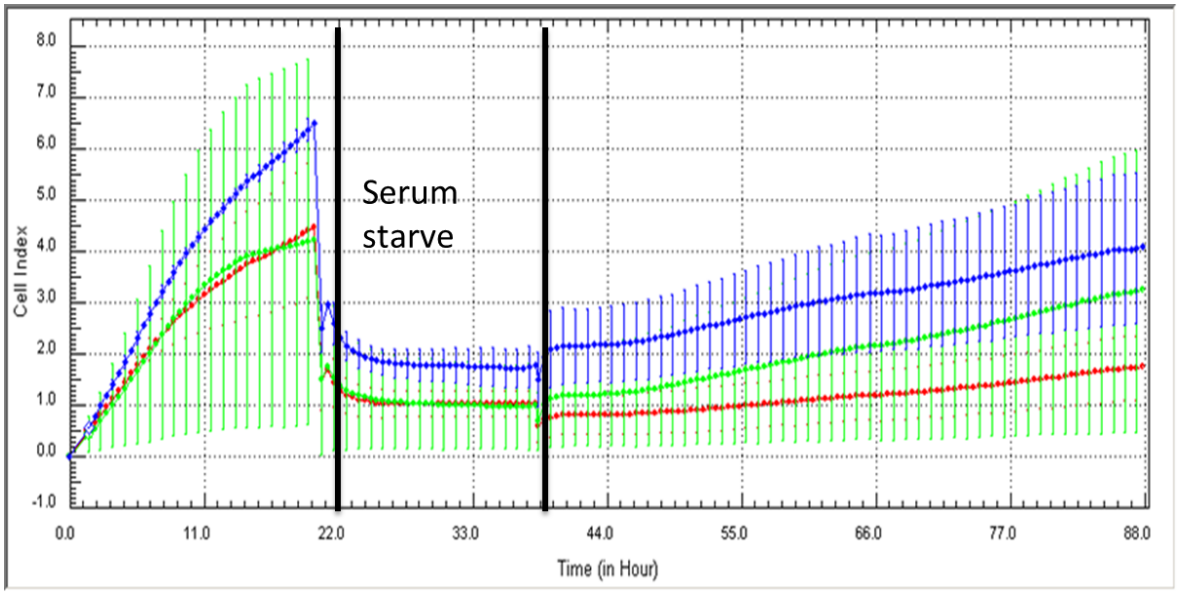


Figure C.4 Real-time cell proliferation and viability of the MCF-7 cell line over 88 hours. Cells were serum starved for 22 hours prior to drug treatment.

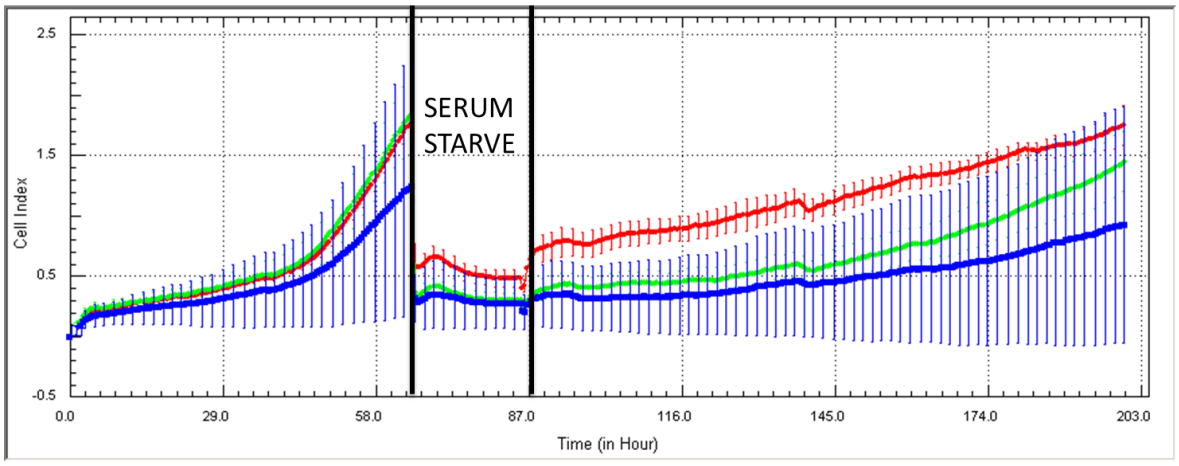


Figure C.5 Real-time cell proliferation and viability of the MD-MB-231 cell line over 200 hours. Cells were serum starved for 22 hours prior to drug treatment.

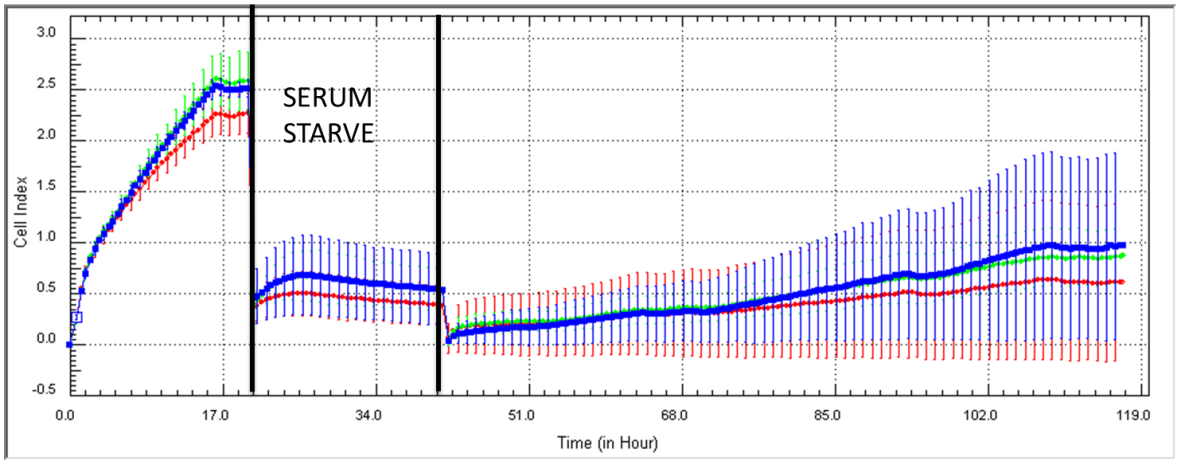


Figure C.6 Real-time cell proliferation and viability of the MDA-MB-231 cell line over 119 hours. Cells were serum starved for 22 hours prior to drug treatment.

Appendix D: Indirect immunofluorescence

Negative controls of immunofluorescence

D.1 Negative controls for the Notch-1 intracellular component signalling expression and localisation

Negative controls included cells incubated with the primary antibody but excluded the secondary antibody and those incubated with secondary antibody but exclude the primary antibody. Images to represent these may be viewed below (Figure. D.1-3):

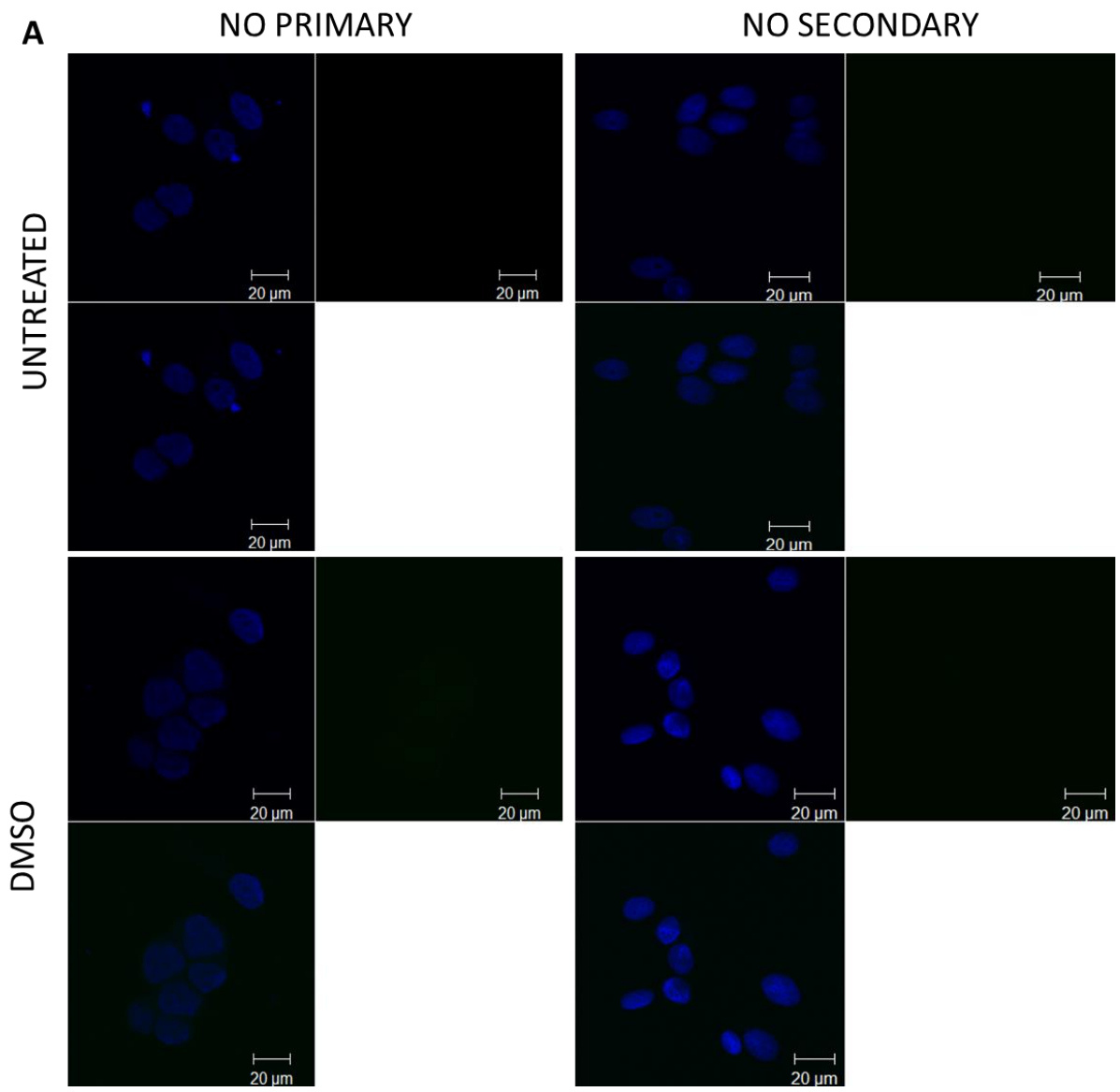


Figure D.1. A) Negative controls of MCF-7 cell line in confocal microscopy. Where the primary antibody was excluded it was marked "no primary" and when a secondary antibody was excluded it was marked "no secondary". The top panel shows the controls for the untreated cells and the bottom panel shows controls for DMSO vehicle control**.**

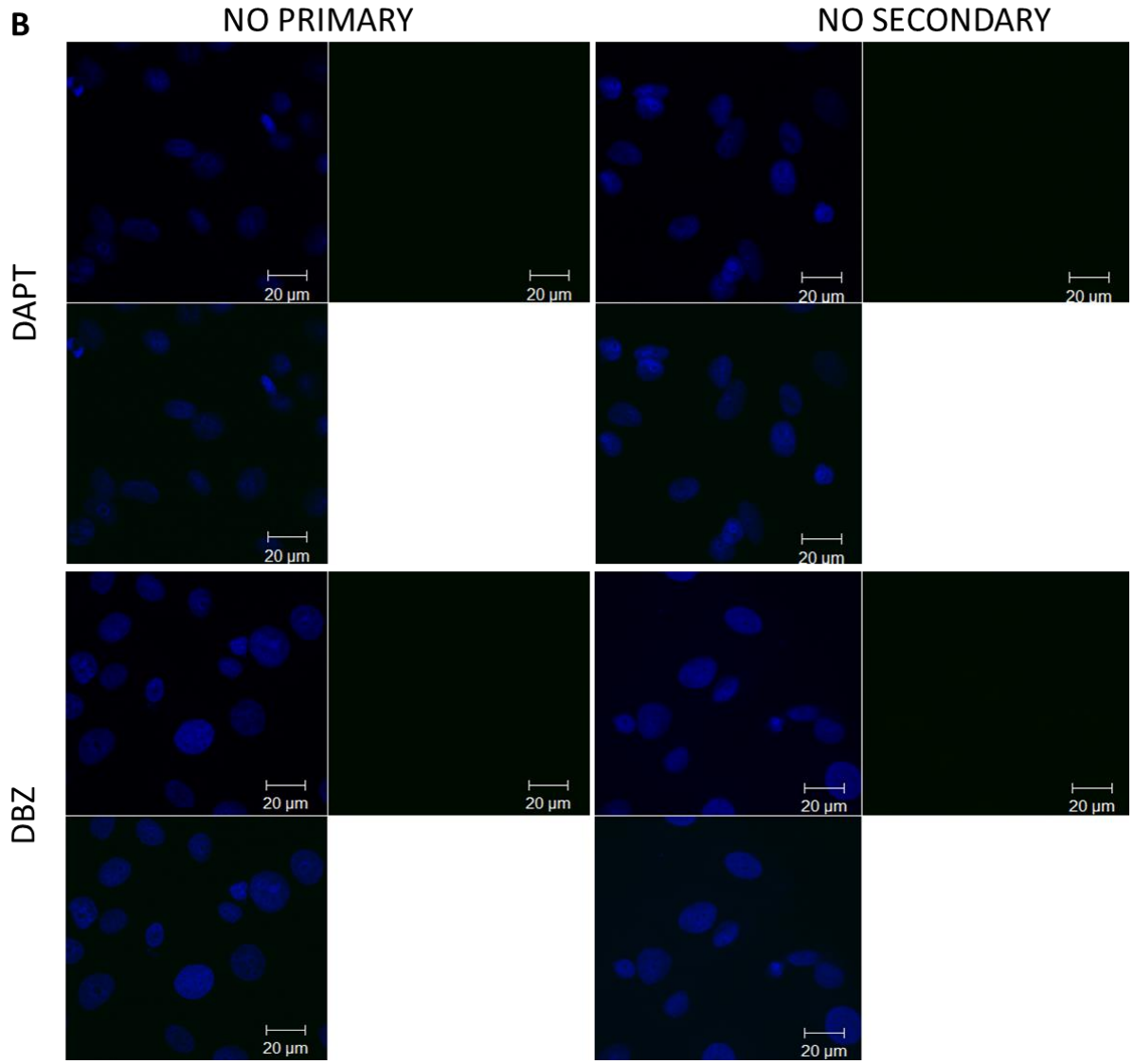


Figure D.1.B) Negative controls of MCF-7 cell line in confocal microscopy. Where the primary antibody was excluded it was marked "no primary" and when a secondary antibody was excluded it was marked "no secondary"**.** The top panel shows the controls for the DAPT treated cells and the bottom panel shows controls for DBZ treated cells.

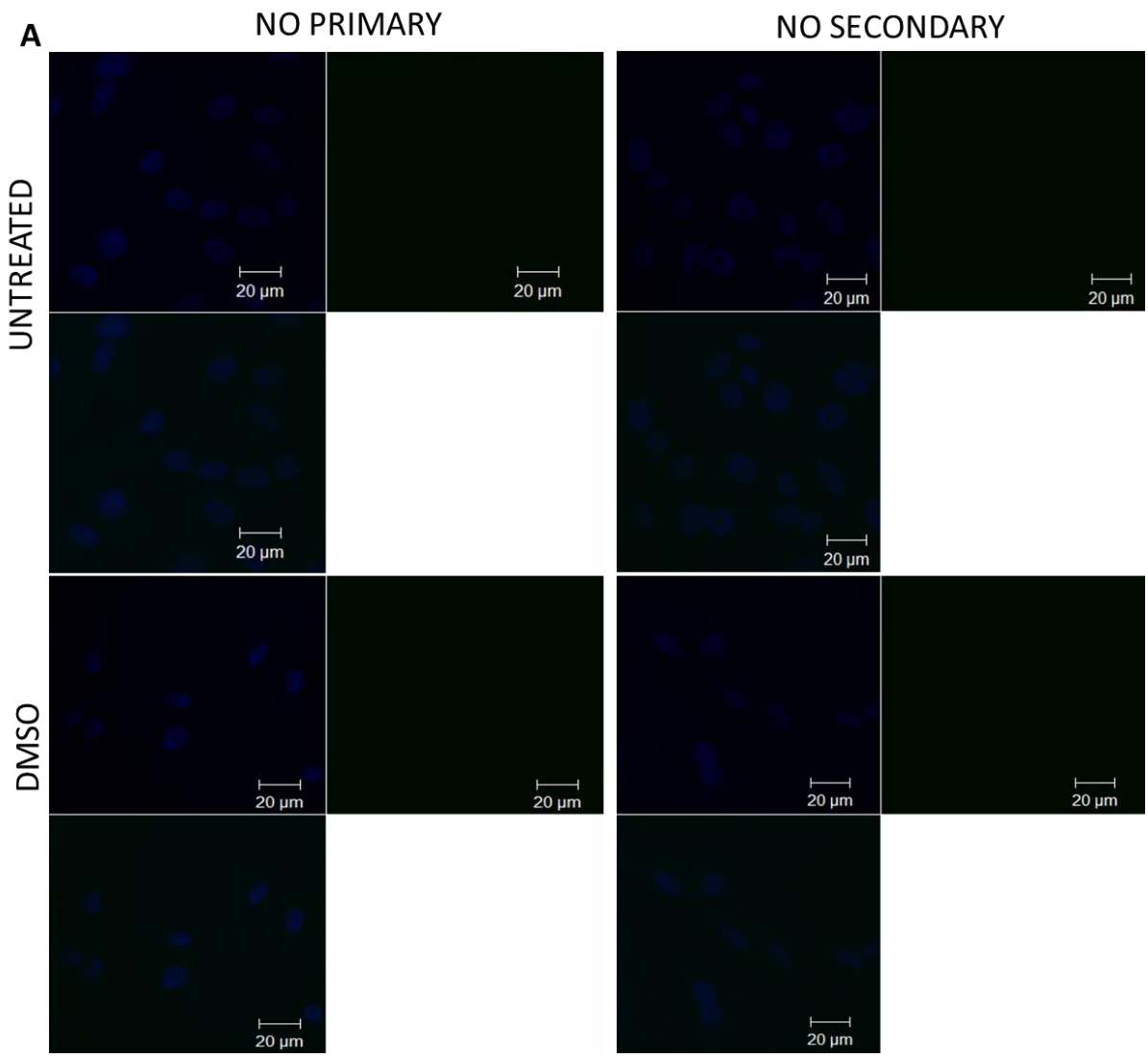


Figure D.2. A) Negative controls of MDA-MB-231cell line in confocal microscopy. Where the primary antibody was excluded it was marked "no primary" and when a secondary antibody was excluded it was marked "no secondary". The top panel shows the controls for the untreated cells and the bottom panel shows controls for DMSO vehicle control.

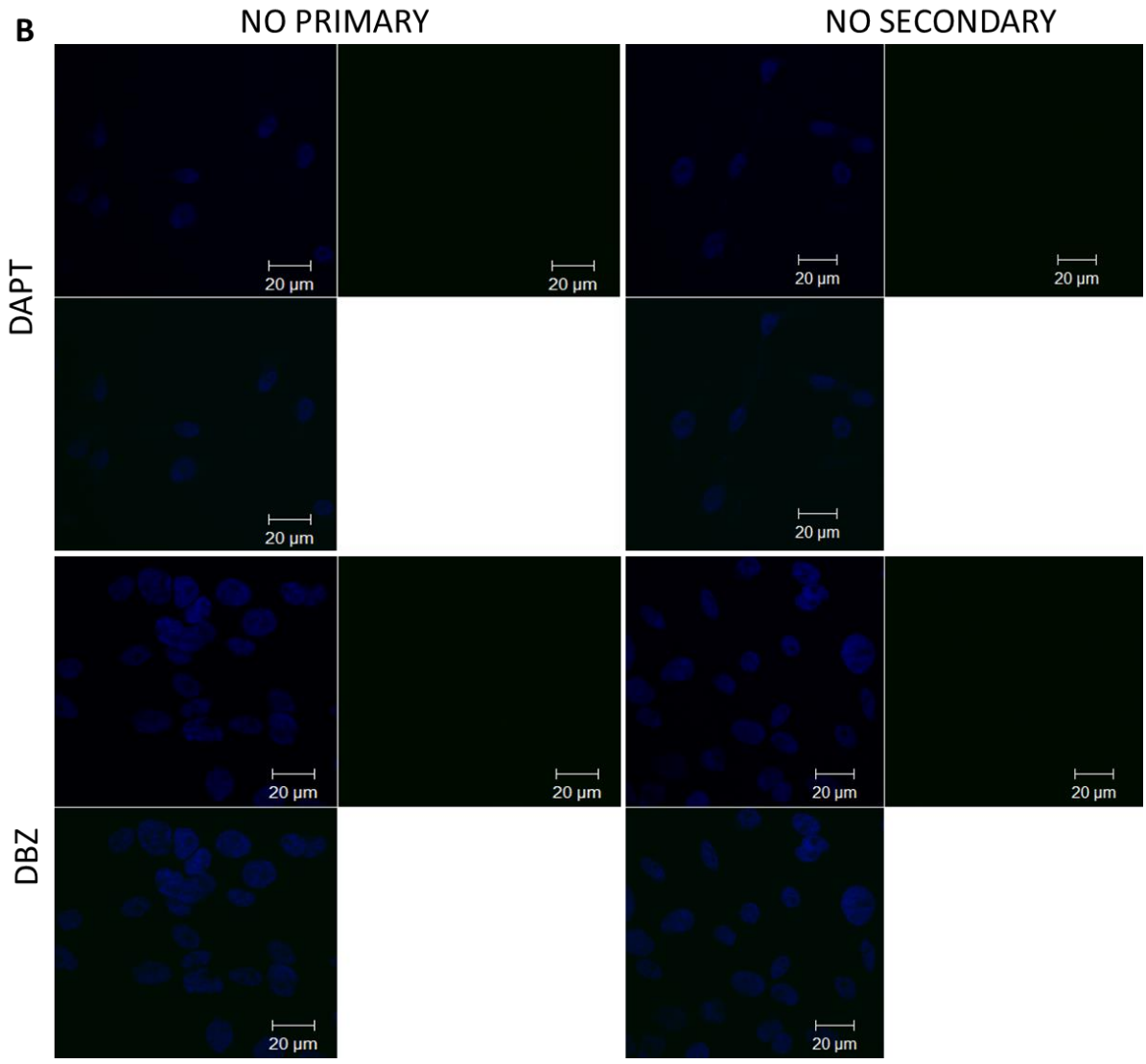


Figure D.2 B) Negative controls of MDA-MB-231cell line in confocal microscopy. Where the primary antibody was excluded it was marked "no primary" and when a secondary antibody was excluded it was marked "no secondary". The top panel shows the controls for the DAPT treated cells and the bottom panel shows controls for DBZ treated cells.

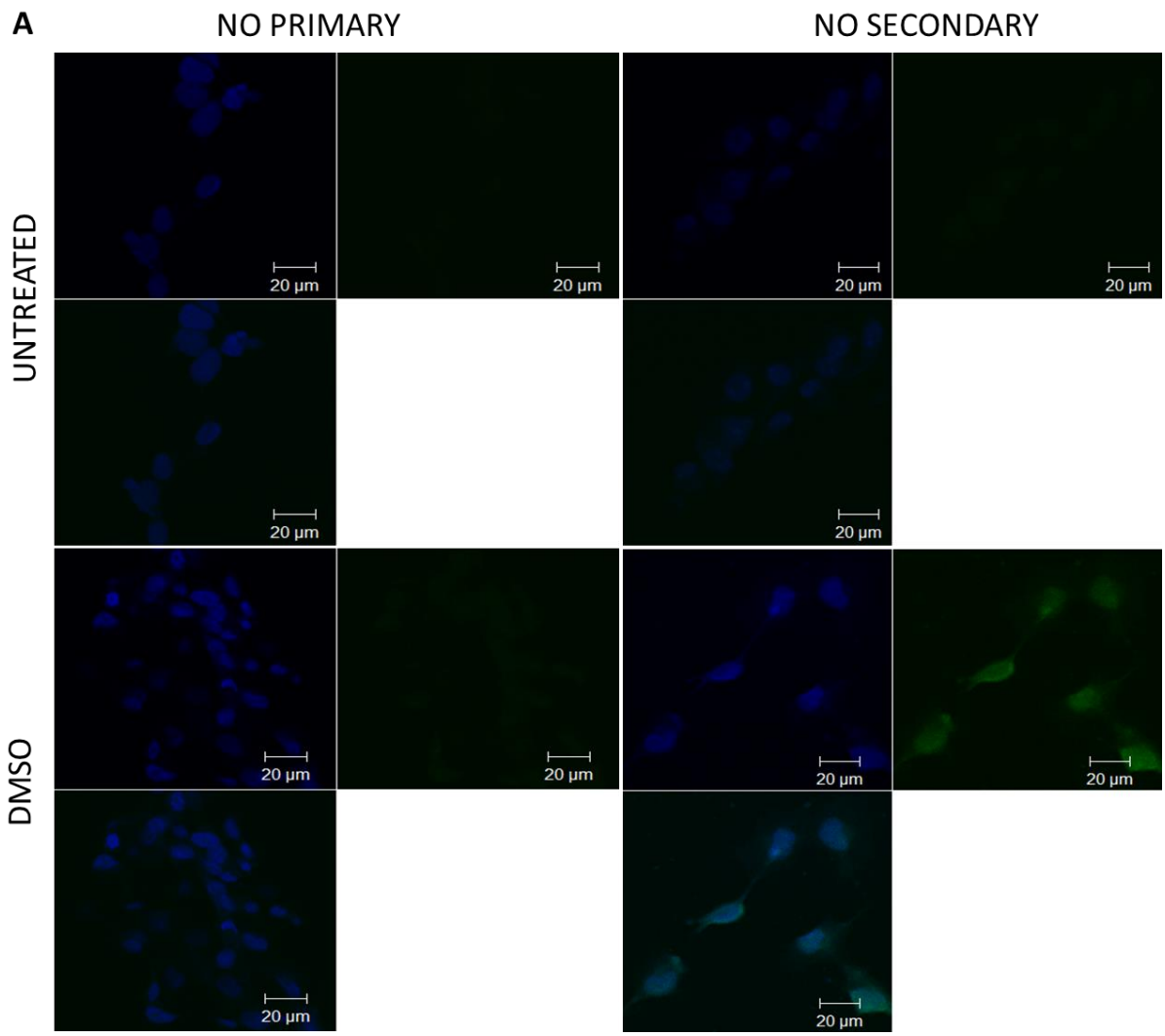


Figure D.3. A) Negative controls of MDA-MB-436 cell line in confocal microscopy. Where the primary antibody was excluded it was marked "no primary" and when a secondary antibody was excluded it was marked "no secondary". The top panel shows the controls for the untreated cells and the bottom panel shows controls for DMSO vehicle control.

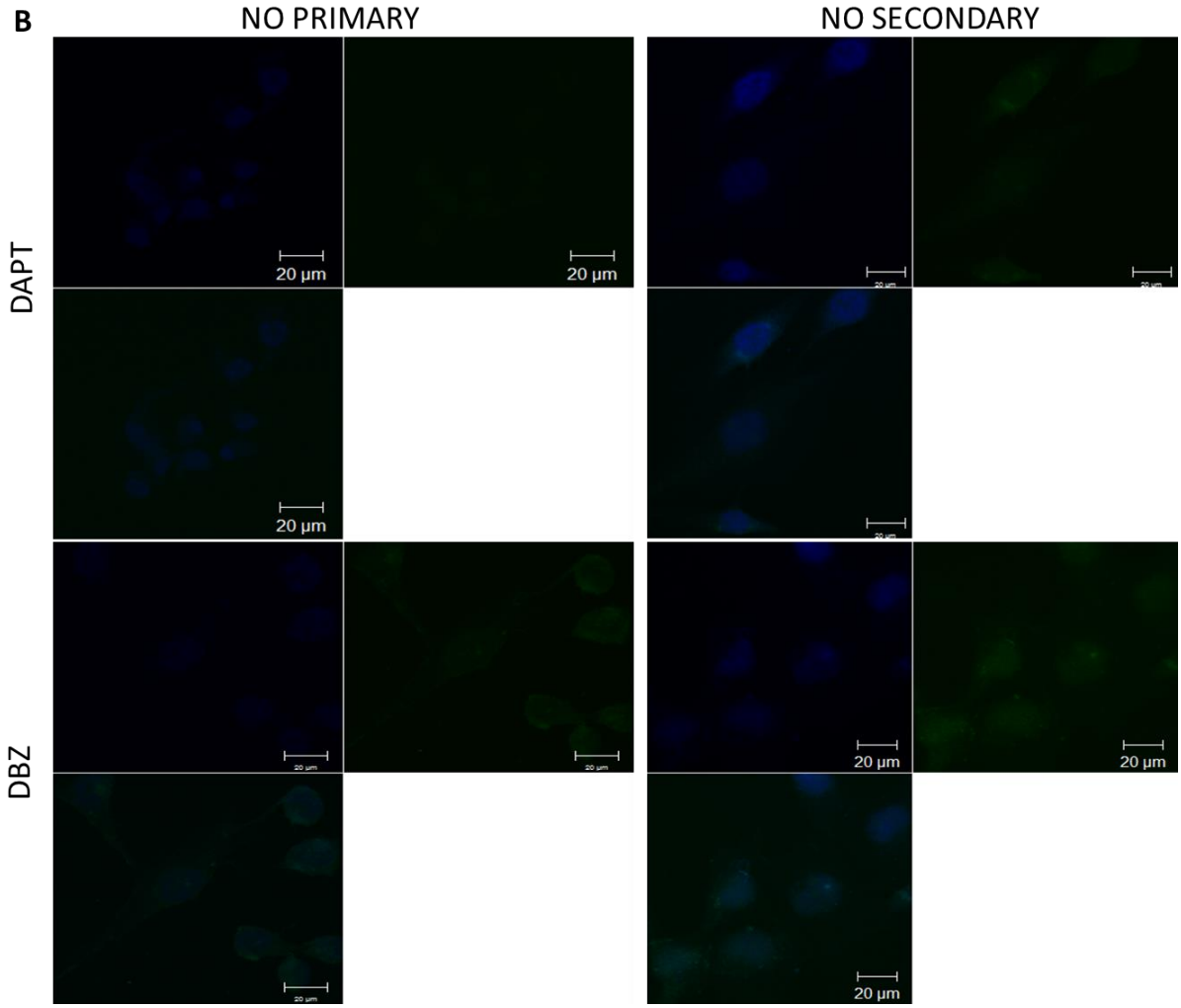


Figure D.3. B) Negative controls of MDA-MB-436 cell line in confocal microscopy. Where the primary antibody was excluded it was marked "no primary" and when a secondary antibody was excluded it was marked "no secondary". The top panel shows the controls for the DAPT treated cells and the bottom panel shows controls for DBZ treated cells.

D.2 Negative controls for the expression and localisation of E-cadherin

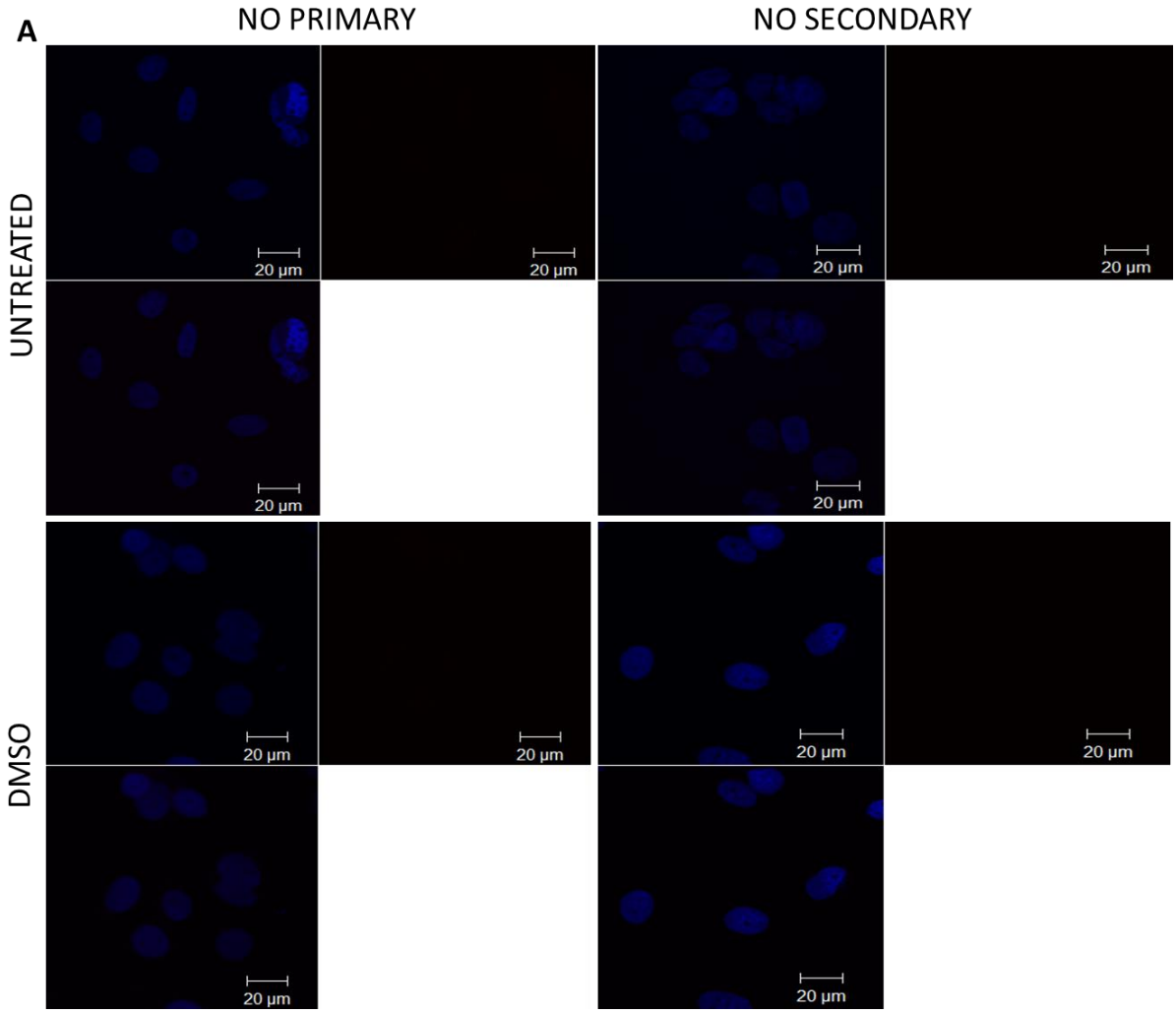


Figure D.4. A) E-cadherin negative controls of MCF-7cell line in confocal microscopy. Where the primary antibody was excluded it was marked "no primary" and when a secondary antibody was excluded it was marked "no secondary". The top panel shows the controls for the untreated cells and the bottom panel shows controls for DMSO vehicle control.

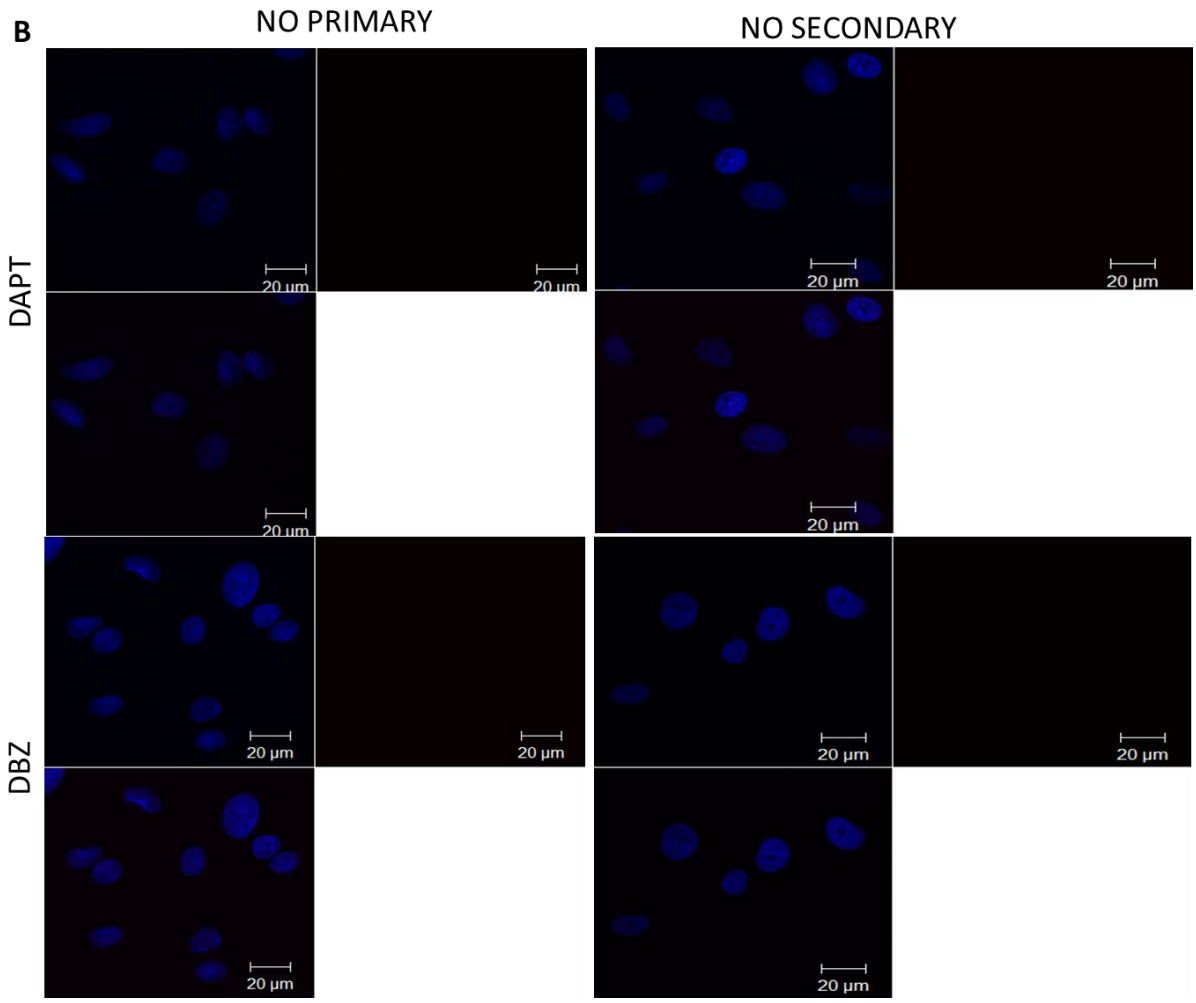


Figure D.4. B) E-cadherin negative controls of MCF-7cell line in confocal microscopy. Where the primary antibody was excluded it was marked "no primary" and when a secondary antibody was excluded it was marked "no secondary". The top panel shows the controls for the DAPT treated cells and the bottom panel shows controls for DBZ treated cells.

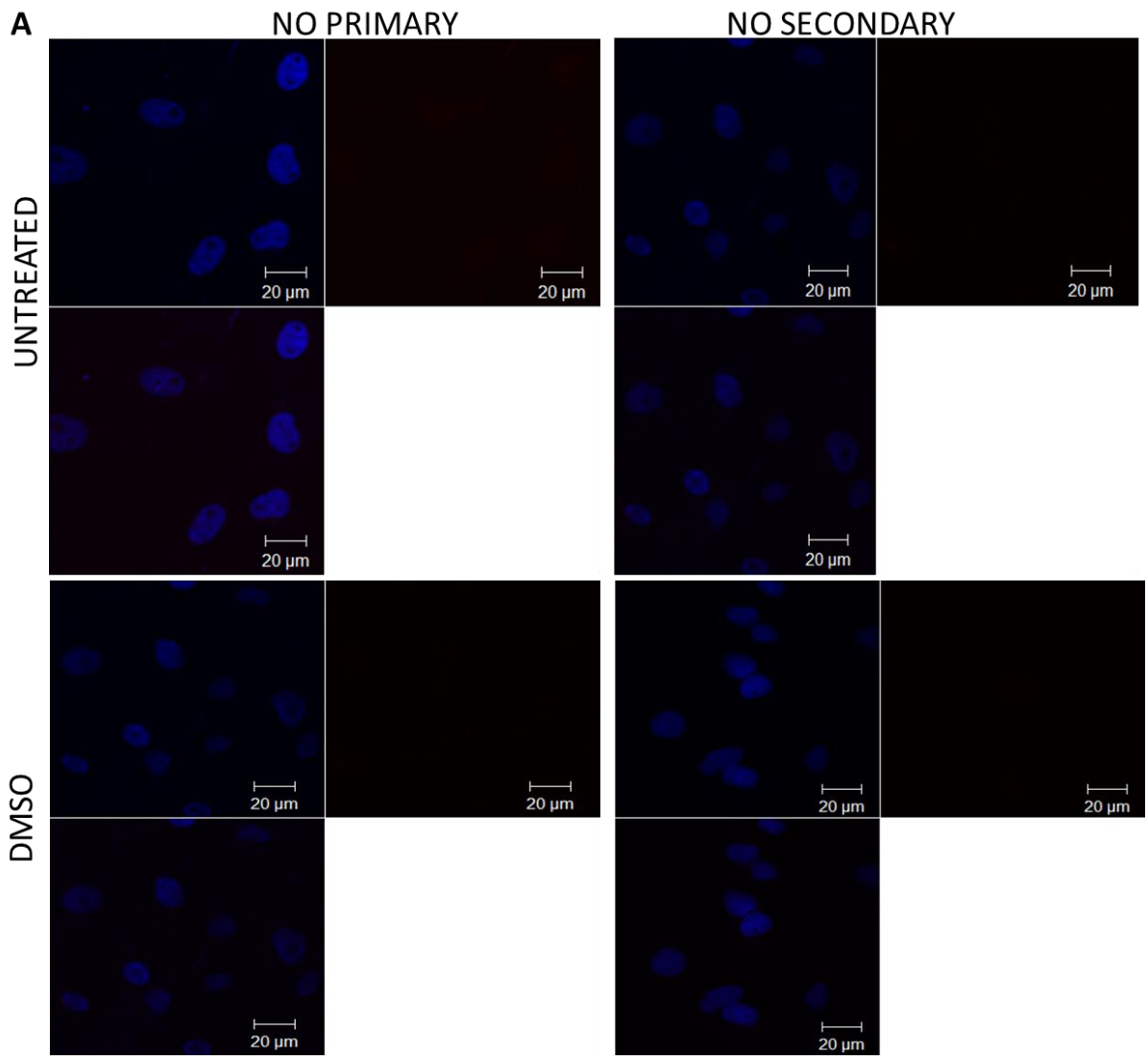


Figure D.5. A) E-cadherin negative controls of MDA-MB-231cell line in confocal microscopy. Where the primary antibody was excluded it was marked "no primary" and when a secondary antibody was excluded it was marked "no secondary". The top panel shows the controls for the untreated cells and the bottom panel shows controls for DMSO vehicle control**.**

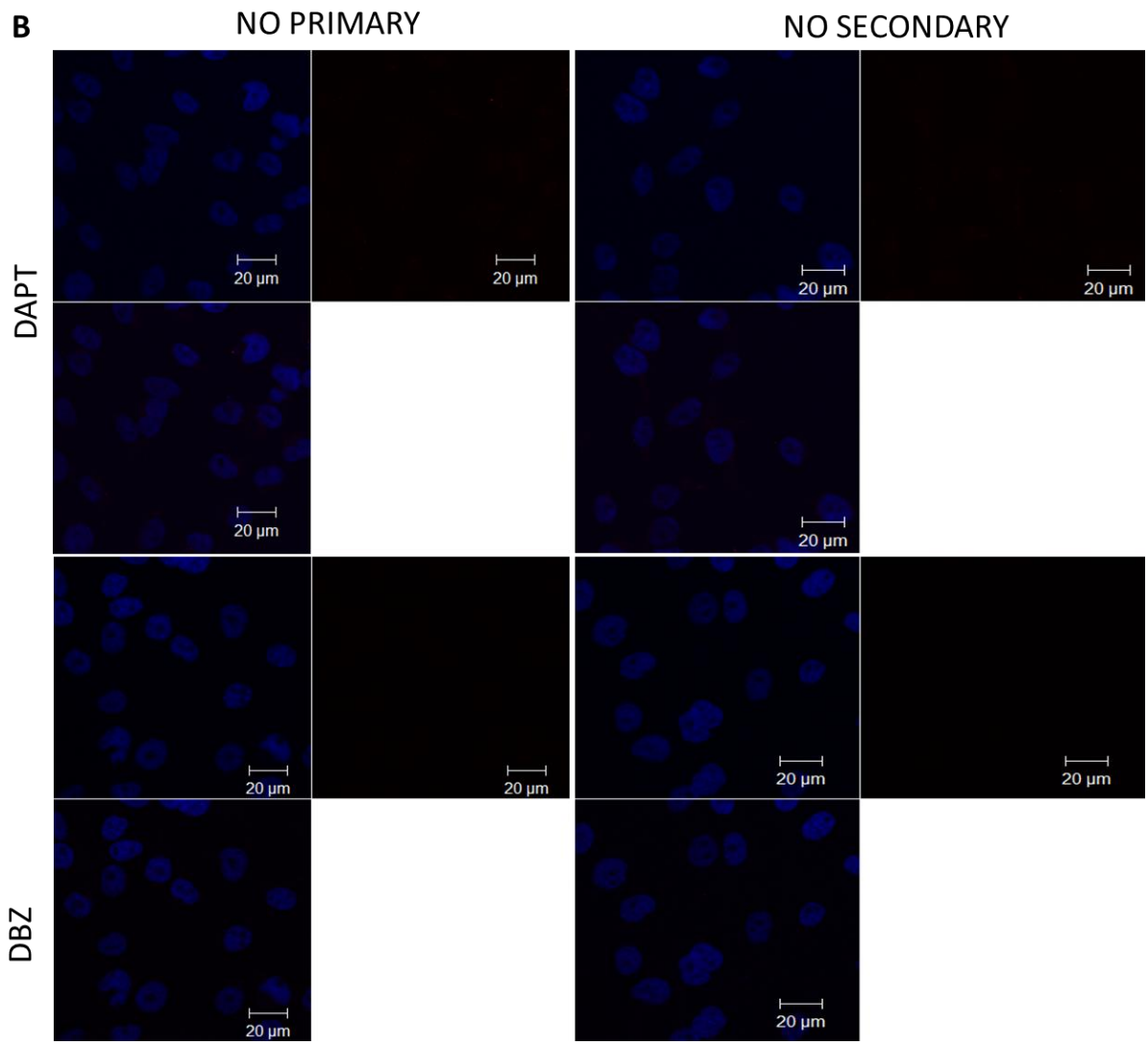


Figure D.5.B) E-cadherin negative controls of MDA-MB-231cell line in confocal microscopy. Where the primary antibody was excluded it was marked "no primary" and when a secondary antibody was excluded it was marked "no secondary". The top panel shows the controls for the DAPT treated cells and the bottom panel shows controls for DBZ treated cells.

B)

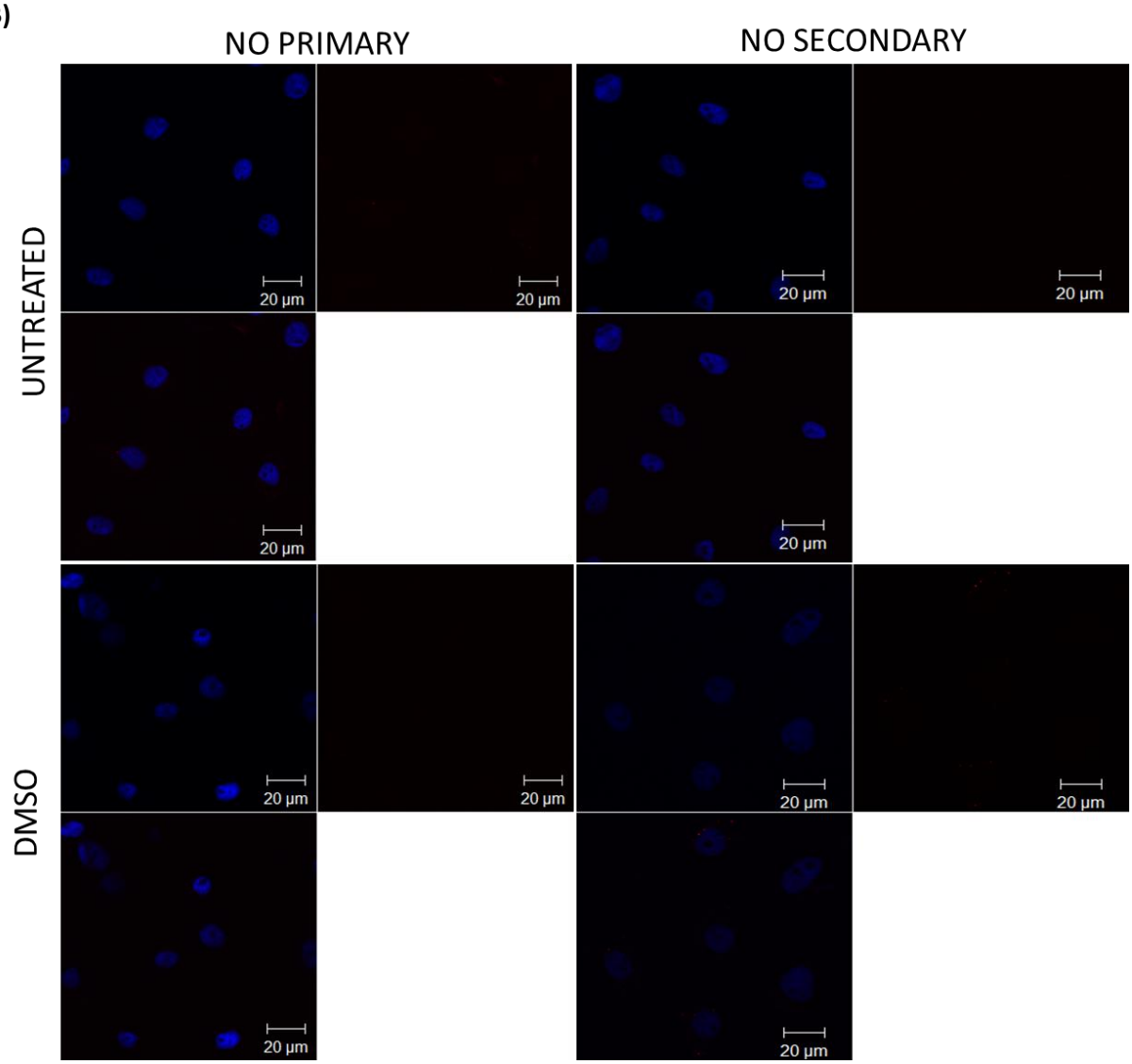


Figure D.6.A) E-cadherin negative controls of MDA-MB-436 cell line in confocal microscopy. Where the primary antibody was excluded it was marked "no primary" and when a secondary antibody was excluded it was marked "no secondary". The top panel shows the controls for the untreated cells and the bottom panel shows controls for DMSO vehicle control**.**

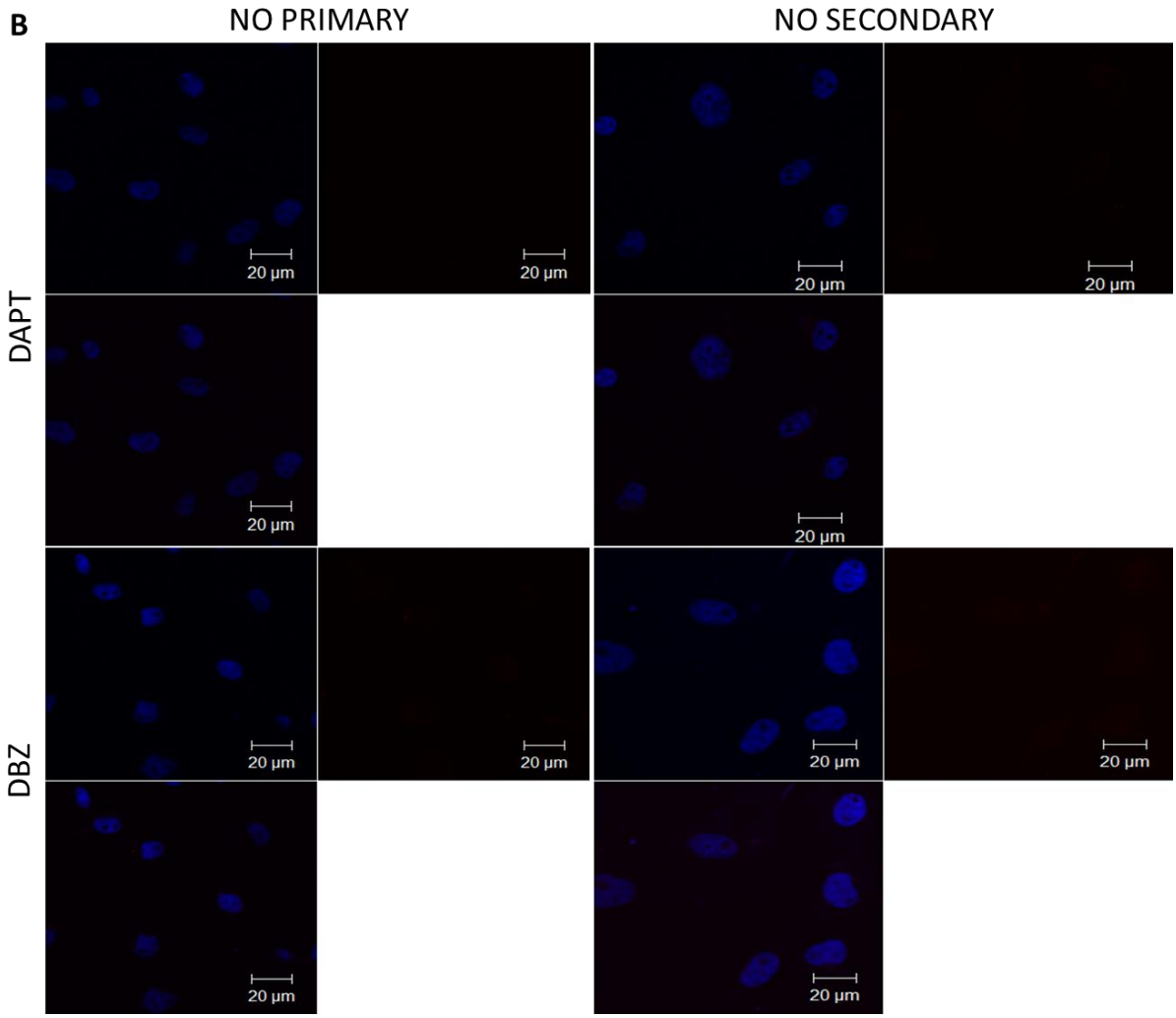


Figure D.6 B) E-cadherin negative controls of MDA-MB-436 cell line in confocal microscopy. Where the primary antibody was excluded it was marked "no primary" and when a secondary antibody was excluded it was marked "no secondary". The top panel shows the controls for the DAPT treated cells and the bottom panel shows controls for DBZ treated cells.

D.3 MCF-7 cell line E-cadherin expression

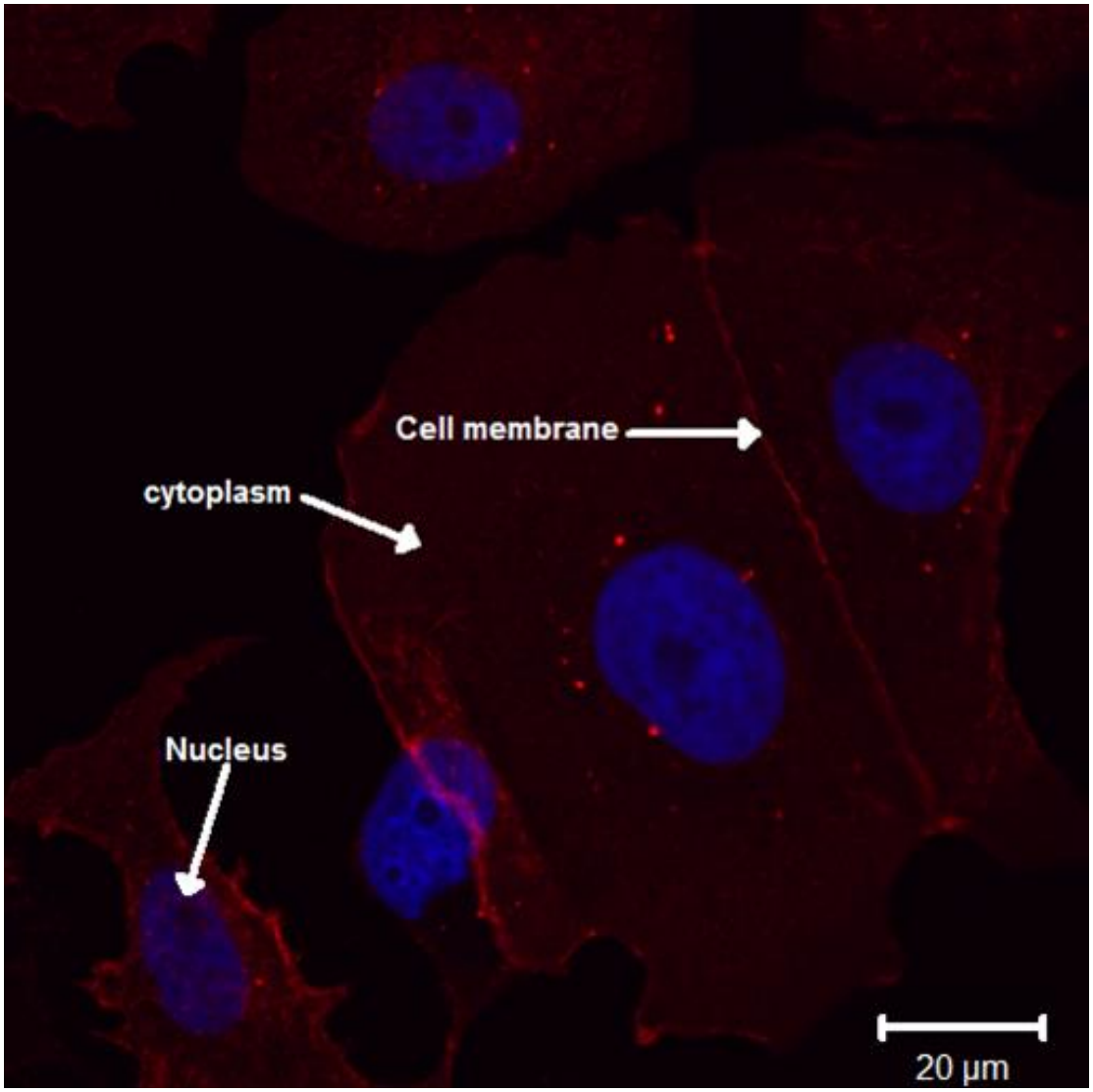


Figure D.7. The E-cadherin expression and localisation in MCF-7 cell line. E-cadherin (red) appears to be expressed in the cytoplasm, the cell membrane as well as the nucleus (blue).

Appendix E: Scratch/Migration assay analysis

E.1 Calculations of cell migration

The distance between two borders of the cells created by the scratch, was measured at 3 points on the image (Figure E.1 orange arrows), using the Imagej software. The distance was calculated in pixels. The distance in pixel/µm was given by the formula Distance in pixels\known distance X 1.0 pixel aspect ratio which is performed by ImageJ automatically. The averages of the 3 were calculated as the average distance for one scratch. As each experiment included 3 biological repeats (Figure E.2-4) every gap on each image was measured using this method. The average distance for each triplicate was regarded as the average distance in pixels/µm.

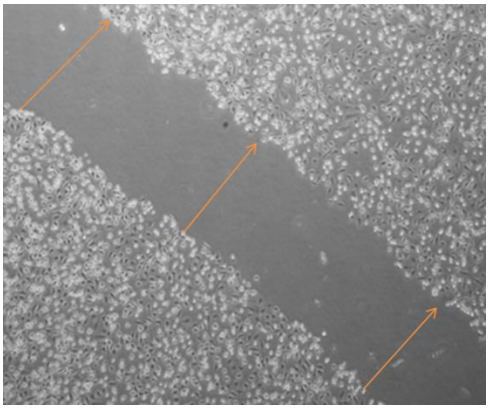


Figure E.1.Scratch image analyses. An example of the three points (orange arrows) at which the gap was measured using Imagej Software.

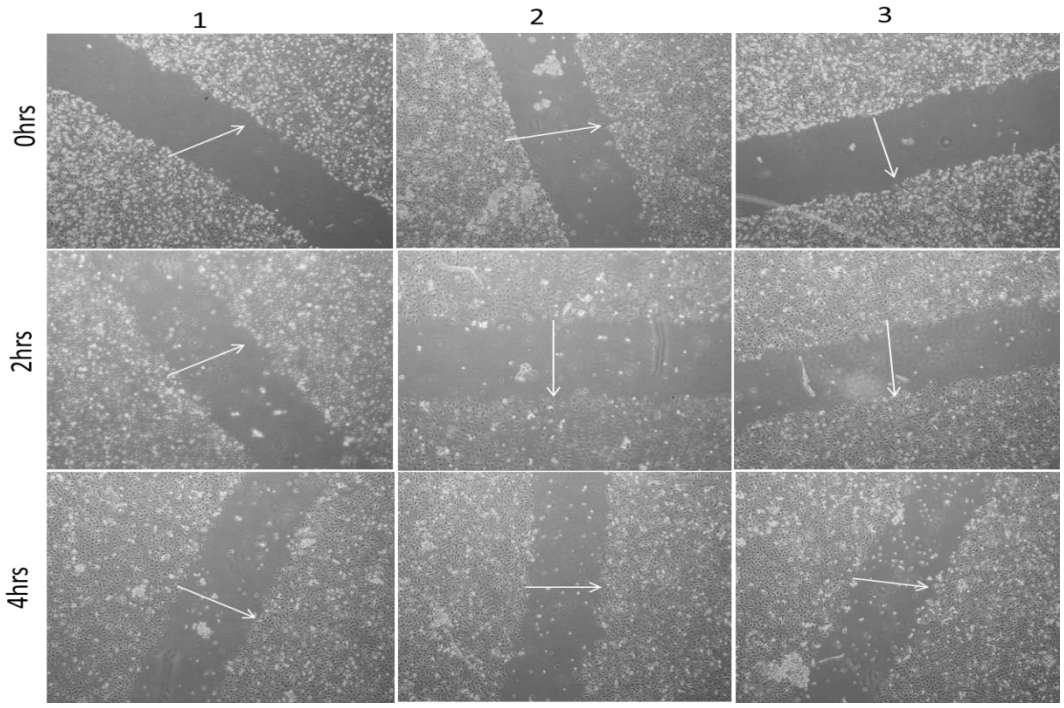


Figure E.2 Scratch image analyses. An example of DAPT treated cells in triplicates at 0 hours, 2 hours and 4 hours. The white arrows indicate gap closure

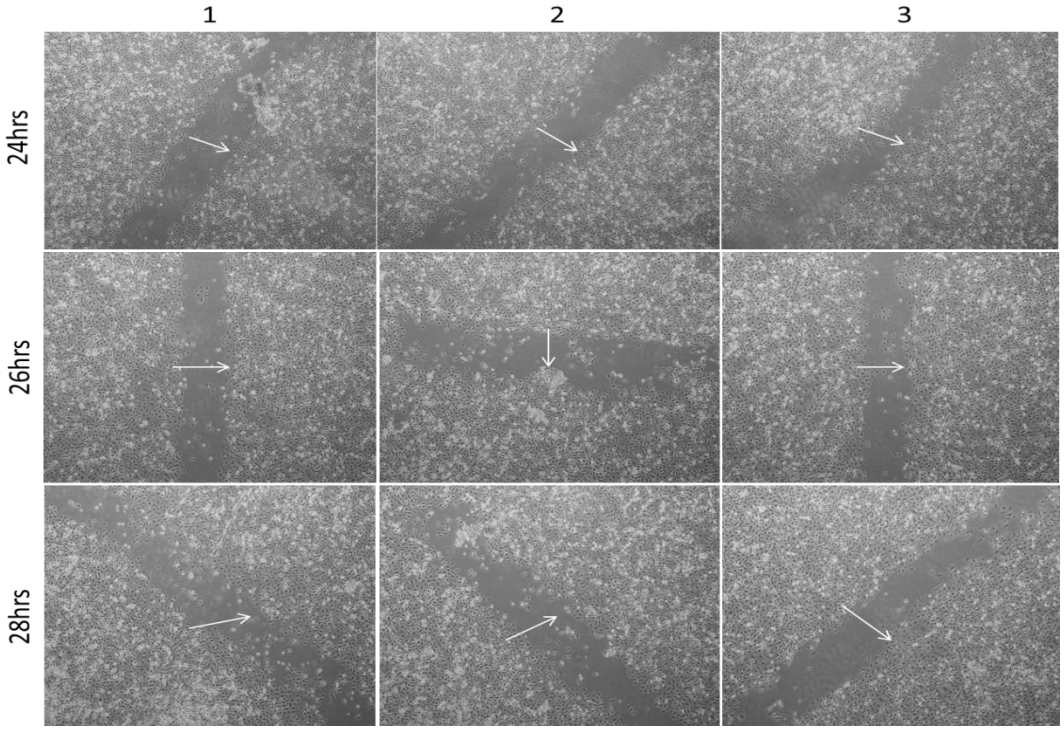


Figure E.3. Scratch image analyses. An example of DAPT treated cells in triplicates at 24 hours, 26 hours and 28 hours. The white arrows indicate gap closure

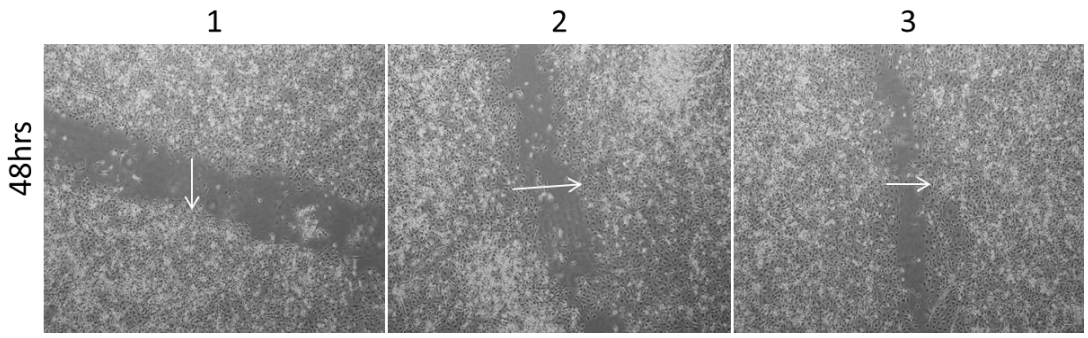


Figure E.4 Scratch image analyses. An example of DAPT treated cells in triplicates at 48 hours. The white arrows indicate gap closure.

E.2 Raw data for gap closure plots

Table E.1: The average distances of MCF-7 cell line pixel/μm calculated on ImageJ.

		average		
Time (hours)	UNTREATED	DMSO	DAPT	DBZ
0	5.405	6.111333333	4.665667	6.683
2	4.557333333	4.604	6.32	4.918667
4	5.899	5.397	5.668	4.196667
24	3.301333333	4.269	4.112333	5.429667
26	3.193333333	3.918666667	3.385667	3.609
28	3.271	3.883	3.539667	2.476
48	1.886333333	2.302333333	2.483667	2.769333

Table E.2: The standard deviations of MCF-7 cell line pixel/µm calculated on ImageJ.

		SDV		
Time (hours)	UNTREATED	DMSO	DAPT	DBZ
0	0.54086875	0.175845	0.85770411	0.077788
2	0.13875278	0.366283	0.32261897	0.453244
4	0.56357165	0.534506	0.91279571	0.299067
24	0.58704032	0.543617	0.57189626	0.314607
26	0.74377707	0.605004	0.68207429	0.313651
28	1.14852993	1.423559	0.42602856	0.116052
48	0.52401559	0.432551	0.57452618	0.368138

Table E.3: The average distances of MDA-MB-231 cell line pixel/µm calculated on ImageJ.

		average		
Time (hours)	UNTREATED	DMSO	DAPT	DBZ
	4.252	3.555	6.020667	5.709667
2	4.24	4.36533333	4.330667	3.832667
4	4.62133333	4.727	4.397667	4.100667
24	4.09333333	3.80366667	2.513333	3.895333
26	3.287	3.096	3.723	3.241333
28	2.619	3.03833333	4.225667	3.224333
48	1.277	2.614	2.594667	0.930333

Table E.4: The standard deviation MDA-MB-231cell line pixel/µm calculated on ImageJ.

		SDV		
Time (hours)	UNTREATED	DMSO	DAPT	DBZ
0	0.245036732	0.495254	0.588145	0.15232
2	0.50610572	0.190264	0.350423	0.441799
4	0.595760299	0.527787	0.190327	0.83001
24	0.525178382	0.628673	0.707094	0.369197
26	0.424625718	0.659737	0.838485	0.443741
28	0.847488643	0.694784	0.473407	0.393983
48	0.459568276	0.522943	0.876286	0.366757

Table E.5: The averages distances of MDA-MB-436 cell line pixel/µm calculated on ImageJ.

		averages		
Time (hours)	UNTREATED	DMSO	DAPT	DBZ
0	6.432	6.223	6.228667	6.089667
2	5.999333333	5.61366667	5.597333	4.828667
4	5.483333333	5.10233333	5.917	5.108333
24	4.118666667	3.927	4.115	4.960667
26	4.235666667	4.08466667	3.587667	4.909333
28	4.615	3.62166667	4.274333	5.071333
48	3.899333333	4.501	3.672	4.468667

Table E.6: The standard deviations of MDA-MB-436 cell line pixel/µm calculated on ImageJ.

		SDV		
Time (hours)	UNTREATED	DMSO	DAPT	DBZ
0	0.488430138	0.138156	0.182506	0.45581
2	0.246579264	0.105406	0.40721	0.183664
4	0.334156151	0.205432	0.117478	0.368419
24	0.311872303	0.330002	0.792121	0.434403
26	0.148708888	0.105078	0.639207	0.426809
28	0.476087177	0.162312	0.492526	0.366571
48	0.173727756	0.681954	0.822658	0.577243

APPENDIX F: Statistical analyses and turn-it-in report

All statistical data was calculated with Graphpad Prism 5 Software version 5 below are all the outputs from the analysis.

Table F.1: Results from the Kruskal-Wallis test of the effect of DBZ on MCF-7, MDA-MB-231 and MDA-MB-436 cell lines.

Table Analysed	Effect of DBZ on MCF-7,MDA-MB-231 and MDA-MB-436
Kruskal-Wallis test	
P value	P<0.0001
Exact or approximate P value?	Gaussian Approximation
P value summary	***
Do the medians vary signif. (P < 0.05)	Yes
Number of groups	3
Kruskal-Wallis statistic	206.4

Table F.2: Results from the Kruskal-Wallis test of the effect of DAPT on MCF-7,MDA-MB-231 and MDA-MB436 cell lines.

Table Analysed	Effect of DAPT on MCF-7,MDA-MB-231 and MDA-MB-436
Kruskal-Wallis test	
P value	P<0.0001
Exact or approximate P value?	Gaussian Approximation
P value summary	***
Do the medians vary signif. (P < 0.05)	Yes
Number of groups	3
Kruskal-Wallis statistic	201.0

Table F.3: Results from the Kruskal-Wallis test of the normal growth curves of MCF-7, MDA-MB-231, and MDA-MB-436 cell lines.

Table Analysed	Growth curve
Kruskal-Wallis test	
P value	P<0.0001
Exact or approximate P value?	Gaussian Approximation
P value summary	***
Do the medians vary signif. (P < 0.05)	Yes
Number of groups	3
Kruskal-Wallis statistic	174.8

Table F.4: Results from the unpaired student's t-test between the growth curves of MCF-7 and MDA-MB-231 cell lines.

Table Analysed	Growth curve MCF-7 VS MDA-231
Column A	MCF-7
vs	vs
Column B	MDA-MB-231
Unpaired t test	
P value	P<0.0001
P value summary	***
Are means signif. different? (P < 0.05)	Yes
One- or two-tailed P value?	Two-tailed
t, df	t=16.05 df=294
How big is the difference?	
Mean ± SEM of column A	6.265 ± 0.1685 N=148
Mean ± SEM of column B	3.177 ± 0.09299 N=148
Difference between means	3.088 ± 0.1924
95% confidence interval	2.711 to 3.465
R squared	0.4669
F test to compare variances	
F,DFn, Dfd	3.282, 147, 147
P value	P<0.0001
P value summary	***
Are variances significantly different?	Yes

Table F.5: Results from the unpaired student's t-test between the growth curves of MCF-7 and MDA-MB-436.

Table Analysed	Growth curve MCF-7 vs MDA-MB-436
Column A	MCF-7
vs	vs
Column B	MDA-MB-436
Unpaired t test	
P value	P<0.0001
P value summary	***
Are means signif. different? (P < 0.05)	Yes
One- or two-tailed P value?	Two-tailed
t, df	t=17.70 df=294
How big is the difference?	
Mean ± SEM of column A	6.265 ± 0.1685 N=148
Mean ± SEM of column B	3.165 ± 0.04780 N=148
Difference between means	3.099 ± 0.1751
95% confidence interval	2.756 to 3.442
R squared	0.5159
F test to compare variances	
F,DFn, Dfd	12.42, 147, 147
P value	P<0.0001
P value summary	***
Are variances significantly different?	Yes

Table F.6: Results from the unpaired student's t-test between the effects of DAPT on the cell proliferation and viability of the MCF-7 and MDA-MB-231 cell lines.

Table Analysed	DAPT comparison between MCF-7 and MDA-MB-231
Column A	MCF-7
vs	vs
Column B	MDA-MB-231
Unpaired t test	
P value	P<0.0001
P value summary	***
Are means signif. different? (P < 0.05)	Yes
One- or two-tailed P value?	Two-tailed
t, df	t=28.90 df=193
How big is the difference?	
Mean ± SEM of column A	2.240 ± 0.06337 N=98
Mean ± SEM of column B	0.3982 ± 0.001644 N=97
Difference between means	1.841 ± 0.06372
95% confidence interval	1.717 to 1.966
R squared	0.8123
F test to compare variances	
F,DFn, Dfd	1501, 97, 96
P value	P<0.0001
P value summary	***
Are variances significantly different?	Yes

Table F.7: Results from the unpaired student's t-test between the effects of DAPT on the cell proliferation and viability of the MCF-7 and MDA-MB-436 cell lines.

Table Analysed	DAPT comparison between MCF-7 and MDA-MB-436
Column A	MCF-7
vs	vs
Column B	MDA-MB-436
Unpaired t test	
P value	P<0.0001
P value summary	***
Are means signif. different? (P < 0.05)	Yes
One- or two-tailed P value?	Two-tailed
t, df	t=28.74 df=192
How big is the difference?	
Mean ± SEM of column A	2.240 ± 0.06337 N=98
Mean ± SEM of column B	0.3452 ± 0.01582 N=96
Difference between means	1.894 ± 0.06591
95% confidence interval	1.765 to 2.024
R squared	0.8114
F test to compare variances	
F,DFn, Dfd	16.37, 97, 95
P value	P<0.0001
P value summary	***
Are variances significantly different?	Yes

Table F.8: Results from the unpaired student's t-test between the effects of DBZ on the cell proliferation and viability of the MCF-7 and MDA-MB-231 cell lines.

Table Analysed	DBZ comparison between MCF-7 and MDA-MB-231
Column A	MCF-7
vs	vs
Column B	MDA-MB-231
Unpaired t test	
P value	P<0.0001
P value summary	***
Are means signif. different? (P < 0.05)	Yes
One- or two-tailed P value?	Two-tailed
t, df	t=16.93 df=193
How big is the difference?	
Mean ± SEM of column A	1.421 ± 0.06245 N=98
Mean ± SEM of column B	0.3579 ± 0.002118 N=97
Difference between means	1.064 ± 0.06281
95% confidence interval	0.9404 to 1.187
R squared	0.5977
F test to compare variances	
F,DFn, Dfd	878.3, 97, 96
P value	P<0.0001
P value summary	***
Are variances significantly different?	Yes

Table F.9: Results from the unpaired student's t-test between the effects of DBZ on the cell proliferation and viability of the MCF-7 and MDA-MB-436 cell lines.

Table Analysed	DBZ comparison between MCF-7 and MDA-MB-436
Column A	MCF-7
vs	vs
Column B	MDA-MB-436
Unpaired t test	
P value	P<0.0001
P value summary	***
Are means signif. different? (P < 0.05)	Yes
One- or two-tailed P value?	Two-tailed
t, df	t=17.55 df=192
How big is the difference?	
Mean ± SEM of column A	1.421 ± 0.06245 N=98
Mean ± SEM of column B	0.3024 ± 0.009160 N=96
Difference between means	1.119 ± 0.06375
95% confidence interval	0.9941 to 1.244
R squared	0.6161
F test to compare variances	
F,DFn, Dfd	47.45, 97, 95
P value	P<0.0001
P value summary	***
Are variances significantly different?	Yes

Table F.10: Results from the paired student's t-test between the effects of DAPT vs DBZ on the cell proliferation and viability of the MCF-7 cell line.

Table Analysed	MCF-7 DAPT VS DBZ
Column A	DAPT
vs	vs
Column B	DBZ
Paired t test	
P value	P<0.0001
P value summary	***
Are means signif. different? (P < 0.05)	Yes
One- or two-tailed P value?	Two-tailed
t, df	t=94.01 df=97
Number of pairs	98
How big is the difference?	
Mean of differences	0.8182
95% confidence interval	0.8009 to 0.8355
R squared	0.9891
How effective was the pairing?	
Correlation coefficient (r)	0.9905
P Value (one tailed)	P<0.0001
P value summary	***
Was the pairing significantly effective?	Yes

Table F.11: Results from the paired student's t-test between the effects of DAPT vs DBZ on the cell proliferation and viability of the MDA-MB-231 cell line.

Table Analysed	MDA-MB-231 DAPT vs DBZ
Column A	DAPT
vs	vs
Column B	DBZ
Paired t test	
P value	P<0.0001
P value summary	***
Are means signif. different? (P < 0.05)	Yes
One- or two-tailed P value?	Two-tailed
t, df	t=23.98 df=96
Number of pairs	97
How big is the difference?	
Mean of differences	0.04034
95% confidence interval	0.03700 to 0.04369
R squared	0.8569
How effective was the pairing?	
Correlation coefficient (r)	0.6257
P Value (one tailed)	P<0.0001
P value summary	***
Was the pairing significantly effective?	Yes

Table F.12: Results from the paired student's t-test between the effects of DAPT vs DBZ on the cell proliferation and viability of the MDA-MB-436 cell line.

Table Analysed	MDA-MB-436 DAPT vs DBZ
Column A	DAPT
vs	vs
Column B	DBZ
Paired t test	
P value	P<0.0001
P value summary	***
Are means signif. different? (P < 0.05)	Yes
One- or two-tailed P value?	Two-tailed
t, df	t=6.363 df=95
Number of pairs	96
How big is the difference?	
Mean of differences	0.04285
95% confidence interval	0.02946 to 0.05624
R squared	0.2989
How effective was the pairing?	
Correlation coefficient (r)	0.9968
P Value (one tailed)	P<0.0001
P value summary	***
Was the pairing significantly effective?	Yes

Table F.13: Results from the Kruskal-Wallis test on the cell migration of MCF-7 cell lines.

Table Analysed	MCF-7 migration assay anova
Kruskal-Wallis test	
P value	0.3916
Exact or approximate P value?	Gaussian Approximation
P value summary	ns
Do the medians vary signif. (P < 0.05)	No
Number of groups	4
Kruskal-Wallis statistic	3.000

Table F.14: Results from the Kruskal-Wallis t-test on the cell proliferation and viability of the MDA-MB-231 cell line.

Table Analysed	MDA-MB-231 migration assay ANOVA
Kruskal-Wallis test	
P value	0.3916
Exact or approximate P value?	Gaussian Approximation
P value summary	ns
Do the medians vary signif. (P < 0.05)	No
Number of groups	4
Kruskal-Wallis statistic	3.000

Table F.15: Results from the Kruskal-Wallis t-test on the cell migration of the MDA-MB-436 cell line.

Table Analysed	MDA-MB-436 MIGRATION ASSAY ANOVA
Kruskal-Wallis test	
P value	0.3916
Exact or approximate P value?	Gaussian Approximation
P value summary	ns
Do the medians vary signif. ($P < 0.05$)	No
Number of groups	4
Kruskal-Wallis statistic	3.000

Table F.16: Results from the paired student's t-test between the effects of DAPT vs DBZ on the cell migration of the MCF-7 cell line.

Table Analysed	Migration assay MCF-7 DAPT VS DBZ
Column A	DAPT
vs	vs
Column B	DBZ
Paired t test	
P value	0.9804
P value summary	ns
Are means signif. different? (P < 0.05)	No
One- or two-tailed P value?	Two-tailed
t, df	t=0.02564 df=6
Number of pairs	7
How big is the difference?	
Mean of differences	0.01324
95% confidence interval	-1.250 to 1.277
R squared	0.0001096
How effective was the pairing?	
Correlation coefficient (r)	0.5431
P Value (one tailed)	0.1039
P value summary	ns
Was the pairing significantly effective?	No

Table F.17: Results from the paired student's t-test between the effects of DAPT vs DBZ on the cell proliferation and viability of the MDA-MB-436 cell line.

Table Analysed	MDA-MB-436 migration assay
Column A	DAPT
vs	vs
Column B	DBZ
Paired t test	
P value	0.4015
P value summary	ns
Are means signif. different? (P < 0.05)	No
One- or two-tailed P value?	Two-tailed
t, df	t=0.9026 df=6
Number of pairs	7
How big is the difference?	
Mean of differences	-0.2921
95% confidence interval	-1.084 to 0.4998
R squared	0.1195
How effective was the pairing?	
Correlation coefficient (r)	0.6763
P Value (one tailed)	0.0476
P value summary	*
Was the pairing significantly effective?	Yes

Table F.18: Results from the paired student's t-test between the effects of DAPT vs DBZ on the cell proliferation and viability of the MDA-MB-231 cell line.

Table Analysed	MDA-MB-231 migration assay
Column A	DAPT
vs	vs
Column B	DBZ
Paired t test	
P value	0.2867
P value summary	ns
Are means signif. different? (P < 0.05)	No
One- or two-tailed P value?	Two-tailed
t, df	t=1.169 df=6
Number of pairs	7
How big is the difference?	
Mean of differences	0.4102
95% confidence interval	-0.4483 to 1.269
R squared	0.1856
How effective was the pairing?	
Correlation coefficient (r)	0.7637
P Value (one tailed)	0.0228
P value summary	*
Was the pairing significantly effective?	Yes